VOLUME XLVII NUMBER 3

THE
JOURNAL OF GEOLOGY

April-May 1939

CREEP OF ROCKS[1]

DAVID GRIGGS
Harvard University

ABSTRACT

"Creep" is the name applied to the slow deformation of solids under small loads acting over long periods of time. Two types of apparatus have been developed for the purpose of investigating the creep of rocks in response to stresses below the "elastic limit," as ordinarily defined. The present paper describes results obtained with these instruments during runs of various duration, up to 550 days. It is found that in many cases there is measurable flow at stresses below the "elastic limit." An empirical law has been derived which resolves this deformation into two types of flow, termed "elastic flow" and "pseudoviscous flow." The creep characteristics of several materials at room temperature and atmospheric confining pressure are described. Preliminary experiments on creep at high pressure and on creep by recrystallization are reported.

INTRODUCTION

It has long been recognized that materials may support, without permanent set, shear stresses of short duration and yet yield continually when subject to smaller stresses for a long period of time. There is no direct connection between creep and elastic rigidity; for example, the substratum in the earth transmits the short-period shear waves of seismic origin in a way which indicates high rigidity, yet the load of a glacial icecap is sufficient to cause a deep-seated flow producing isostatic compensation for this increment of material. The velocity of seismic waves indicates that the continental rocks are less rigid than the substratum, but they apparently support the localized loads of volcanic cones and of deltas without yielding appreciably.

[1] Paper No. 54, published under the auspices of the Committee on Geophysics and the Society of Fellows of Harvard University.

Seeking for a graphic illustration of these phenomena in common materials, geologists have repeatedly turned to Lord Kelvin's classic example of the beeswax and the candle.[2] A temporary tuning-fork may be fashioned of the former, but it will, in the course of time, flow of its own weight into a shapeless mass. In the candle, on the other hand, acoustic vibrations are damped almost immediately, but it will resist flow under its own weight indefinitely.

Some rocks, notably clays and shales, are observed to flow slowly or "creep" under relatively low loads acting over a few years; but other rocks do not creep appreciably under much higher stresses in buildings. These same rocks will, however, exhibit the properties of creep when high differential stresses are applied under high confining pressure in the laboratory.

From measurements of the response to release of the glacial load, Haskell has calculated the equivalent viscosity of the substratum.[3] This viscosity is so great that it could not be noticed in ordinary building applications. A 10-foot cube of rock, loaded to its breaking-point, would shorten only about three-thousandths of an inch in 10 years. Hence, our ordinary observations do not exclude the possibility that the continental rocks may actually be deforming continuously by flow with this extremely high "viscosity." Present laboratory methods, however, are capable of detecting flow even at this low velocity in a few months. This paper reports the results of an investigation of creep in some rocks at atmospheric confining pressure.

This discussion is concerned entirely with creep in specimens subject to a direct compressive force. This type of loading was chosen because it is the only way in which a rock may be loaded with a homogeneous stress, and thus it has the advantage of avoiding one possible source of confusion. Measurements of creep from the deflection of a loaded beam are much more sensitive than these straight compressive tests, and their behavior is in many ways entirely different from the latter. These differences will be brought out in a paper by Dr. George W. Bain, which was kindly shown to the writer

[2] Lord Kelvin, *Baltimore Lectures* (Cambridge, Eng.: Cambridge University Press, 1904), pp. 9–10. (Apiezon wax at 20° C. is a better medium than beeswax.)

[3] N. A. Haskell, "Viscosity of Asthenosphere," *Amer. Jour. Sci.*, Vol. XXXIII (1937), p. 24.

in manuscript form. The bending of the beam is very sensitive to any changes in humidity or any vibration—much more so than specimens loaded in compression. These difficulties and others which may be connected with the anomalous behavior of rocks under the tensile stresses present in bending influenced the writer's choice of compressive tests.

DEFINITIONS

Many of the terms which physicists and engineers use to describe the behavior of matter, while sufficiently accurate for ordinary tests, are not applicable to tests of long duration and great sensitivity. In other words, some of the properties are functions of time. To avoid ambiguity in this text, it seems wise to define operationally the terms used in this discussion.

The terms "elastic limit," "set point," and "strength" lose their ordinary meaning when tests of long duration are undertaken. In such tests the "elastic limit" is known to be a strong function of the limit of sensitivity of the measurements. The present series of experiments are not concerned with the existence of a true elastic limit of stress below which no permanent set occurs regardless of duration of the test. No attempt was made to find whether such a limiting stress exists. "Strength" is also a function of the duration of the test in a way which has not been determined in the present series of experiments. These terms have, in general, been avoided in the text because they are not necessary to an understanding of the phenomena involved. When "strength" is used, it refers merely to the breaking-strength under ordinary conditions in the testing machine and is mentioned to give an idea of the magnitude of the stress applied relative to that which will cause instantaneous fracture.

"Flow" is considered to have occurred whenever a body is so strained that the deformation does not instantly disappear on the complete removal of the external forces acting on the body and when this deformation does not result in a notable loss of cohesion. "Fracture" is deformation with concomitant loss of cohesion. In high-pressure experiments the writer has found fracture and flow to be inseparably associated. A distinction has been made by various authors between "plastic" and "viscous" flow, but in the present experiments it is impossible to differentiate between these two sorts

of flow because the criteria on which this distinction is based have not been evaluated.

When a solid is subject to constant differential stress, it may creep or deform continuously. This deformation is termed "elasticoviscous flow" and may be analyzed as an aggregate effect of two types of flow: (1) "pseudoviscous flow," which is deformation at a constant rate; and (2) "elastic flow," which decreases logarithmically with time. It is possible to represent the total fractional deformation (S) as a function of time (t) by the equation

$$S = A + B \log t + Ct , \tag{1}$$

in which the term ($B \log t$) applies to the elastic flow and Ct applies to the pseudoviscous flow.

The logarithmic term has a further significance justifying the name "elastic flow," for on release of stress the body slowly recovers according to the equation

$$S = A' - B \log t . \tag{2}$$

This return has been called variously "elastic after-working," *Nachwirkung*, and "creep recovery" by engineers and physicists. The writer introduces here the term "elastic flow," applying to both phases of this reversible deformation. It is obvious that the foregoing equations do not describe the relation adequately for short-time intervals, since the logarithmic term approaches minus infinity as the time approaches zero. The writer has not tried to represent accurately the early part of the deformation because it is of no importance in long-time tests. Similarly, the logarithmic term approaches infinity as time approaches infinity. For any finite time longer than a few days, however, this expression gives a reasonable result.

This dependence of elastic flow on time may be visualized more easily if the creep-rates are considered. An expression for the velocity (v) of creep is obtained by differentiating equation (1) with respect to time:

$$\frac{dS}{dt} = v = \frac{B}{t} + C ; \tag{3}$$

and it is seen that the equations for the rate of elastic flow on loading (v_1) and unloading (v_2) are

$$v_1 = \frac{B}{t}, \qquad v_2 = -\frac{B}{t}. \tag{4}$$

Because the rate of elastic flow decreases inversely in proportion to the duration of the experiment, it eventually becomes very small in comparison with the rate of pseudoviscous flow, and the deformation will then proceed at a constant rate ($v = C$). This pseudoviscous flow resembles the viscous flow of liquids only in that the rate of shear is constant under constant stress. An equivalent viscosity may be calculated to describe this flow further and to give the geologist some appreciation of the behavior of the solid by comparison with the equivalent viscosities which are calculated for the deformation of the earth's substratum. This solid "viscosity" is, in general, different from the conventional liquid viscosity in that it is not constant with varying magnitudes of shear stress. For this reason it is impossible to extrapolate the equivalent viscosity to small values of stress difference until the dependence of this viscosity on stress has been determined. (Half the difference of the principal stresses is approximately equal to the shear stress acting on the body.)

CALCULATION OF EQUIVALENT VISCOSITY

The experiments described herein all deal with creep of solids under compressive loading. When there is a constant rate of deformation under constant pressure, one can calculate the equivalent viscosity with a fair degree of accuracy, using the standard equations of elasticity[4] and Jeffreys' term for elasticoviscous flow:

$$S = e_{zz} = \frac{P(\lambda + \mu)}{\mu(3\lambda + 2\mu)},$$

$$\lambda = k - \tfrac{2}{3}\mu,$$

$$S = P\left[\frac{1}{9k} + \frac{1}{3\mu}\right],$$

[4] A. E. H. Love, *Mathematical Theory of Elasticity* (4th ed.; Cambridge, Eng.: Cambridge University Press, 1934), p. 103.

where S is the fractional shortening; P the compressive pressure; λ the elastic constant; μ the coefficient of rigidity; k the compressibility; and η the equivalent viscosity. For elasticoviscous flow Jeffreys[5] replaces μ by

$$\frac{\mu}{1 + \frac{1}{t(d/dt)}}.$$

The compressibility is not a function of time.

$$S = P\left[\frac{1}{9k} + \frac{1 + \frac{1}{t(d/dt)}}{3\mu}\right]$$

$$= \frac{P}{9k} + \frac{P}{3\mu} + \frac{P}{3\mu t(d/dt)},$$

$$\frac{dS}{dt} = \frac{P}{3\mu t}.$$

Putting $\mu t = \eta$,

$$\eta = \frac{P}{3\frac{dS}{dt}}. \tag{5}$$

Hence, only the compressive stress and the constant rate of shortening must be known in order to calculate the equivalent viscosity of a solid.

METHOD OF OBSERVING CREEP

Two types of apparatus have been employed in the creep experiments. One is designed for materials which show relatively rapid creep, such as shale, glass at high temperatures, etc., where great sensitivity is not required. The other is a machine designed to measure the creep of the solid rocks, such as limestone, marble, granite, etc. Its sensitivity is as high as can conveniently be attained in the laboratory. Both methods measure creep in compression.

[5] H. Jeffreys, *The Earth* (2d ed.; New York: Macmillan Co., 1929), p. 265.

CREEP-TESTER OF MODERATE SENSITIVITY

Figure 1 shows the small creep-tester with a piece of paraffin-coated shale between the platens. The load is applied to the specimen by means of a lever, on the end of which is hung the appropriate

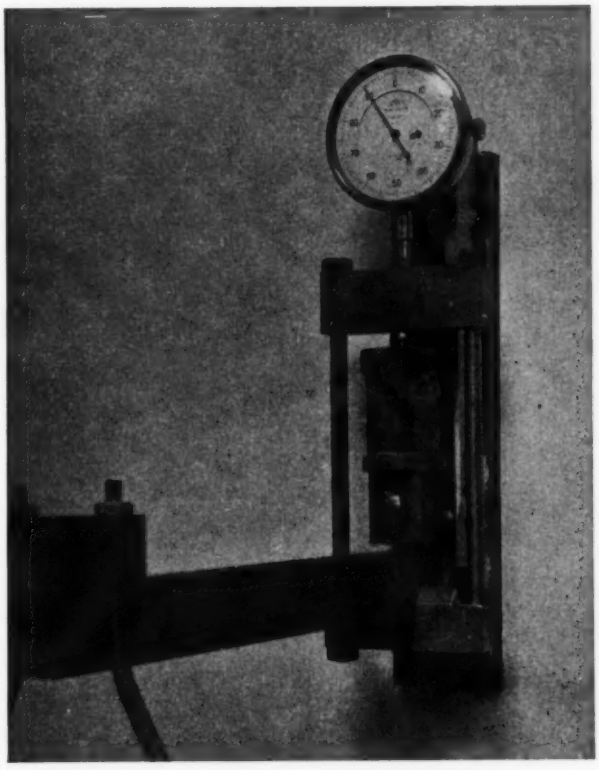

FIG. 1.—Small creep-tester with specimen of shale in position

weight. The lever fulcrums are knife edges, to reduce friction. The shortening of the specimen is measured directly by means of the dial gauge, which can be read to one hundred-thousandth of an inch. A furnace may be placed around the specimen, and tests made at high temperature. In this way tests have been made as high as 400° C.

It is, of course, necessary to have the temperature constant, and for this purpose a Thyratron regulator is used in conjunction with a resistance coil inside the furnace, which maintains the temperature constant within 1°.

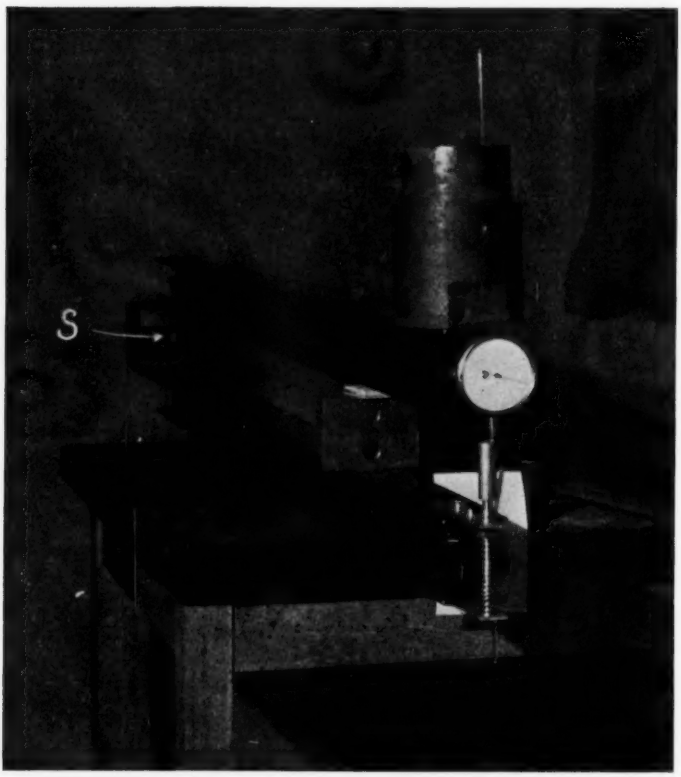

FIG. 2.—Sensitive creep-tester set up in constant-temperature room

SENSITIVE CREEP-TESTER

Figure 2 illustrates the tester used for the hard rocks at room temperature. The specimen (**S**) is loaded by means of the I-beam levers, which are joined at the end by an Emery hinge. This hinge is the heart of the apparatus. Its construction is illustrated in Figure 3.

The solid steel plate $\mathbf{H}_1$ serves as the hinge; the motion of the levers $\mathbf{L}_1$ and $\mathbf{L}_2$ is so small that the metal of the hinge is not strained beyond its elastic limit. The transverse hinge $\mathbf{H}_2$ serves as a stabilizer, preventing lateral motion of the levers. Since the plate $\mathbf{H}_1$ not only serves as a hinge but also supports the same load as the specimen, it must be made of a material which will not itself creep under this load. The success of the method is entirely due to the perfection of a new type of steel which has a very low creep-rate. Dr. A. V. De Forest of the Massachusetts Institute of Technology developed this "iso-elastic" steel and very kindly supplied the author with the

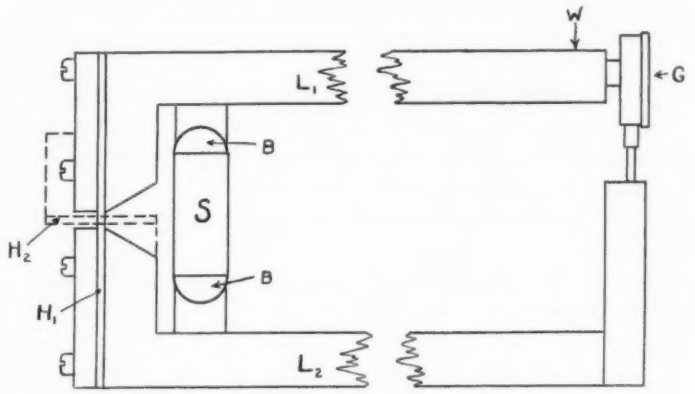

FIG. 3.—Diagram of sensitive creep-tester, showing Emery hinge with specimen in place.

material for this apparatus; and John Chatillon and Sons, makers of the steel, donated a test cylinder for the purpose of calibrating the machine.

The pressure on the specimen is equalized and centralized by means of the ball-and-socket force equalizers, **B**.

The deformation of the specimen is obtained by reading the dial gauge **G**, which measures the movement of the ends of the levers. The ratio of lever arms is 100:1, so that the dial gauge is sensitive to a deformation of the specimen of only one ten-millionth of an inch. The dial-gauge reading is an over-all deformation which includes any

creep in the hinge metal, any bending of the levers, and any motion due to irregularities at the surfaces of contact of the specimen and balls. For this reason it is necessary to make a calibration test with a specimen of known creep properties in place before the exact deformation of the specimen may be determined. Since each test is found to require a year to produce definite determinations, this calibration has not yet been made. Nevertheless, from the over-all deformation one may obtain a minimum figure for the viscosity.

Because of the extreme sensitivity of the apparatus, it is necessary to take some precautions. The temperature must be kept constant within one-tenth of a degree in order that the readings be strictly comparable, since the thermal expansion due to even so small a temperature change can be detected.

The weight **W** is at the end of the lever arm and tends to make the tester act as a seismograph. It was found that construction work in the neighborhood caused the dial gauge to move. Any such deflection was a temporary departure from the creep curve, however, and with the passage of a few weeks the results again returned to the norm.

Presumably, with limestone, humidity may affect the length of the specimen. For this reason a calcium chloride drier was kept in the room.

CREEP OF SOLENHOFEN LIMESTONE OVER A YEAR'S PERIOD

A specimen of Solenhofen limestone has been in the sensitive creep-tester for a year and a half under a pressure of 1,400 kg/cm² (normal strength, 2,560 kg/cm²). During this time it has shown continuous flow at a decreasing rate, as shown in Figure 4. There is no systematic deviation from the straight line drawn through these points. The equation of this straight line is

$$S = (6.10 + 5.20 \log_{10} t)10^{-5}, \qquad (6)$$

where S is the shortening per unit length and t the time in days.

Because of the imperfect knowledge of the mechanism of this creep, one cannot extrapolate this relation with any degree of assurance. Such a direct extrapolation would predict a deformation of only one-twentieth of one per cent in a million years!

No pseudoviscous flow is observed in this creep, and consequently it is impossible to calculate an equivalent viscosity directly. If we assume, however, that equation (1) applies to this creep, as is suggested by the fact that it applies to almost all other substances investigated, then we may conclude that a pseudoviscous flow may be present but is so small that the sensitivity of the measurements does not distinguish it. On this assumption we may calculate a minimum equivalent viscosity for the limestone under these condi-

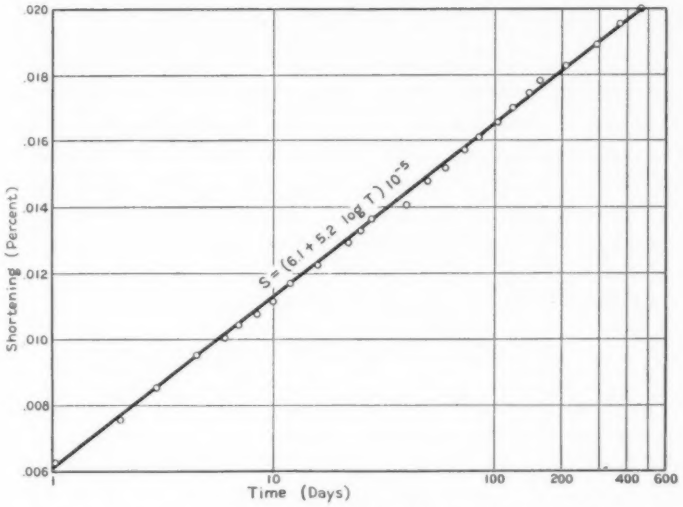

FIG. 4.—Creep of Solenhofen limestone under load of 1,400 kg/cm² at 23° C. (Overall deformation.)

tions. As a basis for this calculation the maximum spread of the observations toward the end of the 550-day period is taken as a measure of the possible deviation from the simple logarithmic curve. This spread is of the order of 0.0001 per cent. Assuming the Ct term to have this magnitude at the end of 550 days, we calculate the minimum equivalent viscosity as about 2.2×10^{22} poises, compared to Haskell's figure of 0.78×10^{22} for the equivalent viscosity of the substratum. To illustrate graphically what these figures mean as to rate of deformation, the limestone block loaded to one-half of its

breaking-strength for 10,000 years would shorten only 1 per cent if this is a valid expression of its deformation.

Taking into consideration the fact that this is a minimum figure for viscosity and that much of the observed spread is probably due to temperature variations and external disturbances, it would appear probable that the equivalent viscosity of the limestone at room temperature is many times as great as that which Haskell calculates for the substratum.

CREEP IN VAN ORSTRAND'S STEEL TAPE

In 1923 Van Orstrand published the results of an experiment on creep in steel.[6] A steel tape was loaded in tension to 970 kg/cm² (about one-twentieth of its breaking-load), and its length was measured accurately over a period of 126 days. Van Orstrand considered that during the last 25 days of the run the strain approximated viscous flow and based his calculations on that hypothesis. It seems, however, that his data may be more closely approximated by a relation of the type discussed above. Figure 5 shows his published data replotted on semilogarithmic co-ordinates. The curve

$$S = (926.0 + 2.47 \log t + 0.0105\, t) \times 10^{-6} \qquad (7)$$

fits his data very closely, as shown in the figure. The last term gives a direct measure of the viscosity, which is calculated as 2.73×10^{21}—nearly twice the viscosity as he calculated it. The perfect fit of this curve to his data gives additional evidence that a relation of this sort may best describe the phenomena of creep. The equation for the elastic flow in this case is

$$S = (926.0 + 2.47 \log t)10^{-6}\,. \qquad (8)$$

It is interesting to note that the limestone, subject to an even greater load than the steel of his experiment, showed an equivalent viscosity many times greater than that of the steel. Curiously enough, the total deformation of the limestone was much greater than the steel, but this was all elastic flow, and in the course of a few

[6] C. E. Van Orstrand, "Notes on Isostasy," *Bull. Geol. Soc. Amer.*, Vol. XXXIV (1923), pp. 300–305.

years the steel would flow much more than the limestone, if the equations give a true picture of the flow.

Van Orstrand also measured the return when the load was removed from the steel tape. His published data for this return are

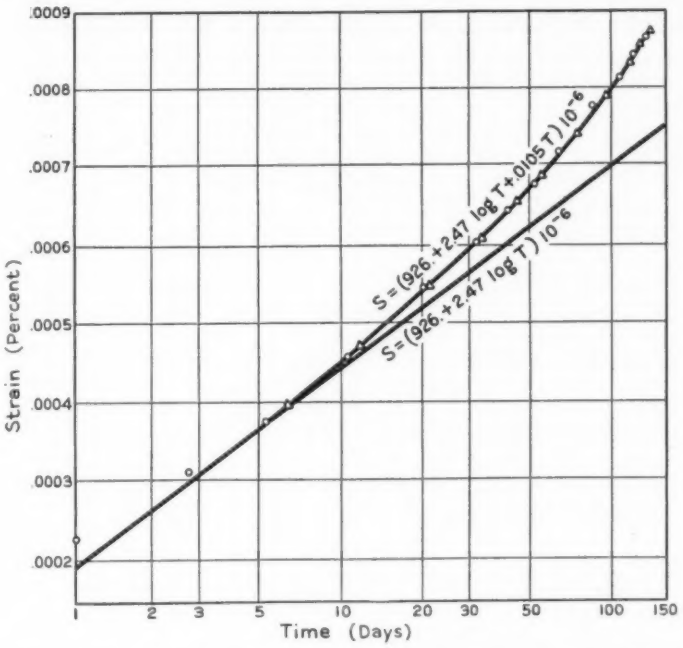

FIG. 5.—Van Orstrand's data on creep of steel (circles) plotted on semi-log paper compared with an equation for *elastic flow* (straight line) and an equation of the form of Equation (1) (triangles and curved line). Steel tape loaded to 970 kg/cm² at 27.1° C.

plotted in Figure 6. This shows the common characteristic of all *Nachwirkung*, namely, flow at a logarithmically decreasing rate. It is interesting to compare the deformation during this return with the supposed elastic flow when the differential stress was acting. In both cases the relation near the origin (time = 0) is not easily dealt

with—it takes some time for the flow to attain the simple logarithmic form of equation (2). It is possible, however, to compare the two types of flow over a given period after the flow assumes the character of this equation. During the interval between 10 days and 100 days the amount of return was 2.51×10^{-6} (fractional part of the original length). During the same interval, when the load was applied, the

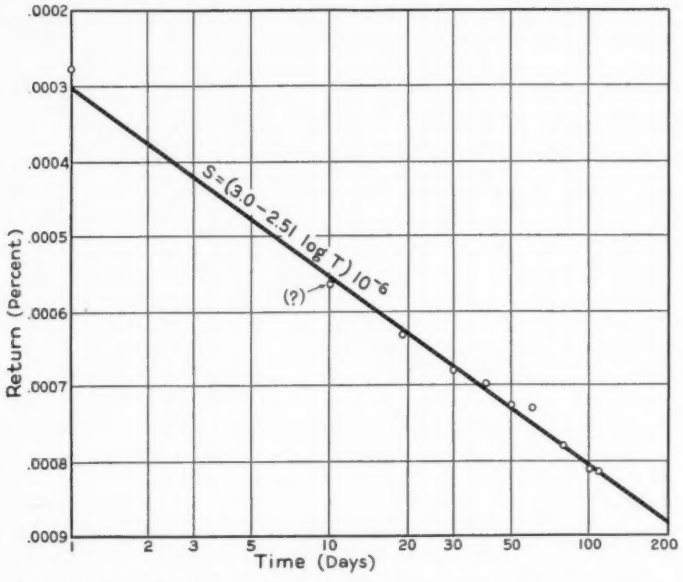

FIG. 6.—Return elastic flow of Van Orstrand's steel tape when load was removed

deformation due to the elastic flow described by equation (8) was 2.47×10^{-6}. This agreement (within the limits of accuracy of the curve-fit in Fig. 6) indicates that the after-working return is due to the same mechanism as the elastic flow on loading.

CREEP OF MISCELLANEOUS SUBSTANCES

BORIC ANHYDRIDE GLASS

It is interesting to compare the behavior of a glass with that of the crystalline solids already investigated. Drs. Francis Birch and E. B. Dane, Jr., gave the writer a cylindrical specimen of boric anhydride

glass 1.55 cm. in diameter and 2.5 cm. long. This cylinder was surrounded by a furnace and mounted in the small creep-tester. At temperatures of from 160° to 260° C. its viscosity was well suited to the sensitivity of this apparatus.

The glass was found to follow the same laws of flow as the steel and limestone. When the load was first applied, deformation oc-

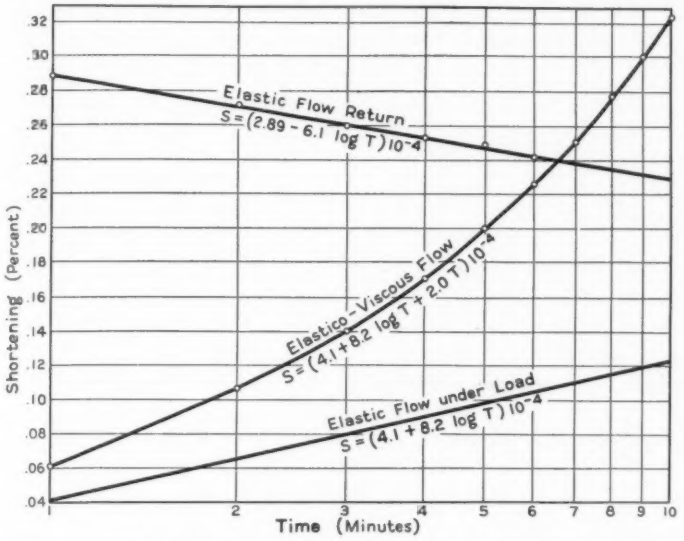

FIG. 7.—Creep of boric anhydride glass under load of 95 kg/cm² at 243° C. (middle curve). Hypothetical elastic flow under load (lower curve). Elastic flow on release of load (upper curve). Plotted to show logarithmic decrease of elastic flow.

curred at a decreasing rate, gradually approaching the constant rate corresponding to viscous flow. Plotting the data on semilog paper showed that the deformation obeyed the equation (see Fig. 7).

$$S = (4.1 + 8.2 \log t + 2.0\, t) \times 10^{-4}. \qquad (9)$$

On release of load, return flow occurred, following the logarithmic relation shown in Figure 7. This return elastic flow does not agree with the elastic flow under load, probably for two reasons: (1) the load was not reduced to zero, for the weight of the lever was still on the specimen; and (2) the amount of the viscous flow was so great

(total flow = 0.56 per cent) that it might be expected to change the structural inhomogeneities of the whole. When these experiments were performed, the importance of elastic flow was not realized, and consequently the measurements are not well suited to demonstrate this phenomenon on return. Experiments in the future will be carried out with this in mind and should furnish a good experimental check on the theory.

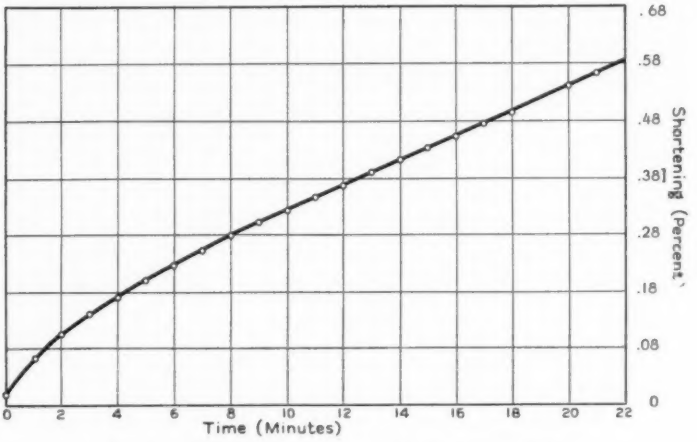

FIG. 8.—Same data as Fig. 7, plotted with normal abscissa

When the equivalent viscosity is as low as in this experiment (4.3×10^{12}), the Ct term of the equation soon becomes much greater than the logarithmic term, and the deformation assumes the nature of pseudoviscous flow. This is shown to the best advantage when the data are plotted on regular cross-section paper, as in Figure 8. In general, the higher the temperature or the lower the viscosity, the more closely does the deformation approach "viscous flow."

Parks and Spaght[7] investigated the viscosity of this glass at temperatures ranging from 267° to 443° C. From qualitative measurements at lower temperatures they predicted a transition in properties

[7] G. S. Parks and M. E. Spaght, "Some Viscosity Data for B_2O_3," *Physics*, Vol. VI (1935), pp. 69–71.

at about 240° C. They found the glass perfectly viscous at 356° C. The writer's experiments definitely indicate this transition in properties but seem to point toward a gradual transition, rather than a sharp one, as the temperature is lowered. Thus, elastic flow becomes more and more important as the temperature is lowered below 260° C., but the present measurements indicate that even at this temperature the flow is not purely viscous.

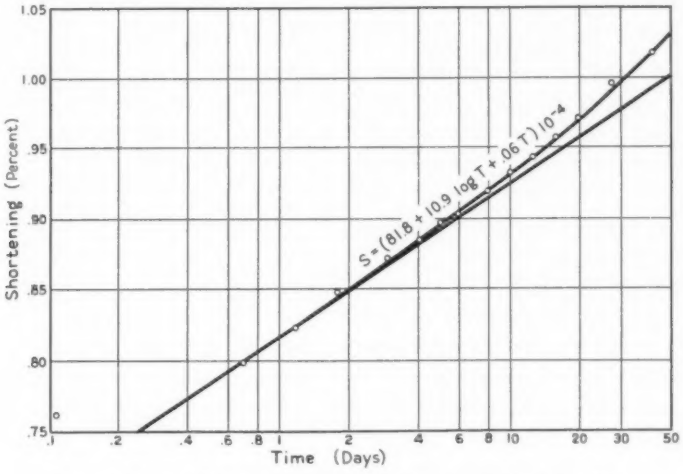

FIG. 9.—Creep of halite single crystal loaded to 61.0 kg/cm² at 23° C.

It is interesting to speculate on Parks and Spaght's empirical conclusion that transitions in general occur in glasses when their viscosity rises above 10^{13} or 10^{14}. One might suggest that a glass in the earth's crust or substratum would not be viscous but would behave as an elasticoviscous material.

HALITE SINGLE CRYSTAL

A square prism, cleaved from a single crystal of halite and measuring 1.1 × 1.1 × 2.05 cm., was mounted in the small creep-tester, loaded to 61 kg/cm²; and its creep at room temperature observed for 42 days. As shown in Figure 9, this creep also obeys equation (1) and seems to show a pseudoviscous flow superimposed on the elastic

flow. The equivalent viscosity is $2.6 \times 10.^{17}$ The elastic flow was not measured after release of load.

The mechanism of flow could not be shown definitely, but there were diagonal lines through the crystal which coincided with the 110 planes, and it is possible that plastic flow occurred by translation on the 110 plane, as is commonly observed in halite at high temperature. When the load was increased, these lines became more prominent; but, also, tensile cracks developed parallel to the direction of compression, so that the test was considered worthless.

CALCITE SINGLE CRYSTAL

A cylinder of calcite cut parallel to the *c*-axis was mounted in the apparatus, loaded to 125.8 kg/cm², and observed for 22 days. The amount of creep was so small that no certain measurements could be made. The stress was increased to 164.7 kg/cm², but again the creep was too small to observe accurately. Since this was near the breaking-point and since the writer wished to use the specimen in a high-pressure investigation, no more measurements were attempted.

One can speculate on the fact that there was no measurable creep in this calcite crystal, although it is easy to deform calcite crystals by mechanical twinning. The specimen was compressed parallel to the *c*-axis, and in this direction the shear stresses on the twin planes are in the wrong sense to produce twinning. It is probable that calcite compressed in this direction is highly brittle and shows no creep; but, if it were compressed in such a way that the shear stresses could produce twinning, creep might ensue.

CREEP OF TALC

A cylinder of pure talc schist was tested for creep at 23°, at 200°, and at 300° C. In all cases the deformation was entirely elastic flow, and the measurements did not suggest any viscous yield. The measurements were accurate enough to exclude the possibility of any yield with an equivalent viscosity of less than 10^{16}—the limit of resolution of the small creep-tester for the loads which could be applied to the talc.

CREEP OF SHALE

At the suggestion of Mr. Irving Crosby, creep tests on shale have been begun, and the first run has yielded unexpected results. A

uniform mudstone (the Conchas shale of New Mexico) was subject to a compressive force of 10.4 kg/cm² for a period of 144 days, and the resultant creep is shown in Figure 10. The anomalous behavior of this specimen is not understood. Mr. Crosby and the writer do not

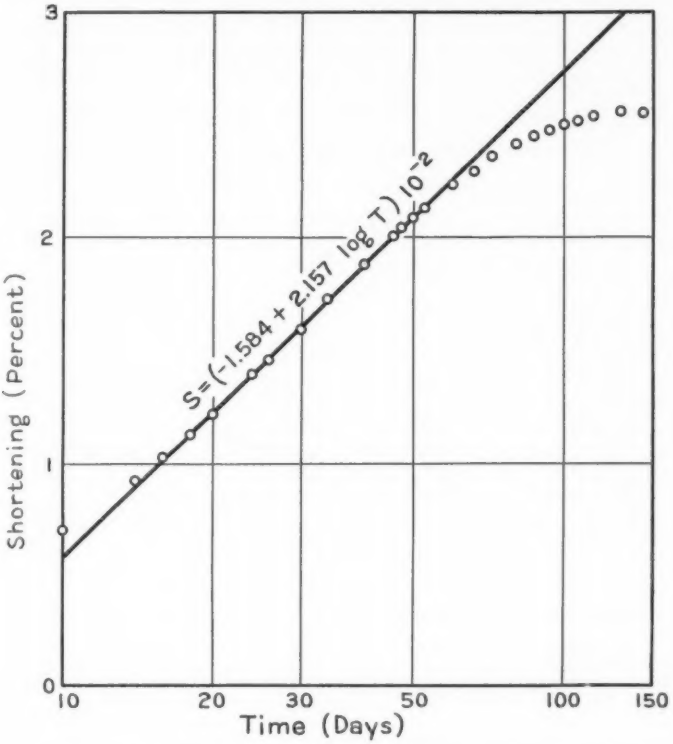

FIG. 10.—Creep of Conchas shale loaded to 10.4 kg/cm² at room temperature

feel that it may be accepted definitely as a true picture of the creep of shale, because of the difficulty in obtaining shale free from fractures and the uncertainty as to whether the water content of this specimen was maintained exactly constant by the paraffin jacket. If this curve be accepted merely for speculative purposes, it predicts a decreasing flow which ceases entirely in less than half a year. Thus, in engineer-

ing application, the shale might be expected to show a fairly rapid flow up to about 2½ per cent, when flow would cease altogether. We are not satisfied with the control on this experiment, however, and are planning to continue the work with different specimens and more accurate moisture control.

CREEP TESTS AT HIGH CONFINING PRESSURES

In 1936 the writer published the results of a few creep tests on Solenhofen limestone under 10,000 atmospheres confining pressure

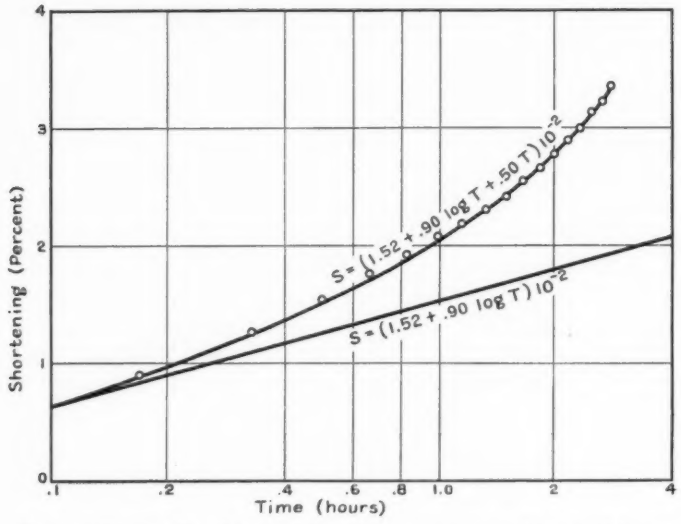

FIG. 11.—Creep of Solenhofen limestone under 10,000 atmospheres confining pressure, subject to 5,500 kg/cm² differential pressure, at room temperature.

and at high values of differential stress.[8] It was found that at high pressures the limestone exhibits properties of flow very different from that at atmospheric pressure, and, similarly, the creep at constant stress is very much more accentuated than at atmospheric confining pressure.

Figure 11 shows that the results of this high-pressure creep investigation may be treated in the same manner as the creep tests

[8] D. T. Griggs, "Deformation of Rocks under High Confining Pressures," *Jour. Geol.*, Vol. XLIV (1936), pp. 561–63.

already described. The curve is again found to be a composite of elastic flow and pseudoviscous flow in the relation of equation (1). Consequently, we can calculate the equivalent viscosity as before and find it to be 1.29×10^{15} for a differential stress of 5,500 kg/cm² and 2.17×10^{14} for a differential stress of 6,760 kg/cm². This dependence of equivalent viscosity on stress is an example of the difference between the observed solid flow of rocks and the flow of a true liquid.

Microscopic study of some artificially deformed calcite aggregates has indicated that the bulk of the deformation has been occasioned by twinning of the calcite grains. It is not known whether this same mechanism is dominant in the creep of rocks under long-continued loads, nor is the relation between equivalent viscosity and magnitude of shear stress known. It is hoped that further experimentation on creep at high confining pressure will furnish information regarding the variation of "viscosity" with stress and that microscopic study of the deformed specimens will enable us to determine what the mechanism of this slow flow is. This particular branch of the creep investigation is regarded as most significant for the understanding of rock flow in orogenic deformations.

OTHER EQUATIONS OF CREEP

The literature of physics and engineering contains many descriptions of experiments on creep of materials (mainly metals), and one may find many different empirical equations derived in an attempt to explain the results. Outstanding among these are Andrade's and Michelson's. Andrade,[9] experimenting with lead and copper deformed at a constant tensile stress above the elastic limit, derived the equation

$$S = (1 + \beta t^{1/3})e^{kt}, \tag{10}$$

where β and k are arbitrary constants; this formula fits his data closely. Michelson,[10] working with many different types of substances deformed in torsion, derived the equation

$$S = A + B(1 - e^{\alpha t^{1/2}}) + Ct^{\beta}, \tag{11}$$

[9] E. N. da C. Andrade, "Viscous Flow in Metals," *Proc. Roy. Soc.*, Vol. A-LXXXIV (1910), pp. 1–12.

[10] A. A. Michelson, "Elastico Viscous Flow," Part I, *Jour. Geol.*, Vol. XXV (1917), pp. 405–10; Part II, *ibid.*, Vol. XXVIII (1920), pp. 18–24.

where A, B, C, α and β are arbitrary constants, and found the average value of β for fifteen substances to be 0.35.

These experiments dealt with relatively short-time tests and high stresses. Recently, engineers interested in failure of metals under low stresses applied for long periods have obtained a large mass of data dealing with long-time tests. In 1936 Weaver[11] suggested that an equation of exactly the same form as equation (1) describes the results of long-time tests on steel at high temperatures better than the older equations.

The writer quite independently derived equation (1) as an expression of the data presented in this paper. It is interesting, therefore, to note Weaver's suggestions that engineers may formulate their results on creep of metals at high temperature in a similar manner.

MECHANISM OF CREEP

Elastic flow is probably due to rearrangement of those atoms around structural inhomogeneities which move to new positions of equilibrium when the external stress field is changed. Various pictures of these movements have been presented, and, in the case of some metals, experimental evidence has been adduced which indicates this rearrangement is confined to the intercrystalline boundaries.[12] Considerable evidence has been obtained by metallurgists that the atoms along an intercrystalline border are in an amorphous or cryptocrystalline state. The writer suggests that elastic flow occurs as the atoms in this intergranular film slowly assume their new positions of equilibrium in response to the external stress, and that, when this stress is removed, the deformation is reversed as the atoms return to their old positions of equilibrium, except as the relations of the grains have been changed by concomitant pseudoviscous flow.

Pseudoviscous flow has been explained as due to a process of solid diffusion in response to the shear stress by Kanter,[13] who has shown

[11] S. H. Weaver, "Creep Curve of Steel," *Trans. Amer. Soc. Mech. Eng.*, Vol. LVIII (1936), pp. 745–51.

[12] R. Becker, "Über die Plastizität amorpher und krystalliner fester Körper," *Physik Zeitschr.*, Vol. XXVI (1925), p. 919; "Elastische Nachwirkung und Plastizität," *Zeitschr. f. Physik*, Vol. XXXIII (1925), pp. 185–213; "Über den Gleitwiderstand von Metallkristallen," *ibid.*, pp. 413–28.

[13] J. J. Kanter, "Temperature Coefficient of Creep Rate" (New York: Amer. Inst. Min. Met. Eng., 1937), pp. 1–24 (mimeographed).

that the creep-rate of steel depends on stress and temperature in the manner that would be expected if creep were due to solid diffusion. Moore, Betty, and Dollins[14] present evidence that creep in lead is largely due to intergranular motion, whereas rapid deformation of lead occurs largely by intracrystalline slip.

The possibility that creep occurs by an entirely different mechanism from the more rapid plastic flow of short-time tests is of great significance in the interpretation and application of laboratory results on rock deformation for geologic purposes. This intergranular motion would probably tend to produce a much more pronounced preferred orientation of the constituent crystal grains in a rock deformed slowly than in a rock deformed to the same degree by rapid flow under higher shear stress. The evaluation of the influence of this effect should be of great importance to the laboratory investigations undertaken to determine the effect of deformation on the rock fabric.

It is evident that this hypothesis of solid diffusion in the intergranular film does not apply to the pseudoviscous flow in glass and the single crystal of halite. In the case of the single crystal of halite the same mechanism of solid diffusion may be operative at the boundaries of the intracrystalline structural inhomogeneities which are known to exist; and solid diffusion may occur throughout the amorphous glass.

CREEP BY RECRYSTALLIZATION

All the experiments described above deal with creep of dry specimens, with the exception of the shale. Since deforming rocks are frequently, if not always, filled with interstitial solutions, it seemed highly important to attempt to produce flow by solution and recrystallization in the laboratory and to determine the physical and chemical laws governing this flow. Geologists have recognized the possible importance of this type of flow ever since Riecke's principle was set forth,[15] but to the author's knowledge no experiments have been performed in which deformation of this type was observed in rock-forming minerals.

[14] H. F. Moore, B. B. Betty, and C. W. Dollins, "Creep and Fracture of Lead," *Univ. Ill. Eng. Sta. Bull. 272*, Vol. XXXII (1935).

[15] E. Riecke, "Über das Gleichgewicht zwischen einem festen, homogen, deformirten Körper und einer flüssigen Phase, insbesondere über die Depression des Schmelzpunkt durch einseitige Spannung," *Ann. Physik*, Vol. LIV (1895), pp. 731–38.

As this paper goes to press, a series of experiments has been started which seem to indicate flow of this sort. The method of experimentation is to observe the creep properties of a specimen under a given load when dry, and then, keeping the load constant, to observe the effect of surrounding the specimen by solutions.

The results of the first experiment are shown in Figure 12. A specimen of alabaster was mounted in the small creep-tester and its

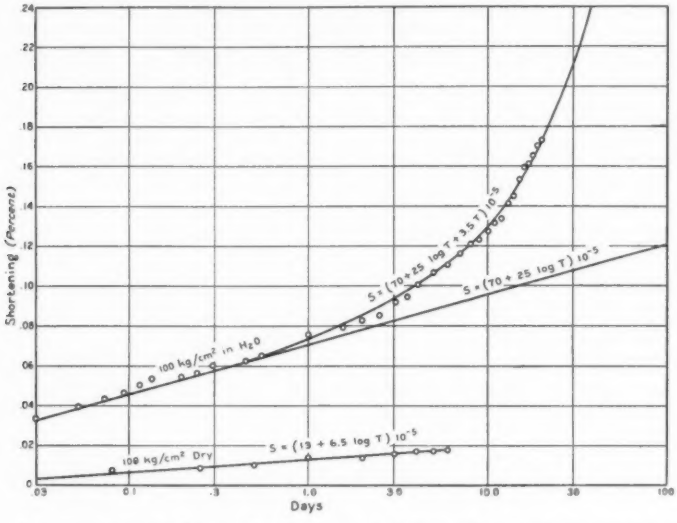

FIG. 12.—Creep of alabaster loaded to 100 kg/cm² at 23° C. Both curves for same specimen: dry, and in distilled water.

creep observed for 6 days under a compressive stress of 100 kg/cm² (just below its elastic limit, as ordinarily defined). The observed deformation followed the law of elastic flow but was of such a small magnitude that it was close to the limit of sensitivity of the apparatus. This creep of the dry specimen is shown at the bottom of Figure 12. A similar experiment on another piece of alabaster has shown that the creep follows this logarithmic curve for 20 days at least—the duration of the wet test. At the end of the 6-day dry creep of the first specimen it was surrounded by a small jacket of distilled water, while the load was maintained constant. The creep-

rate immediately increased very greatly, and the nature of the deformation is shown in the upper curve of Figure 12.

Although this curve is of the same type as that previously suggested for elasticoviscous flow, the conditions of the experiment imply a different interpretation here. The flow at decreasing rate (the logarithmic term of the equation) is thought to be the sum of three types of flow: (1) ordinary elastic flow, probably of very small magnitude; (2) flow due to solution of the gypsum until the distilled water is saturated; and (3) flow due to more rapid solution at the points of local stress concentration, until the stress becomes homogeneous throughout the cross section of the specimen. That this was not the normal type of reversible elastic flow was proved by the fact that the specimen did not show a significant return flow when the load was removed.

The pseudoviscous flow is interpreted as due to recrystallization under stress according to Riecke's principle. This predicts that solution will take place at the surfaces of maximum stress and recrystallization at the surfaces of no stress. Thus, the specimen will tend to shorten in the direction of compression, and deposition may be expected either on the unstressed sides of the specimen or on the walls of the jacket.

This recrystallization hypothesis is only one of many that may be applied to the data at present. There is a possibility that the plastic properties of the crystals are so changed as to produce more rapid deformation. The correct interpretation can only be assured by more creep data, supplemented by microscopic examination.

The importance of flow of this type may be inferred from the equivalent viscosities calculated for the dry flow and the wet flow. The first is greater than 2×10^{18}, and the latter is 8×10^{16}. This means that under the constant load of 100 kg/cm^2 the wet alabaster would flow continuously more than twenty-five times as fast as when it was dry.

Gypsum was selected for this experiment as being one common mineral which promised measurable recrystallization in the times available in the laboratory and at room temperature and low pressure. If it illustrates one mechanism of rock deformation in the earth, then it is very important to determine the nature of this creep

more fully. For this reason a series of long-time tests have been initiated which are designed to determine the relation between the applied stress and the rate of flow by recrystallization. It is hoped that from this relation a satisfactory physicochemical theory may be derived to guide speculation about the nature of recrystallization flow under other conditions and with other materials.

A similar experiment on marble immersed in boiling water failed to show measurable creep—presumably because of its low solubility.

CONCLUSION

These tests have demonstrated that rocks loaded well below their normal breaking-strength may be observed to creep in the laboratory. An empirical equation has been derived which very accurately fits the data on this elasticoviscous flow. This independently derived equation differs markedly from the earlier equation of Michelson but is identical with that which engineers have come to use in recent years to describe the creep of metals.

The equation analyzes creep as composite: (1) pseudoviscous flow and (2) elastic flow. The rate of elastic flow decreases inversely in proportion to the time the stress is applied and hence is of small importance in geologic applications over long periods. The pseudoviscous flow, on the other hand, is constant under a constant stress difference. Hence, if we assume that this equation gives an accurate description of the behavior of rock, we may calculate an equivalent viscosity which may be useful in speculation about the forces causing rock deformation in geology.

Before this equivalent viscosity is really useful to the geologist, however, its dependence on magnitude of shear stress and temperature must be determined. Experimental information on these dependencies is not yet available, although from studies on solid diffusion physicists have suggested the nature of these relations.

Now that the role of pseudoviscous flow has been inferred and methods have been devised to measure the equivalent viscosity, it should not be difficult to measure these relations of stress and temperature at atmospheric pressure and perhaps to determine also the effect of a superimposed confining pressure. With the aid of a grant from the Penrose Fund of the Geological Society of America, ap-

paratus permitting such measurements is being constructed by the writer.

The equation of elasticoviscous flow is found to apply not only to crystalline aggregates in the form of limestone and steel but also to a glass and to a single crystal of halite.

The fact that limestone is observed to have an equivalent viscosity at atmospheric pressure and room temperature greater than the equivalent viscosity calculated for the flow at depth which produces isostatic compensation is in accord with the geologic evidence that the earth's crust is "strong" and will not flow in response to small stresses even when applied over long periods. The much lower equivalent viscosity of limestone under a confining pressure equal to that at a depth of 22 miles and at high differential stresses may show something about the mechanism of rock deformation in the mountain-building deformations. This change in the manner of flow with pressure may even make one speculate whether the same materials which are so exceedingly "viscous" at the surface may not possess a smaller "viscosity" at depth. As yet, measurements of sufficient sensitivity have not been made to ascertain the equivalent viscosity for small differential stresses acting under high confining pressure.

Preliminary results of a series of experiments designed to produce flow by recrystallization indicate that this type of flow is highly important in the deformation of gypsum and may give an indication of the importance of recrystallization as a factor in rock deformation in general.

ACKNOWLEDGMENTS.—The writer wishes to acknowledge gratefully the joint grant from the Committee on Geophysics and the Society of Fellows which made this experimental investigation possible. Thanks are due also to Professor Theodore Lyman, director of the Jefferson Physical Laboratory, for the continuous use of a constant-temperature room. Dr. Robert W. Vose aided materially in designing the apparatus. Drs. Francis Birch, T. S. Lovering, and W. W. Rubey improved the manuscript. Professor P. W. Bridgman's advice and criticism have been invaluable at every step in the work.

PROPERTIES OF SATURATED AQUEOUS SOLUTIONS OF POTASSIUM CHLORIDE AT TEMPERATURES ABOVE 250° C.[1]

MANSON BENEDICT
Jersey City, New Jersey

ABSTRACT

Equilibrium pressures of the three-phase system—steam, solid KCl, and saturated aqueous solution—have been determined between 250° and 600° C. A maximum pressure of 225 atm. is found at 565° C. This maximum is evidence that critical phenomena do not occur in aqueous solutions saturated with solid KCl. The specific volume of solid KCl and the apparent volume of water in the saturated solution were also determined. From the measured volumes and certain assumptions about other properties of the system, the specific volume of the liquid phase and the volume change and latent heat in the reaction: Steam + Solid KCl → Saturated liquid solution, were evaluated.

INTRODUCTION

Detailed knowledge of the physicochemical properties of hydrothermal systems is indispensable for the solution of many problems relating to the synthesis and decomposition of minerals. As Bowen's study of the phase diagrams of silicate melts has been of great help to the geologist in explaining the genesis of the igneous rocks, so a study of the phase equilibria of hydrothermal solutions should clarify the mechanism of ore deposition from them.

This report summarizes the first of a series of investigations in this laboratory on the properties of simple aqueous solutions in equilibrium with a vapor phase at temperatures between 250° and 600° C. The principal objects of this program are: (1) development of experimental methods for studying hydrothermal solutions and (2) accumulation of data on simple representative systems to provide a basis for generalization to the complex systems of geologic interest. This first report is concerned with properties of the three-phase system—solid KCl, steam, and saturated aqueous solution.

Two properties of saturated solutions of KCl were directly measured. These were: (1) the three-phase vapor pressure and (2) the apparent volume of water in the saturated solution. Property (1) is

[1] *Paper No. 49* published under the auspices of the Committee on Geophysical Research and the Division of Geological Sciences at Harvard University.

the pressure at which the three phases—solid KCl, steam, and saturated aqueous solution—can coexist; (2) is the difference between the volume of a saturated solution containing 1 gram of water and the volume of that quantity of solid salt present in the solution.

The specific volume of solid KCl was also determined at elevated temperatures. The solubility of KCl in water has been determined semi-quantitatively by Benrath.[2] From the specific volume of solid KCl, its solubility in water, and the apparent volume of water in the saturated solution, it was possible to estimate the specific volume of the saturated solution.

From the assumption that the vapor phase contained no KCl, the known properties of steam,[3] and the apparent volume of water in the saturated solution, the volume change in the reaction

$$\text{Steam} + \text{Solid KCl} \rightarrow \text{Saturated solution}$$

was calculated. From this volume change and the observed three-phase vapor pressures, the latent heat of the foregoing reaction was evaluated by means of the exact Clapeyron equation.

HISTORICAL

Morey and Ingerson[4] have given an extensive bibliography of previous work on hydrothermal solutions, so that only articles closely related to the present problem will be discussed. Reference may be made to their article for a detailed description of possible types of phase diagrams encountered in systems composed of a nonvolatile solid, such as KCl, and a volatile solvent near its critical temperature, such as water. Here it is sufficient to state that two possible cases are encountered. In case 1 the three phases—solid salt, saturated liquid solution, and saturated gaseous solution—can be in equilibrium at every temperature between the eutectic temperature and the melting-point of the salt; no critical phenomena are found in

[2] A. Benrath, F. Gjedebo, B. Schiffers, and H. Wunderlich, "Solubility of Salts and Salt Mixtures in Water at Temperatures above 100°," *Zeit. anorg. allgem. Chem.*, Vol. CCXXXI (1937), pp. 285–97.

[3] J. H. Keenan and F. G. Keyes, *Thermodynamic Properties of Steam* (New York: John Wiley & Sons, 1936).

[4] G. W. Morey and Earl Ingerson, "The Pneumatolytic and Hydrothermal Alteration and Synthesis of Silicates," *Econ. Geol.*, Vol. XXXII (1937), pp. 607–760.

saturated solutions. In case 2, saturated liquid and saturated gaseous solutions merge at two critical points; between the two critical temperatures only one saturated fluid phase and the solid may coexist. Case 2 is typical of systems containing solids relatively insoluble in water near its critical temperature, such as SiO_2, Na_2CO_3, and Na_2SO_4. Case 1 is typical of solids whose solubility in water is relatively high and increases with increasing temperature, such as K_2SiO_3 and KCl.

Experimental work on the phase diagrams of hydrothermal systems has been concerned with two different types of solutions. The first type consists principally of molten silicates and contains relatively little water. The system K_2SiO_3–H_2O was studied by Morey,[5] and the systems granite–H_2O, albite–H_2O, and orthoclase–H_2O have been studied by Goranson.[6] The method used is the rapid quenching of the system and subsequent analysis of the glassy supercooled solution. The method is limited to viscous solutions, containing relatively little water, which may be cooled without change in composition. In the second type of system the liquid phase consists of a relatively dilute aqueous solution of inorganic salts.

Benrath and collaborators[7] have determined the solubility of KCl and many other salts in water up to 450° C. They employed a synthetic method in which weighed amounts of salt and water were sealed in a glass tube and heated to the temperature at which salt just disappeared. Their method may be in error by as much as 3 per cent, owing to transfer of an indeterminate amount of water to the vapor phase. Nevertheless, their results for KCl are in substantial agreement, up to 300° C., with those of Akhumov and Vasiliev,[8] who employed a more reliable analytic method.

[5] G. W. Morey, "Ternary System: Water-Potassium Silicate-Silica," *Jour. Amer. Chem. Soc.*, Vol. XXXIX (1917), pp. 1173–1229.

[6] R. W. Goranson, "The Solubility of Water in Granite Magmas," *Amer. Jour. Sci.*, Vol. XXII (1931), pp. 481–502; "Some Notes on the Melting of Granite," *ibid.*, Vol. XXIII (1932), pp. 227–36; "Silicate-Water Systems: The Solubility of Water in Albite-Melt," *Trans. Amer. Geophys. Union*, Vol. XVII (1936), p. 257.

[7] *Op. cit.*

[8] E. I. Akhumov and B. B. Vasiliev, "The Technological Calculations for the Equilibrium of the Chlorides of Potassium, Sodium, and Magnesium in Water at High Temperatures," *Jour. Chem. Ind.* (Moscow), Vol. VIII, No. 17 (1931), pp. 17–23.

Above the critical temperature of pure water there have been no determinations of the vapor pressures of aqueous solutions of this second type and no measurements on the specific volumes of aqueous solutions of any kind.

PRINCIPLE OF THE EXPERIMENTAL METHOD

A schematic diagram of the apparatus is shown in Figure 1. Weighed amounts of salt and water are confined over mercury in a stainless steel bomb. The temperature of the bomb is maintained

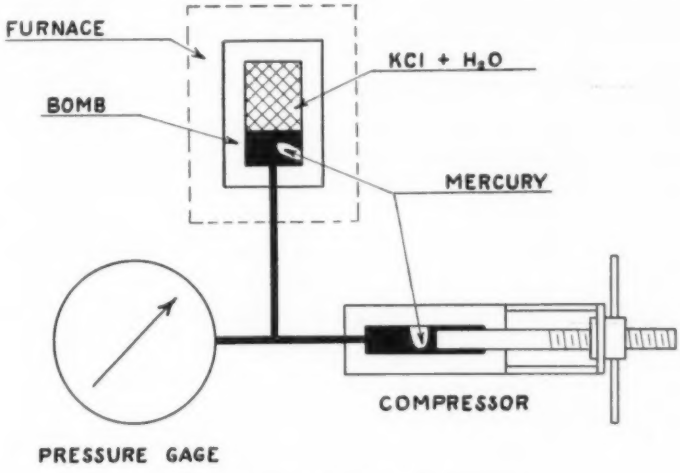

FIG. 1.—Schematic diagram of the apparatus

constant by a thermostated copper block, which surrounds it. The volume of mercury in the bomb is controlled and measured by the screw compressor; the volume occupied by salt, solution, and steam is the difference between the internal volume of the bomb and the volume of mercury in the bomb. Pressure is measured by means of a dead-weight piston gauge.

The result of varying the amount of mercury in the bomb at constant temperature is illustrated by the pressure-volume diagram (Fig. 2). The solid line is the curve which would be observed in an idealized experiment if mercury had no vapor pressure and if it were

possible to free the contents of the bomb completely from air. At the point *A* the volume in the bomb occupied by KCl and H_2O is so great

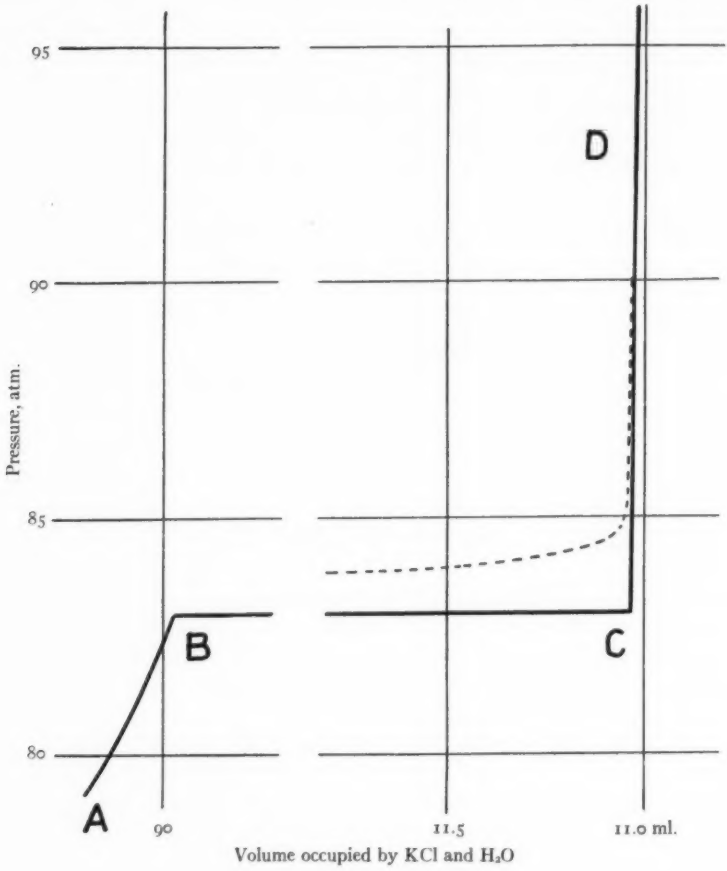

FIG. 2.—Pressure-volume diagram

that only two phases—saturated gaseous solution and solid (besides liquid mercury)—are present. As the volume of salt and H_2O is reduced by injection of mercury, the pressure rises until the dew point

B is reached, and saturated liquid solution appears. Three phases—solid, saturated gaseous solution, and saturated liquid solution—are now present, and the two-component system KCl–H_2O is univariant. As the volume is further reduced, the pressure remains constant along the line *BC*, and more and more of the gaseous solution condenses. Finally, one of two things can happen. If the quantity of salt in the bomb is in excess of that required to form a saturated liquid solution with the H_2O present, the pressure remains constant until all gaseous solution has been condensed, as at the boiling-point *C*. However, if less salt were present, the solid phase might disappear before all the gaseous had condensed, and another break in the curve would be found. This second case is not illustrated in Figure 2 and did not occur in any of the experiments to be described in this article because a large excess of salt was present at all times. As still more mercury is injected, the pressure rises rapidly (along the line *CD*) because the system is again bivariant, and the two phases present—solid salt and saturated liquid solution—are relatively incompressible. The pressure represented by the horizontal line *BC* is the three-phase vapor pressure of the system. The combined volume of solid salt and saturated liquid solution may be calculated from the volume of mercury present in the bomb at the point *C*.

DETAILED DESCRIPTION OF THE APPARATUS

The apparatus is very similar to that used by Keyes and Beattie[9] in their investigations of the *P-V-T* properties of pure fluids. It is illustrated in Figure 3 and shown in the photograph, Figure 4.

Piston gauge.—The dead-weight piston gauge used to measure pressure is illustrated at *G*. The piston diameter is approximately $\frac{1}{4}$ inch. Bridgman's design[10] is followed, in that the outside of the cylinder is exposed to pressure so that leak at high pressures is reduced. The gauge was calibrated by comparison with Massachusetts

[9] F. G. Keyes, "Methods and Procedures Used in the Massachusetts Institute of Technology Program of Investigation of the Pressures and Volumes of Water to 460° C.," *Proc. Amer. Acad. Arts Sci.*, Vol. LXVIII (1933), pp. 505–64; J. A. Beattie, "The Apparatus and Method Used for the Measurement of the Compressibility of Several Gases in the Range 0° to 325° C.," *ibid.*, Vol. LXIX (1934), pp. 389–405.

[10] P. W. Bridgman, "The Measurement of High Hydrostatic Pressure. I. A Simple Primary Gauge," *Proc. Amer. Acad. Arts Sci.*, Vol. LXIV (1909), pp. 201–17.

Institute of Technology type piston gauge, kindly lent us by Professors Keyes and Beattie of that institution. The factor for our gauge, 3.0509 atm/kg of brass in air, showed an average deviation of only 0.01 per cent up to 460 atm. in this comparison. The constant of the M.I.T. gauge had been determined by standardization against the vapor pressure of CO_2 at 0° C., 34.4009 atm.[11] The pressures re-

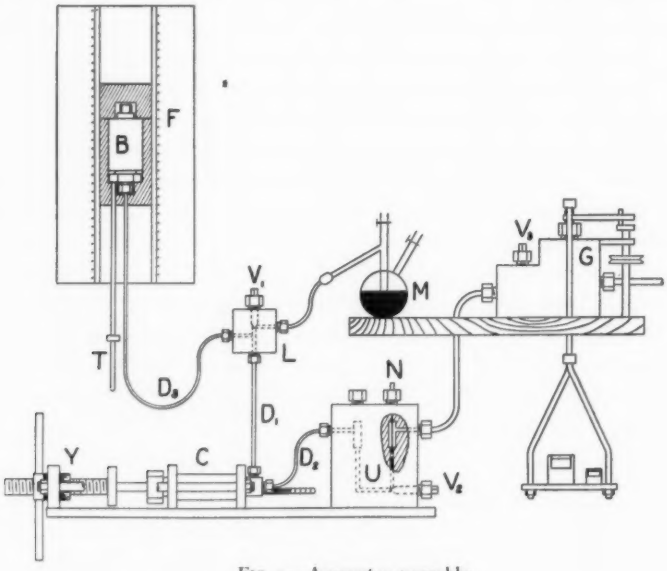

FIG. 3.—Apparatus assembly

ported in this work have been corrected for the head of liquids intervening between the gauge and the fluid whose pressure is to be measured. Observed pressures are expressed in international atmospheres and are accurate to 0.05 per cent, or 0.1 atm., whichever is larger.

The trap *U* is used to separate the mercury, filling the compressor *C* and connecting tubing D_1 and D_2, from the oil in the piston gauge. The insulated needle *N* serves to locate the mercury-oil interface and

[11] O. C. Bridgeman, "A Fixed Point for the Calibration of Pressure Gages: The Vapor Pressure of Liquid Carbon Dioxide at 0° C.," *Jour. Amer. Chem. Soc.*, Vol. XLIX (1927), pp. 1174–83.

to detect pressure balance. A $\frac{1}{4}$-watt neon glower, in series with 1 megohm, 110 volts, and the needle, indicates contact.

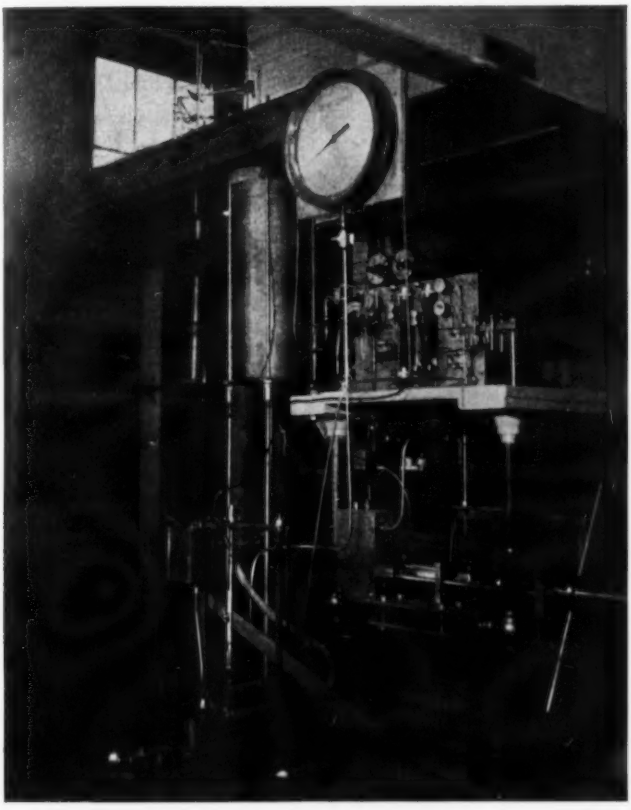

FIG. 4.—Photograph of the apparatus

Compressor.—The compressor *C* is similar in principle to those described by Keyes.[12] The piston diameter is $\frac{1}{2}$ inch, effective stroke 6.7 inches, and displacement 21.6 ml. of mercury. The driving nut *V* has a pitch of 10 threads per inch. Its position can be determined

[12] *Op. cit.*

to 0.001 turn, so that a volume change of 0.0003 ml. can be estimated.

The compressor was not thermostated. In order to correct its setting to the value it would have at a room temperature of 25° C., the volume contained by the compressor with the nut at zero, by the trap U up to the needle point, and by the connectors D_1 and D_2 was determined by weighing the mercury required to fill this portion of the apparatus. The volume of mercury expelled from the compressor for every five turns of the nut was determined in the manner recommended by Keyes.[13] Volume was proportional to turns of the nut within 0.005 turn over the entire range.

After calibration the compressor was connected to loading block L. The latter is connected to a supply of mercury M and, through D_3, to bomb B. Valve V_1 is used to isolate the apparatus from the mercury supply after the former had been evacuated and filled with mercury.

Bomb.—Connector D_3 and bomb B are made throughout of Allegheny 44, a stainless steel mechanically strong and resistant to corrosion at high temperatures. Preliminary tests had indicated that this material was wholly unattacked by mercury and only slightly acted on by water, steam, and KCl solutions. The action of the latter consists of formation of a dark superficial coating which protects against further attack up to 550° C.

The bomb is shown in longitudinal section in Figure 5. Its internal volume is about 16 ml. There is no provision for stirring the bomb's contents; hence, it was made small and free from constricted places, so that equilibrium could be rapidly attained by diffusion alone. No gasket material was found which would withstand the combined action of mercury and salt solution. All connections were made by forcing a 57° cone into a 60° seat. The closure piece K is pierced by a $\frac{3}{16}$-inch hole, so that the bomb may be filled with solid KCl after K has been driven tight by retaining screw R bearing against slip washer M. In this way the bomb can be tested for tightness under 1,000 atm. gas pressure before the KCl is weighed in. Potassium chloride is retained in the bomb by a stainless-steel disk,

[13] *Ibid.*

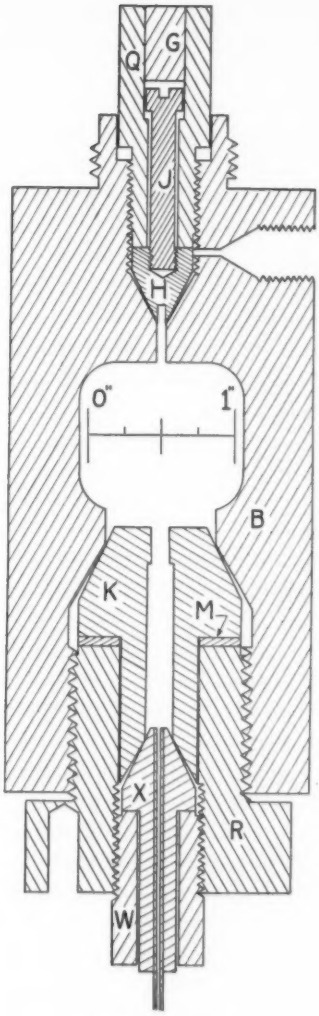

FIG. 5.—The bomb

pierced with a number of small holes, which is forced into the axial hole in K. The disk is not shown in Figure 5. The cone X is welded to the upper end of connector D_3 (Fig. 3).

The valve for sealing the opening through which water is introduced is shown at the top of Figure 5. With valve stem H closed, the bomb is first baked out and evacuated through the lower opening at as high a temperature as is subsequently to be used in measurements. When sufficiently degassed, the bomb is allowed to cool and is removed from the furnace. Mercury is run into the bomb till it stands above the opening in K. A rubber washer is slipped over the outside of valve screw Q and retained by a cap nut. A stainless-steel connector leading to vacuum and a source of air-free water is screwed into the side outlet of the valve. These auxiliary fittings are not shown in Figure 5. After the connections have been pumped down, valve H is opened and water is distilled into the bomb. Finally, valve H is closed, the auxiliary fittings are removed from the bomb, and the bomb is returned to the furnace, ready for vapor-pressure measurements.

Temperature control and measurement.—The bomb is surrounded in the furnace by a hollow copper cylinder capped at each end by copper disks. The copper parts, shown cross-hatched in Figure 3, are hung in the center of a vertical tube furnace, F. The empty spaces below and above the copper blocks are plugged with insulating fire brick. In this way convection currents are eliminated and a uniform temperature distribution throughout the bomb is insured. Interior of the bomb was explored with a thermocouple; the temperature gradient was less than 0°.1 C. per inch at 480° C.

The copper cylinder is wound with a resistance thermometer of "Hytemco" wire. This thermometer forms one arm of an alternating-current bridge. The output of the bridge is amplified and fed to a phase-shifting thyratron circuit.[14] The thyratron plate current decreases as the furnace temperature rises, and conversely, and thus maintains the furnace temperature constant.

Bomb temperature is measured by means of a platinum, platinrhodium thermocouple T, Figure 3, inserted in the well in R, Figure 5.

[14] M. Benedict, "Use of an Alternating Current Bridge in Laboratory Temperature Control," *Rev. Sci. Inst.*, Vol. VIII (1937), pp. 252–54.

The thermocouple wires are sealed in a Pyrex case filled with dry air. The maximum error caused by thermoelectric inhomogeneity in the assembled couple was investigated and found to be 0°.05 C. Electromotive force was measured with a potentiometer and galvanometer sensitive to 0.1 μv., or 0°.02 C. Precautions were taken to keep parasitic electromotive forces below this voltage. The thermocouple was standardized against a mercury thermometer up to 200° C. and in vapor baths of condensing mercury at 356°.58 C. and condensing sulphur at 444°.60 C. Each calibration temperature was known within 0°.1 C. Thermocouple e.m.f. E was related to standard e.m.f. e, taken from Adams' table,[15] by the equation

$$e = 0.9975E\,, \qquad (1)$$

with an error of less than 0°.2 C. Up to 450° C., the temperature, calculated from this equation and Adams' table, is believed to be within 0°.5 C. of the temperature of the contents of the bomb. The error may increase to 1° C. between 450° and 600° C.

MATERIALS

Potassium chloride.—Dr. Marjorie A. Benedict kindly purified the KCl for this work. Chemically pure material was thrice recrystallized from conductivity water, dried, and fused.

Water.—Distilled water was de-aerated by distillation between two bulbs *in vacuo*. After each distillation any air that had been liberated was pumped off. The process was repeated until the pressure of residual air, read on a McLeod gauge, was less than 0.005 mm. The water was distilled directly into the bomb *in vacuo*.

Mercury.—Mercury was purified by electrolysis at the anode of a cell containing a dilute solution of HNO_3. Electrolysis was continued until mercury began to plate out at the cathode. The mercury was washed with distilled water and dried.

EXPERIMENTAL PROCEDURE AND REDUCTION OF DATA

Blank run.—In Run 1 the bomb contained mercury only. Observation was made of the compressor setting x at 5 pressures between 20 and 300 atm. at each of six temperatures between 250° and 500° C. Observations were also made at 25° C. before and after work

[15] L. H. Adams, *International Critical Tables*, Vol. I (New York: McGraw-Hill Co., 1926), p. 57.

at higher temperatures in order to demonstrate the absence of leak, gas evolution, and volume hysteresis. The maximum volume change was 0.006 ml.

Specific volume of KCl.—In Run 2 the bomb contained 14.8179 gm. of purified KCl in addition to mercury. Compressor settings y were determined at the same pressures and temperatures as in Run 1. Volume hysteresis was again less than 0.006 ml. From the compressor settings in Run 1 and Run 2, the known density of mercury d, and the known specific volume of KCl at 25° C. and 20 atm., v_{oo}, its specific volume v_{pt} at pressure P, and temperature t, could be determined as follows. For the other symbols, also, let the subscripts $(_{pt})$ refer to the value of the symbol at pressure P and temperature t, and let the subscripts $(_{oo})$ refer to its value at 20 atm. and 25° C. Let C be the factor required to convert the number of revolutions of the compressor nut into volume displacement. Then

$$v_{pt} = \frac{\dfrac{C[d_{oo}(y_{oo} - x_{oo}) - d_{po}(y_{pt} - x_{pt})]}{14.8179}}{d_{pt}} + v_{oo}d_{oo} \qquad (2)$$

Properties of mercury.—As may be seen from equation (2), the volumes measured in this work are based on the density of mercury

TABLE 1

PROPERTIES OF MERCURY

t (° C.)	Density of Mercury at t° C. and 20 atm., d_{ot} (g./ml.)	$\beta \times 10^6$ (atm.)$^{-1}$
0	13.5965	3.7
25	13.5350	3.8
250	12.9951	5.1
300	12.8766	5.4
350	12.7576	5.6
400	12.6379	5.9
450	12.5170	6.2
500	12.3947	6.4
550	12.2706	6.7
600	12.14	.....

at elevated temperatures and pressures. Table 1 and equations (3) and (4) summarize the properties assumed for mercury at the temperatures and pressures encountered in this work. In Table 1, d_{ot} is

based on a density of 13.5955 gm/ml at 0° C. and 1 atm., the equation of Sears[16] for the change in density with temperature between 0° and 25° C., and the equation of Hoffmann and Meissner[17] for the change in density between 0° and temperatures above 250° C. Equation (4) summarizes the data of Smith and Keyes[18] on the isothermal compressibility β of mercury.

$$d_{pt} = d_{ot}(1 + \beta P) . \tag{3}$$

$$\beta = 3.7 \times 10^{-6} + 5.5 \times 10^{-9} t . \tag{4}$$

Saturated aqueous solutions of KCl.—Without changing the quantities of KCl and mercury remaining in the system after Run 2, 2.8839 gm. of air-free water was distilled into the bomb through valve H, Figure 5. The weight of water added in this way was calculated from the volume of mercury M displaced by the water at 25° C. and atmospheric pressure. If w is the weight fraction of water in a saturated solution of specific volume V, and v, as before, is the specific volume of solid KCl, the weight of water added, W, is given by

$$W = \frac{M}{\frac{V - wv}{1 - w}} . \tag{5}$$

$(V - wv)/(1 - w)$ is the volume increase caused by the addition of 1 gm. of H_2O to an excess of solid KCl; it will be called the apparent volume of H_2O and will be denoted by A. At 25° C. and 1 atm.,[19]

$$w = 0.2648 ,$$
$$v = 0.50335 \text{ ml/gm KCl} ,$$

and

$$V = 0.8487 \text{ ml/gm solution} ;$$

hence,

$$A = 0.9731 \text{ ml/gm } H_2O .$$

[16] Sears, *International Critical Tables*, Vol. II, p. 457.

[17] F. Hoffmann and W. Meissner, "Expansion of Mercury at Temperatures up to 500° C.," *Zeit. Instrumentkunde*, Vol. XXXIX (1919), p. 212.

[18] L. B. Smith and F. G. Keyes, "The Compressibility of Mercury from 30° to 300° C.," *Proc. Amer. Acad. Arts Sci.*, Vol. XLIX (1934), pp. 313–14.

[19] *International Critical Tables*, Vol. III, pp. 43 and 106.

Run 3 was made on the saturated solution at 250°, 300°, and 350° C. At each temperature a pressure-volume curve similar to the dotted line of Figure 2 (actually measured at 350° C.) was determined. At the same volume, pressures on the horizontal branch of the curve measured with increasing or decreasing volume agreed within 0.05 atm. This indicates that the measured pressure was a true equilibrium property. Equilibrium was rapidly attained without stirring, because the KCl and water in the bomb were in close contact.

The dotted line is somewhat rounded near the boiling-point, owing to the presence of about 0.2 ml. of foreign gas, measured at 1 atm. and 25° C. The source of this gas is not known; it may have been occluded by the salt or formed in superficial action of salt solution on steel. Below 550° C. the amount of gas did not increase progressively during a run.

It is necessary to determine, from the experimental curve, the pressure and volume co-ordinates of the boiling-point *C*. *C* is the intersection of the two branches of the ideal curve which would have been observed if foreign gas were absent and mercury had zero vapor pressure. First, a horizontal asymptote is drawn to the observed curve. Its ordinate is the equilibrium pressure P_1 of a system consisting of liquid mercury, solid KCl, and saturated liquid and gaseous solutions, uncontaminated by foreign gas. It lay from 0.1 to 0.5 atm. below the lowest observed pressure. It was assumed that the three-phase vapor pressure in the system KCl–H_2O was the difference between P_1 and the vapor pressure of mercury at the total pressure P_1. The vapor pressures of mercury used are given under the heading P_2 in Table 2. This correction may well be in error by 10 per cent of the vapor pressure of mercury, and, at high temperatures, is the principal uncertainty in the measurements. Application of this correction for the presence of mercury gives the horizontal ideal line *BC*.

The ideal line *CD* is drawn asymptotic to the right-hand branch of the dotted experimental curve. It represents the volume of the contents of the bomb as a function of pressure in the absence of foreign gas. The compressor setting Z_{pt} at the intersection of *CD* with *BC* is the setting that would be observed at the three-phase

pressure of the system KCl–H_2O if foreign gas were absent. Z_{pt} could be located within 0.020 turn; this corresponds to an error of 0.003 ml/gm in the apparent volume.

A_{pt}, the apparent volume of water in a liquid solution saturated with mercury and KCl, is given by the equation

$$A_{pt} = \frac{C(y_{pt} - Z_{pt})d_{po}}{W d_{pt}} . \qquad (6)$$

Since mercury undoubtedly is insoluble in a saturated liquid solution of KCl in H_2O, A_{pt} may be regarded as the apparent volume of water in a solution saturated with KCl alone.

After 350° C. the bomb connector became plugged, and Run 3 was stopped. Run 4, made with a fresh charge of KCl, was similar to Run 2 except that a temperature range from 350° to 550° C. was covered. Then 1.7097 gm. of water was charged to the bomb, and Run 5 was made over the same temperature range.

In Run 5, compressor settings were determined at 25° C. before and after the work at higher temperatures. This check-up showed there had been no leak but that 0.2 ml. of foreign gas, measured at 25° C. and 1 atm., had appeared. Nevertheless, the apparent volumes of water and equilibrium pressures at 350° C. measured in Runs 3 and 5 were in good agreement, and it is believed that error due to the presence of gas was largely eliminated by the graphical procedure outlined above.

After Run 5 the foreign gas was pumped out through valve *H*. In Run 5*a* the equilibrium pressure at 550° C. was redetermined. It checked the value determined in Run 5. But when, in Run 5*a*, the temperature was raised to 600° C., a slow, progressive accumulation of gas, later proved to be hydrogen, began. The equilibrium pressure at 600° C. was measured as a function of time and extrapolated back to the time at which this temperature was first reached. A correction of 1.5 atm. was required. Hence, the pressure at this temperature is much less reliable than the pressure at lower temperatures.

RESULTS

Saturated solution.—The measured properties of saturated aqueous solutions of KCl are given in Table 2. P_t is the observed equilib-

TABLE 2

THE MEASURED PROPERTIES OF SATURATED AQUEOUS SOLUTION OF KCl

Temperature (° C.)	Run	P_1 (atm.)	P_2 (atm.)	P (atm.)	A_{pt} (ml/gm)
250	3	24.52	0.10	24.42	1.109
300	3	48.97	0.32	48.65	1.155
350	3	83.87	0.91	82.96	1.205
350	5	83.98	0.91	83.07	1.205
400	5	127.74	2.15	125.59	1.263
450	5	173.32	4.48	168.84	1.331
500	5	213.33	8.47	204.86	1.414
550	5	238.51	14.77	223.74	1.531
550	5*a*	238.52	14.77	223.75	.....
600	5*a*	244	24.11	220	.....

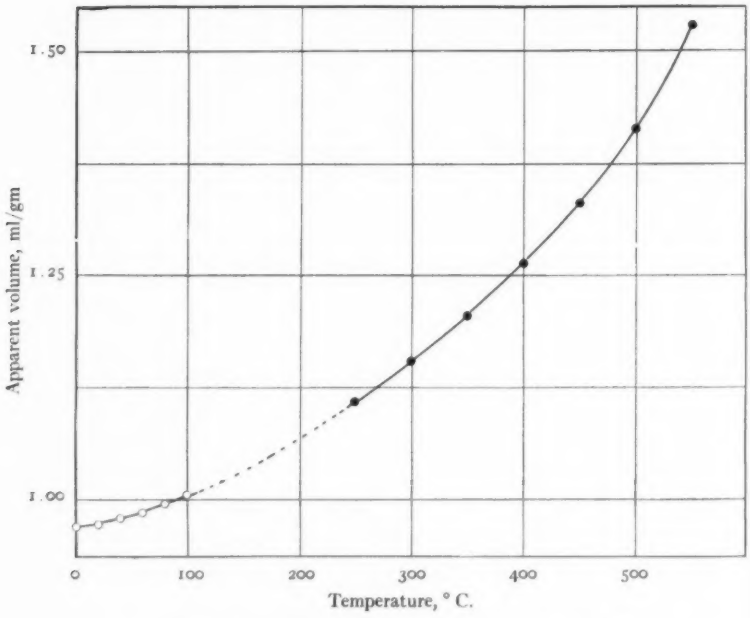

FIG. 6.—Apparent volume of water in saturated solution

rium pressure in the system KCl–Hg–H_2O. P_2 is the vapor pressure of mercury at P_1; it is obtained by applying the Poynting correction to the vapor pressure of pure mercury.[20] P is the three-phase vapor pressure in the system KCl–H_2O; $P = P_1 - P_2$. A_{pt} is the apparent volume of water in the saturated liquid solution at P.

The apparent volume of water and the three-phase vapor pressure in the system KCl–H_2O are illustrated in Figures 6 and 7, respectively. The vapor pressure of pure water is also given for comparison. C is the critical point of pure water; T is the triple point of pure KCl, the high-temperature end of the three-phase curve.

It will be noted that the three-phase vapor pressure passes through a maximum pressure of 225 atm. at 565° C. This maximum is slightly greater than the critical pressure of pure water, 217 atm. The maximum in the three-phase curve is conclusive evidence that this system does not show critical phenomena in solutions saturated with the solid phase and hence belongs to case 1 described by Morey and Ingerson.[21]

Solid KCl.—In Table 3, v_{ot} is the measured specific volume of KCl at 20 atm. and t° C., v_{pt} is its measured specific volume at the

TABLE 3

PROPERTIES OF SOLID KCl

Temperature (° C.)	Specific Volume		$\alpha_{25}^{t} \times 10^{6}$ $(°C.)^{-1}$
	At 20 Atm. v_{ot} (ml./g.)	At P v_{pt} (ml/gm)	
250	0.51736	0.5174	123
300	.52065	.5207	126
350	.52397	.5240	126
400	.52779	.5275	130
450	.53177	.5313	133
500	0.53556	.5348	135
550	.....	0.539*	.....

* Extrapolated.

[20] *International Critical Tables*, Vol. III, p. 206.

[21] *Op. cit.*

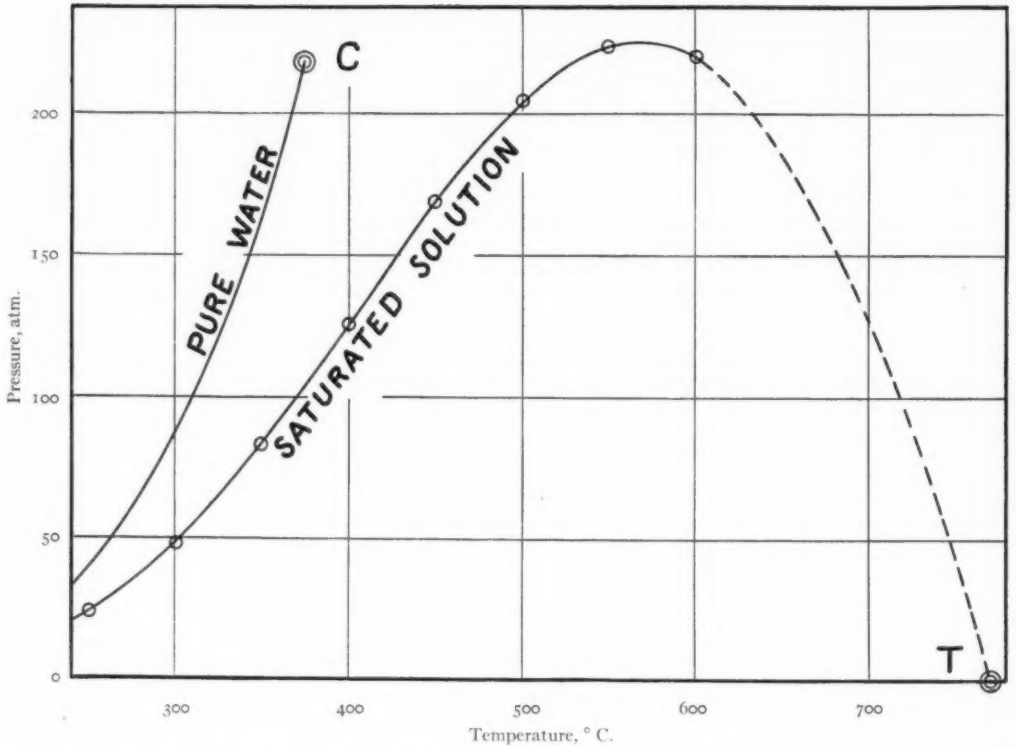

FIG. 7.—Three-phase vapor pressure in system KCl–H_2O

three-phase pressure P and $t°$ C., and a^t_{25} is its coefficient of cubical expansion at 20 atm., defined by the equation

$$a^t_{25} = \frac{v_{0t} - v_{00}}{t v_{00}} . \tag{7}$$

In Figure 8 our values of a^t_{25} are compared with determinations at lower temperatures by other workers.[22] The radius of the circles is

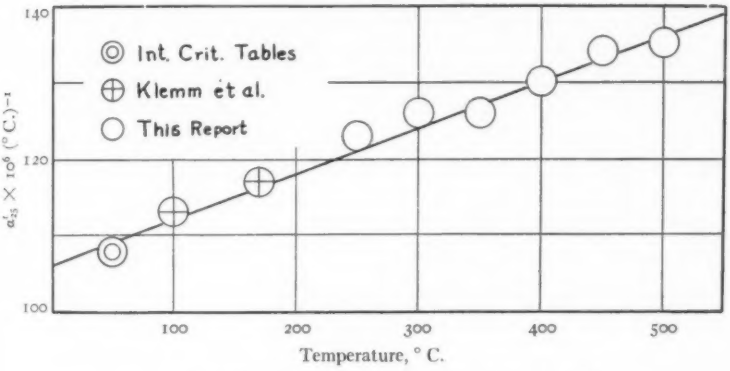

FIG. 8.—Coefficient of cubical expansion of solid KCl

2 per cent, our estimated maximum error. The equation of the straight line is

$$a^t_{25} = 106 \times 10^{-6} + 60 \times 10^{-9} t . \tag{8}$$

The measured specific volumes were too irregular to permit reliable calculation of the isothermal compressibility.

DERIVED PROPERTIES OF SATURATED SOLUTION

From the observed properties of the system KCl–H_2O given in Tables 2 and 3, a number of other properties may be evaluated if certain additional assumptions are made.

[22] *International Critical Tables*, Vol. III, pp. 43 and 106; W. Klemm, W. Tilk, and S. von Müllenheim, "Dilatometric Measurement of the Thermal Expansion of Crystalline Salts," *Zeit. anorg. allgem. Chem.*, Vol. CLXXVI (1928), pp. 1–22.

FIG. 7.—Three-phase vapor pressure in system KCl-H_2O

If the vapor phase contains no dissolved KCl, the volume change in the reaction

Saturated liquid solution → Solid KCl + Steam

may be evaluated. This assumption is very plausible because the specific volume of steam at the three-phase pressure and temperature of the saturated solution is much greater than the critical volume of steam, 3 ml/gm; no pronounced solution of KCl in steam is anticipated until the specific volume of the gas phase approaches the critical volume of steam. If ΔV is the volume change in the foregoing reaction per gram steam evaporated,

$$\Delta V = V_{\text{steam}} - \frac{V_{\text{soln}} - wv_{\text{KCl}}}{1 - w} \tag{9}$$

$$= V_{\text{steam}} - A_{pt} .$$

The specific volume of steam[23] at P and t and the volume change ΔV calculated in this way are given in Table 4.

TABLE 4

VOLUME CHANGE AND LATENT HEAT PER GRAM STEAM EVAPORATED

Temperature (° C.)	V_{steam} (ml/gm)	ΔV (ml/gm)	$\frac{dP}{dt}$ (atm/° C.)	ΔH (cal/gm)
250	88.06	86.95	0.378	416
300	46.12	44.96	.590	368
350	28.16	26.96	.784	319
400	19.57	18.31	.882	263
450	15.64	14.31	.827	207
500	14.09	12.68	.573	136
550	14.23	12.70	.169	43
600	16.01	14.30	−0.329	−100

The Clausius-Clapeyron equation

$$\Delta H = T\Delta V \frac{dP}{dt} \tag{10}$$

applies to any univariant system. Hence, ΔH, the latent heat of evaporation of 1 gm. of steam from the saturated aqueous solution,

[23] Keenan and Keyes, *op. cit.*

may be calculated from the three-phase vapor pressures and values of ΔV. The derivative dP/dt, evaluated from the pressure data of Table 2 by residual means, and ΔH are given in Table 4. The sign of ΔH changes at the temperature at which the three-phase pressure is a maximum. The physical interpretation of this fact is as follows: ΔH may be regarded as the resultant of two processes, the evaporation of steam from the solution and the crystallization of KCl from the solution. At low temperatures only a small amount of KCl is precipitated for every gram of steam evaporated, and ΔH has the sign of the heat required to evaporate the steam. However, at high temperatures many grams of solid KCl are precipitated for every gram of steam evaporated, and ΔH has the sign of the heat evolved in the crystallization of KCl.

The volume and heat changes given in Table 4 are for a process in which 1 gm. of steam is evaporated. For many purposes it is preferable to have these quantities referred to a process in which 1 gm. of solution is evaporated. It is also desirable to know the specific volume of the solution. These quantities can be derived from the data of Tables 2, 3, and 4 when the weight fraction of KCl, w, in the saturated solution is known.

The weight fraction of KCl has been determined up to 450° C. by Benrath.[24] His results are plotted in Figure 9. The solid line has been drawn through his data and extended by the dotted portion to the melting-point of KCl at which $w = 1$. Values of w, read from the curve at even temperatures, are given in Table 5. The specific volume of the saturated solution, V_{pt}, and the volume change and latent heat of evaporation per gram of solution, $\Delta' V$ and $\Delta' H$, are also given in Table 5. These were calculated by the equations

$$V_{pt} = (1 - w)A_{pt} + wv_{pt}\,, \tag{11}$$

$$\Delta' V = \Delta V(1 - w)\,, \tag{12}$$

$$\Delta' H = \Delta H(1 - w)\,. \tag{13}$$

V_{pt} is plotted in Figure 9, and $\Delta' V$ and $\Delta' H$ are plotted in Figure 10. At the triple point of KCl, 770°.3 C., $\Delta' H$ should be the latent heat of

[24] Benrath *et al.*, *loc. cit.*

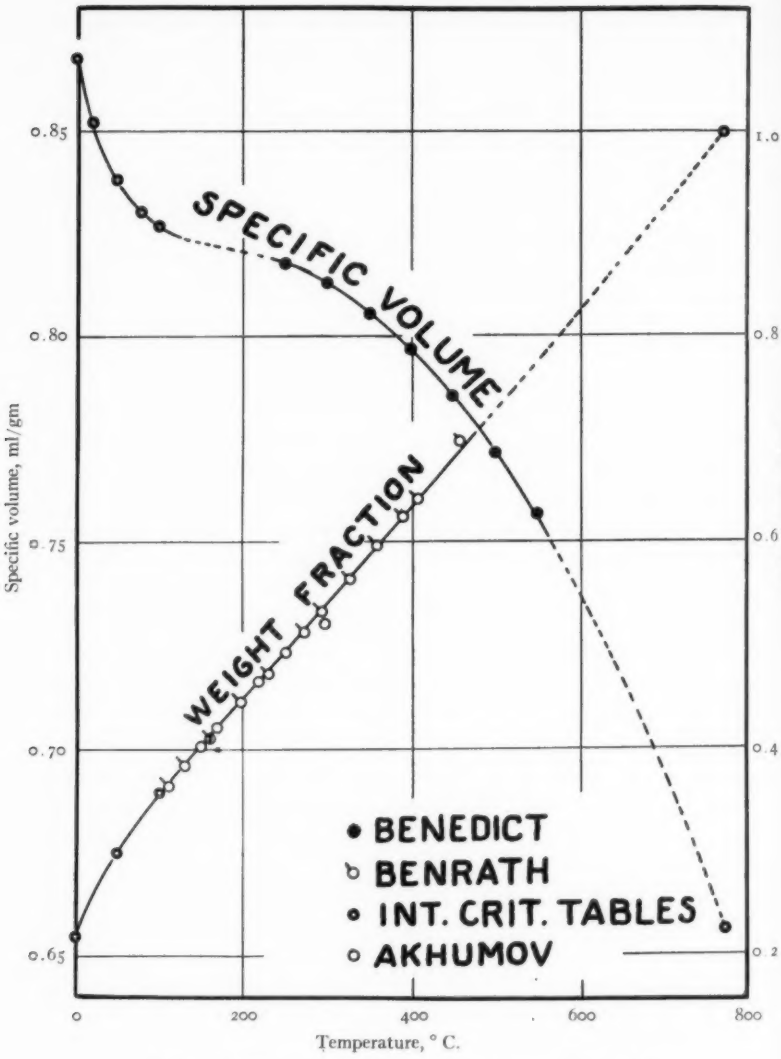

FIG. 9.—Composition and specific volume of saturated solution

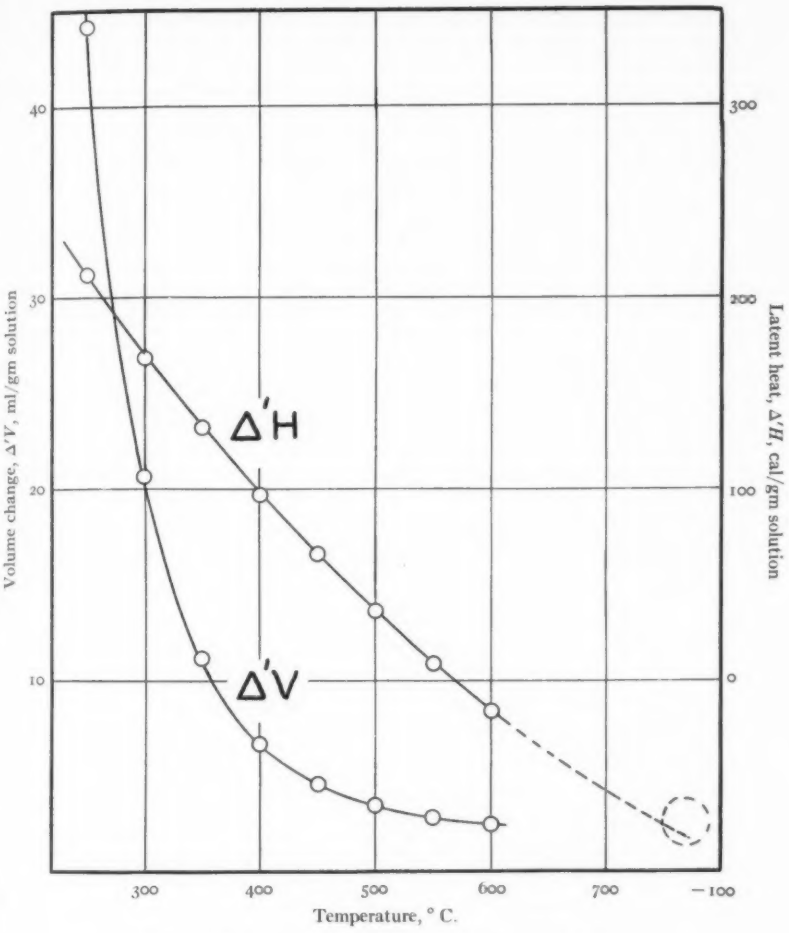

FIG. 10.—Volume change and latent heat per gram solution

crystallization of molten KCl. $\Delta' H$ can be extrapolated to the latent heat of crystallization of pure KCl within the rather large error in this datum.

TABLE 5

PROPERTIES OF 1 GRAM OF SATURATED SOLUTION

Temperature t (° C.)	Weight of KCl per Gram of Solution w (gm.)	Specific Volume V_{pt} (ml/gm)	Volume Change of Evaporation $\Delta' V$ (ml/gm)	Latent Heat of Evaporation $\Delta' H$ (cal/gm)
250	0.493	0.817	44.08	211
300	0.540	.813	20.68	169
350	0.587	.805	11.13	132
400	0.634	.797	6.701	96
450	0.682	.786	4.551	66
500	0.730	.772	3.424	37
550	0.779	0.758	2.807	9
600	0.829	.....	2.445	− 17
770.3	1.000	.....	.....	− 74 ± 12*

* *International Critical Tables*, Vol. V, p. 131.

Estimated accuracy of data.—The three-phase pressures P are probably absolutely accurate to 1 per cent. The principal error is in the correction for the vapor pressure of mercury. The change of pressure with temperature is probably correct to 2 per cent; this is the principal source of error in the latent heat of evaporation ΔH. The main error in the apparent volume of water in the saturated solution is caused by the presence of foreign gas in the bomb; this introduces an uncertainty of, at most, 0.005 ml/gm. The data of Table 5 is less reliable because it depends on the uncertain composition of the saturated solution. The error in the specific volume of the saturated solution probably lies between 1 and 2 per cent.

ACKNOWLEDGMENTS.—The writer wishes to express his appreciation of the support of the Committee on Geophysical Research at Harvard University under whose auspices this work was done. He especially wishes to thank Professors L. C. Graton and Francis Birch for their interest in the problem. The assistance of Mr. H. J. Ames in the construction of the apparatus is gratefully acknowledged.

END MORAINES OF NORTH-CENTRAL OHIO

GEORGE W. WHITE
University of New Hampshire

ABSTRACT

North-south projected profiles of eighteen quadrangles in north-central Ohio were constructed with sufficient vertical exaggeration to show the end moraines. From a study of these profiles and of supplementary east-west and northwest-southeast profiles of parts of the area and from field work the positions of the end moraines were mapped.

The Powell moraine in the area trends northward from Delaware County through Morrow County and dies out in southwestern Richland County. The Broadway moraine is traced from northeastern Logan County eastward to Morrow County where it turns north across Morrow County to join the Wabash moraine in eastern Crawford County. In much of Morrow County it lies very close to the Powell moraine but does not join it. The St. Johns moraine is traced eastward across Hardin County to central Marion County, thence north through Marion to join the Wabash moraine in southwestern Crawford County. The Wabash moraine extends across Hardin, Marion, southeastern Wyandot, and Crawford counties, joining the Fort Wayne moraine in the eastern part of the latter county and continuing eastward across northern Richland County. The Fort Wayne moraine is traced in a general easterly direction across the area. The Defiance moraine is strongly developed across the whole area.

INTRODUCTION

The last ice sheet to invade Ohio advanced in a series of lobes. The Scioto lobe advanced farthest to the south in the lowland between the Allegheny plateau on the east and the Bellefontaine outlier on the west. The Miami lobe advanced into the lowland west of the Bellefontaine outlier. As the ice melted back, there were stages of halting and slight readvance marked by end moraines. When the ice had retreated to the Erie and Maumee lowland, a position north of the Bellefontaine outlier, the Miami and Scioto lobes were no longer existent.

The moraines here described lie in the area shown in Figure 2, the position of which is indicated on the index map, *ABCD*, Figure 1. The moraines in the southern part of the area bend in southward arcs and register halts of the retreating edge of the diminishing Scioto lobe. Those in the northern part show that the Scioto lobe had disappeared at the time of their formation and are referred to a Maumee lobe. Parts of several of these moraines were described

almost seventy years ago by early workers of the Geological Survey of Ohio,[1] and in 1902 were treated in Leverett's monographic study of the glacial features of Ohio.[2] Topographic maps now available

FIG. 1.—Index map. *ABCD*, location of map, Figure 2, and profiles shown in Figure 3; *EBCF*, location of profiles shown in Figure 4; *JKLM*, location of profiles shown in Figure 5.

[1] G. K. Gilbert, "On Certain Glacial and Post-glacial Phenomena of the Maumee Valley," *Amer. Jour. Sci.*, Vol. I (3d ser., 1871), pp. 339–45, also *Rept. Geol. Surv. Ohio*, Vol. I (1873), pp. 535–56; N. H. Winchell, "The Surface Geology of Northwestern Ohio," *Proc. Amer. Assoc. Adv. Sci., 1872* (1873), pp. 152–86, also county reports in *Rept. Geol. Surv. Ohio*, Vol. I (1873), pp. 593–645; *ibid.*, Vol. II (1874), pp. 227–438.

[2] Frank Leverett, "Glacial Formations and Drainage Features of the Erie and Ohio Basins," *U.S. Geol. Surv. Mono. 41* (1902).

for the whole state make it possible to follow various glacial features more closely and in certain areas to fill in gaps and to follow structures more exactly than formerly. From these topographic maps it has been possible by constructing profiles to get a picture of a large

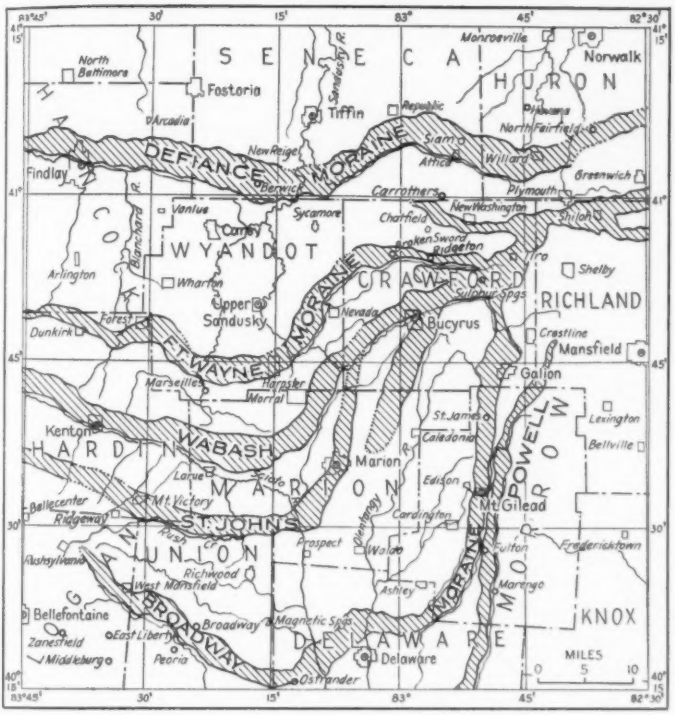

FIG. 2.—Map of north central Ohio showing end moraines

area at a single view and to follow the ridgelike structures of the end moraines across quadrangle after quadrangle.

THE PROFILES

Projected profiles of 1-inch strips running north-south were constructed from the topographic maps covering the area shown in Figure 2 (*ABCD*, Fig. 1). The horizontal scale is that of the topo-

graphic maps, 1 inch to 1 mile, and the vertical scale is 1 inch to 100 feet. By using such a vertical exaggeration the end moraines are brought out most sharply. The profiles were transferred to card-

FIG. 3.—View southeast across north-south projected profiles of area *ABCD*, Figure 1 and Figure 2 (two quadrangles in southeast corner omitted). Moraines shown by letters: *D*, Defiance; *F*, Fort Wayne; *W*, Wabash; *S*, St. Johns. Cities and towns shown by numbers:

1. Norwalk
2. Shiloh
3. Attica
4. Tiffin
5. Fostoria
6. Sycamore
7. Bucyrus
8. Galion
9. Mount Gilead
10. Nevada
11. Carey
12. Upper Sandusky
13. Marion
14. Kilbourne
15. Delaware
16. Larue
17. Richwood
18. Broadway
19. Findlay
20. Forest
21. Dunkirk
22. Kenton
23. Rushsylvania
24. Bellefontaine
25. West Mansfield

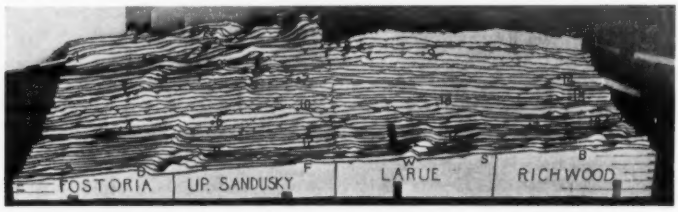

FIG. 4.—Looking east across north-south projected profiles of area *EBCF*, Figure 1 (same profiles as Figure 3, with western row of quadrangles removed). Moraines and towns marked as in Figure 3; *B*, Broadway moraine.

board, cut out, and set up in frames. Photographs were taken from various angles to show various features. The photograph, Figure 3, is of the whole area shown in Figure 2, and the moraines crossing it may be studied. In this photograph (lower right) the highland of the Bellefontaine outlier obscures the Broadway moraine, so the profiles of the western strip of quadrangles were removed and the remainder

(*EBCF*, Fig. 1) photographed (Fig. 4). In this view the Broadway moraine is well shown.

In order for moraines to show up well the profiles must be drawn nearly at right angles to them. Where the Powell and Broadway moraines have a north-south trend, the north-south profiles fail to show them, but they are quite clear in east-west profiles.[3] In the central part of the area the moraines have a northeast trend, and

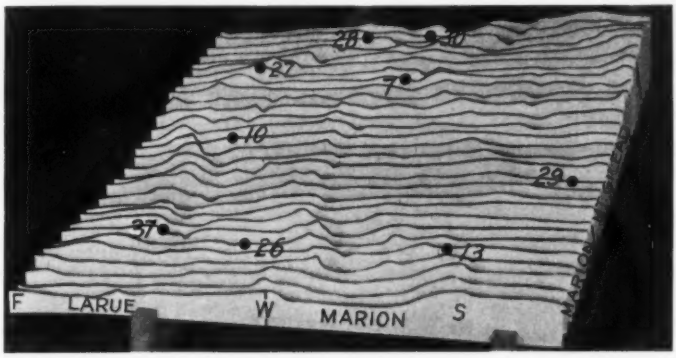

FIG. 5.—Looking northeast across northwest-southeast projected profiles of area *JKLM*, Figure 1. Moraines marked as in Figure 3; towns shown by numbers:

7. Bucyrus	26. Morral	29. Caledonia
10. Nevada	27. Broken Sword	30. Sulphur Springs
13. Marion	28. Ridgeton	37. Harpster

neither north-south nor east-west profiles are satisfactorily clear in delimiting the moraines. Particularly is this true in respect to the weak St. Johns moraine north of Marion. For this central area (*JKLM*, Fig. 1) northwest-southeast profiles were constructed, and in these the moraines are reasonably clear, as shown in Figure 5.

From the profiles set up and from the photographs taken from various angles the moraine borders were plotted on the topographic maps and from these a map of the region, Figure 2, was constructed. Doubtful boundaries are shown by dotted lines. Detailed field study in the eastern part of the area confirms the boundaries mapped from profiles.

[3] G. W. White, "The Powell and Broadway End Moraines," *Amer. Jour. Sci.*, Vol. XXX (1935), p. 38.

POWELL MORAINE

The Powell moraine is a southward arc in the Scioto basin[4] and only its eastern part is within the area here discussed. From Sunbury, just south of the south boundary of Figure 2, the moraine extends northward across northeastern Delaware County and across Morrow County to the northeastern part, where it turns northeast into western Richland County and dies out on the northwestern slope of the Allegheny plateau at about the latitude of Crestline. From Sunbury to Fulton the moraine lies along the border of the low shelf or cuesta formed by the Berea sandstone, which has been referred to as the "Low plateau."[5] Northward from Fulton the moraine lies farther back from the edge of this shelf and dies out on its eastern margin against the higher Allegheny plateau. The Powell moraine is well shown by east-west profiles.[6] Walnut Creek flows along the outer margin of the moraine from Mount Gilead to Sunbury and farther north Whetstone Creek follows this margin for several miles.

BROADWAY MORAINE

The Broadway moraine crosses the Scioto basin in an arc which extends from northeastern Logan County, across Union, Delaware, and Morrow counties to eastern Crawford County, where it joins the Wabash moraine. The moraine first becomes evident on the northeast slope of the Bellefontaine outlier just east of Rushsylvania (Fig. 3). It descends to the till plain and crosses Union County, in a southeasterly course. The village of West Mansfield in eastern Logan County is located on the inner margin and the village of Broadway from which Leverett[7] named this moraine lies along the inner margin in Union County (Fig. 4). Across Delaware County the moraine has a north-northeast course[8] which it continues to

[4] Leverett, *op. cit.*, Pl. XIII.

[5] White, *op. cit.*, p. 35.

[6] *Ibid.*, figure on p. 38; and in profiles of Marengo quadrangle, W. S. Cole, "Development and Structural Control of Erosion Surfaces," *Jour. Geol.*, Vol. XLV (1937), Fig. 2, p. 144.

[7] *Op. cit.*, p. 531.

[8] L. G. Westgate, "Geology of Delaware County," *Geol. Surv. Ohio Bull. 30* (1926), pp. 91–93 and Pl. II.

Fulton, in Morrow County, where it turns northward. At Mount Gilead it rises from the till plain to the margin of the Berea escarpment (Low plateau)—a position it maintains to its union with the Wabash moraine. For part of its course across Morrow County the Broadway moraine almost touches the Powell moraine, but they do not join, being separated by a narrow lowland occupied by Whetstone and Alum creeks.

The Broadway moraine varies in width from a little more than a mile to more than 3 miles. It rises from 30 to 50 feet above the ground moraine along most of its course, but from Mount Gilead to Galion, because of its position on the plateau its crest is 100 feet or more above the till plain to the west. As is the case with many end moraines, the inner margin is often indeterminate, as it merges gradually with the ground moraine.

Along more than half of the moraine streams follow the outer margin with great regularity. On the west, Mill Creek follows the margin from near Rushsylvania to a point southeast of Peoria; on the east, Whetstone Creek and Alum Creek flow southward across Morrow County to northeastern Delaware County.

ST. JOHNS (SALAMONIE) MORAINE

The end moraine immediately north of the Broadway moraine has been called the Mount Victory moraine[9] from the village of that name in Hardin County. However, since the profiles show that this moraine extends westward from the Scioto lobe and is really a continuation of the St. Johns moraine of the Maumee-Miami glacial lobe, the latter name is here preferred. The St. Johns moraine, named "St. Johns Ridge" by Winchell from the village of St. Johns in Auglaize County,[10] has also been called the Salamonie moraine[11] in the Maumee-Miami lobe. This end moraine crosses southern Hardin, northern Union, and southwestern Marion counties, then turns north to southwestern Crawford County where it appears to join the Wabash moraine. As may be seen in the profiles of Figures 3, 4, and 5, it is the weakest of the moraines in the area.

Southwest of Kenton the St. Johns moraine is well developed east-

[9] Leverett, *op. cit.*, p. 543.

[10] "The Surface Geology . . . . ," pp. 161–65.

[11] Leverett, *op. cit.*, p. 509.

ward for several miles, but from south of Kenton it becomes very low and indistinct as far as Mount Victory, as shown by dotted lines on the map (Fig. 2). Eastward from Mount Victory the moraine is fairly well marked as far as Marion (Fig. 4). The southern margin is followed by Rush Creek for 12 miles eastward from Mount Victory. Northward from Marion the St. Johns moraine becomes lower and more indistinct, and question arises whether its continuation is northward from Marion to join the Wabash moraine at a point just east of the Wyandot-Crawford county line or is northeast from Marion to Bucyrus. Profiles constructed along northwest-southeast lines, shown in Figure 5, indicate that the low swell of the St. Johns moraine continues northward from Marion as mapped in Figure 2, and not northeast to Bucyrus. The moraine extending southwestward from the Wabash moraine at Bucyrus dies out just west of Caledonia and does not connect with the St. Johns moraine. This small prong extending toward Caledonia is a very weak and minor feature.

The St. Johns moraine is from 1 to 4 miles wide. Its inner margin is so poorly marked that the exact width is difficult or impossible to determine. This moraine generally rises from 20 to 30 feet above the ground moraine but at a very few places rises as much as 60 feet.

WABASH MORAINE

The Wabash moraine is strongly developed across almost all of the area. It derives its name from its strong development along the Wabash River, farther west. It was first described by Winchell,[12] who named it for the Wabash River, which follows it for a long distance west of the area here discussed, and who traced the "Wabash Ridge" from Indiana eastward to Crawford County. It enters the western edge of the area in Hardin County northwest of Kenton and extends southwest through Kenton to northwestern Marion County where it turns northeast across the southeastern corner of Wyandot County and crosses Crawford County, where in the eastern part of the county it joins the Fort Wayne moraine on the border of the Berea shelf (Low plateau). The combined moraines extend eastward for 10 miles across the Low plateau and divide just east of Shiloh in

[12] "The Surface Geology . . . . ," p. 166.

northern Richland County at the border of the higher Allegheny plateau.

Across Hardin and Marion counties the moraine is generally over 2 miles wide, rising 40–50 feet above the ground moraine. The outer margin is closely followed by the Scioto River as far as Larue, whence the river flows 1–3 miles south of the margin for several miles. For several miles in northeastern Marion County the Little Scioto River flows southwest along the outer margin.

The Wabash moraine is rather weakly developed for several miles northeast of the Wyandot-Crawford county line, where at the junction of the Wabash and St. Johns moraines it is crossed by the Sandusky River. North-south profiles do not show the moraine here at all well because of the direction of the moraine and its lack of strength (Figs. 3 and 4). However, northwest-southeast profiles, cutting the moraine at almost right angles, do show the continuity quite well, as illustrated in Figure 5.

Northeast from a point about 4 miles southwest of Bucyrus the moraine becomes stronger, rising 40–60 feet above the ground moraine. North of the main moraine between Bucyrus and Sulphur Springs a short spur of moraine projects westward from the inner margin of the Wabash moraine. In the vicinity of Sulphur Springs the moraine is almost 4 miles wide and well developed. Although the Fort Wayne moraine to the north appears to touch the Wabash moraine south of Ridgeton, actually the two moraines are separated by the valley of Broken Sword Creek and they may be distinguished from each other as far east as Tiro.

The Sandusky River and its tributary, Loss Creek, follows the outer margin of the Wabash moraine completely across Crawford County—a distance of about 25 miles. The river turns at right angles and crosses the moraine at the Crawford-Wyandot county line. In Richland County, Black Fork or some of its tributaries follow this moraine, but not so closely as does the Sandusky River farther west.

The combined Wabash and Fort Wayne moraines in Richland County make up a belt of higher land from 2 to 4 miles wide. It is 30–60 feet above the ground moraine and, especially in the vicinity of Shiloh, has a well-developed knob and kettle topography. It is

interesting to note that while the Wabash moraine was being formed at the active ice edge in northern Richland County much stagnant ice was still present in the Black Fork Valley in the Allegheny plateau for at least 22 miles to the southeast.[13] The Wabash moraine again becomes separate from the Fort Wayne east of Shiloh. At the eastern boundary of the area shown in the map (Fig. 2) the Wabash moraine is only a mile in width and is exhibited as a single ridge (see profiles, Figs. 3 and 4). This narrow width is maintained to the east of the area here described, across Ashland County and the northwestern part of Wayne County.[14]

FORT WAYNE MORAINE

The Fort Wayne moraine was first described in 1871 by Gilbert,[15] who had studied it in northwestern Ohio and in Indiana. He projected it eastward into the area here discussed on the basis of stream patterns but correlated the moraine that passes through Fort Wayne, Indiana, with that which passes through Kenton, Ohio. The moraine on which Kenton is situated is the Wabash moraine, the Fort Wayne moraine passing 10 miles north of Kenton.

The Fort Wayne moraine is well developed across the whole area. It enters the area along the Hancock-Hardin county line, curves in a southward arc across southern Wyandot County, and crosses Crawford County, where in the eastern part it joins the Wabash moraine and enters Richland County. The two moraines are joined across the Low plateau in northwestern Richland County but become separate near the edge of the higher Allegheny plateau.

Across northern Hardin County (and including a very small portion of southern Hancock County) the Fort Wayne moraine is from 1 to 2 miles wide and rises 30–50 feet above the ground moraine. This part of the moraine past Dunkirk to Forest is well shown on the profiles across the Arlington quadrangle, Figure 3. As pointed out by Leverett,[16] the Fort Wayne moraine has a weak development across

[13] White, "Peripheral Zone of Stagnation of the Last Ice Sheet in North Central Ohio" (abst.), *Proc. Geol. Soc. Amer. 1933* (1934), pp. 455–56.

[14] G. W. Conrey, "Geology of Wayne County," *Geol. Surv. Ohio Bull. 24* (1921), Map V and pp. 30 and 31.

[15] "On Certain Glacial and Post-glacial Phenomena . . . . ," *loc. cit.*

[16] *Op. cit.*, p. 572 and Pl. XIII.

southern Wyandot County as far as Harpster. However, the moraine ridge is recognizable in the profiles across the southern part of the Upper Sandusky and northern part of the Larue quadrangles (Fig. 4). From Harpster, across eastern Wyandot County and western Crawford County to Ridgeton the moraine is quite clear. In the northwest-southeast profiles, Figure 5, its ridgelike character shows best because these profiles are almost at right angles to the structure. In this part of its course the moraine is generally about 2 miles wide and rises from 40 to 50 feet above the ground moraine. The outer border is closely followed by Broken Sword Creek from its source near Tiro to its junction with the Sandusky River—a distance of approximately 27 miles. From Tiro to Ridgeton the Fort Wayne moraine and a spur of the Wabash moraine are very close together, but maintain their identities, separated by the narrow valley of Broken Sword Creek.

From Tiro to Shiloh across the Berea shelf (Low plateau) the Wabash and Fort Wayne moraines form a single prominent belt which is 3–4 miles wide and which rises as much as 100 feet above the surrounding territory. East of Shiloh the Fort Wayne moraine diverges east-northeast from the Wabash moraine and becomes lower, narrower, and less conspicuous a topographic feature in the Allegheny plateau.

In northeastern Crawford County, from a point north of Tiro, a conspicuous spur diverges from the main moraine westward past New Washington to a point 3 miles west of Carrothers. This seems to be a separate spur rather than a local widening of the main moraine, because the area between the main moraine and the spur is very flat and is 40–70 feet lower than either moraine ridge. This spur is shown in the profiles (Figs. 3 and 4) south of Attica.

DEFIANCE MORAINE

The Defiance moraine is a very prominent and well-developed ridge, crossing in this area the northern part of Hancock County and the southern parts of Seneca and Huron counties. In the eastern part of Huron County it becomes less well marked. The position of this moraine was first indicated in a general way in the Maumee

basin to the west by Gilbert, who showed its position from Adrian, Michigan, into Ohio, past Defiance to Findlay.[17]

Across the Findlay and Fostoria quadrangles in north-central Hancock County the moraine is very prominent, as shown by the profiles in Figure 3. Findlay is situated partly on the moraine and partly on the ground moraine to the south. Here the moraine, 2–3 miles or more wide rises about 50 feet above the ground moraine to the south and about 100 feet above the lake plain to the north. The inner border of the moraine, as is so often the case with end moraines on till plains, is indeterminate and might be placed much farther north. Shaffer,[18] who has studied the geology of the Findlay quadrangle, maps the wide, gentle inner slope of the moraine as a "zone of transition" between the higher ridge and the lower plain. Across the western part of the Fostoria and all the Findlay quadrangle the outer margin of the moraine is followed by the Blanchard River and its tributary, the Outlet. Prominently shown in the profiles of Figures 3 and 4 is a group of rock knobs of Niagaran and Monroe[19] dolomite between Carey and the moraine. These have no effect on the course of the moraine as the ice border was just north of the rock knobs.

Westward from the Carey knobs, across the southeastern part of the Fostoria and southwestern part of the Tiffin quadrangles, the moraine is about 3 miles wide and is about 50 feet high. Here the borders of the moraine are less plainly marked, in part because of the dissection by the Sandusky River and Honey Creek, which cross the ridge south of Tiffin.

Across the southeastern part of the Tiffin quadrangle and across the Siam quadrangle the moraine is strongly developed, with a width of 3–4 miles and a height of as much as 100 feet a few miles west of Attica. Here the outer margin is marked by Honey Creek, which follows the moraine westward from just southwest of Willard for 22 miles before turning north through the ridge to join the Sandusky River near Tiffin.

[17] "On Certain Glacial and Post-glacial Phenomena. . . . ."

[18] P. R. Shaffer, "Pleistocene Geology of the Fostoria, Ohio, Quadrangle" (Ohio State University, unpublished thesis [1937]).

[19] Wilber Stout, personal communication.

Across the Norwalk quadrangle the moraine is approaching the Berea bench but does not rise to it until just east of the area here discussed. East of Willard (Chicago Junction on old maps) the moraine is weak, as may be seen from the profiles. It is strong enough to follow, however, as a belt about 2 miles wide, and to the east of North Fairfield it attains a height of 40 feet for several miles.

ACKNOWLEDGMENTS.—The profiles were constructed under the writer's direction by Mr. Ralph E. Abbott, whose careful work has been much appreciated. Thanks are due to Dr. Wilber Stout, director of the Geological Survey of Ohio, who arranged to have the maps, Figures 1 and 2, drafted in the offices of the Ohio Survey.

VISCOSITY OF LAVA

ROBERT L. NICHOLS
Tufts College

ABSTRACT

Palmer, by assuming that the Alika flow of Hawaii when liquid was turbulent, found that its viscosity was 15 times that of water. Becker, who also assumed turbulent motion, found that the viscosty of the 1840 flow of Hawaii was 60 times that of water. Dimensional analysis, however, proves that these flows moved with laminar motion and therefore the viscosities computed by Becker and Palmer are in error.

By using the Jeffreys formula, the viscosity of the Alika flow is found to have been about 287,000 times the value calculated by Palmer.

The specific gravity, the thickness, and the gradient of the last 6 miles of the McCartys flow are known. If it is assumed that the viscosity was similar to that of the 1887 flow of Hawaii, the velocity in this area, calculated by the Jeffreys formula, is 4.8 miles per hour. This figure, together with a consideration of the flow mechanism of the flow, indicates that it covered the last 6 miles in about 12 hours.

The volume of the last 6 miles of the flow is known, and, as the time necessary to cover this distance has been calculated, the rate of extrusion of lava can also be calculated. It is found to be approximately 178,320,000 cubic feet per hour.

INTRODUCTION

The literature on the viscosity of lava flows is meager. Becker[1] computed the viscosity of the 1840 basaltic flow of Hawaii, and found that it was 60 times as viscous as water. Palmer[2] calculated the viscosity of the Alika flow of Hawaii, also basaltic, and found it to be 15 times that of water. Becker and Palmer assumed that the flows were turbulent. However, it will be shown that both flows must have moved by laminar motion and therefore the calculations of both Becker and Palmer produce erroneous results. The viscosity of the Alika flow, assuming laminar motion, has been computed and is of a much higher order of magnitude than the result obtained by Palmer.

Considerable work has been done on the viscosities of dry melts of basalt at temperatures similar to those found in basaltic flows. The viscosities computed by Becker and Palmer are not in harmony with any of this experimental work; but it will be shown that vis-

[1] George F. Becker, "Some Queries on Rock Differentiation," *Amer. Jour. Sci.*, Vol. III (4th ser., 1897), p. 29.

[2] Harold S. Palmer, "A Study of the Viscosity of Lava," *Bull. Hawaiian Vol. Observ.*, Vol. XV (1927), pp. 1–4.

cosities calculated on the assumption that the flows moved by laminar motion are in close agreement with this work.

CHEZY AND KUTTER FORMULAS

The Chezy and Kutter formulas, familiar to hydraulic engineers, apply to water and generally to all liquids that have turbulent flow, i.e., flow with eddies. The velocity of these flows is almost independent of the viscosity of the liquid and depends on the density of the liquid, on the slope, and on the dimensions and roughness of the channel.

The Chezy formula[3] is

$$V = c\sqrt{rs}\,,$$

where V is the mean velocity in feet per second, c is a coefficient depending on the dimensions, slope, and roughness of the channel, r is the hydraulic radius which is defined as the ratio of the area of the cross section to the length of its wetted perimeter, and s is the slope or tangent of the angle of inclination. The coefficient, c, is usually computed from Kutter's formula:

$$c = \frac{\dfrac{1.811}{n} + 41.66 + \dfrac{0.00281}{s}}{1 + \dfrac{n}{\sqrt{r}}\left(41.66 + \dfrac{0.00281}{s}\right)},$$

in which s and r are the same as in the Chezy formula, n is a coefficient expressing the roughness of the channel surfaces, and the various numerical coefficients are those derived empirically from experiments with channels of many types.

PALMER'S CALCULATION OF VISCOSITY

Palmer[4] analyzed the Alika flow (1919) of Mauna Loa by means of the Chezy and Kutter formulas and found that a stream of water with the same cross section, flowing on the same gradient and in a channel of similar roughness, would flow 11 times as fast as did the Alika flow. He drew from this relation and from the fact that the

[3] Charles W. Harris, *Hydraulics* (New York: John Wiley & Sons, 1936), pp. 108–11.

[4] *Op. cit.*, pp. 2–4.

gas-charged fluid lava had a specific gravity of the order of 1.4 the incorrect conclusion that the lava was 15 times as viscous as water, on the assumption that "velocity is inversely proportional to the viscosity." Such an assumption, however, is true only of liquids which move by laminar flow, in which the filaments are parallel in any unit of the liquid. It does not hold for turbulent flows. The correct inference to be drawn from Palmer's calculation is that, because the observed velocity of the lava flow was 11 times as slow as that calculated for the stream of water, the lava flow could not have been turbulent, but must have moved by laminar flow—a state of movement to which the Chezy and Kutter formulas do not apply.

APPLICATION OF DIMENSIONAL ANALYSIS

Since the application of dimensional analysis to flow problems has become accepted, it is customary to plot the resistance of open-channel flows as shown in Figure 1. The ordinate of this diagram is known as the "friction factor" and is the product $8gsd/V^2$, where g is the acceleration of gravity, s is slope, d is the depth, and V is average velocity. The abscissa is known as "Reynold's number" and is the product $4\rho Vd/u$, where V is average velocity, d is the depth, ρ is density of the liquid, and u is viscosity. Roughly, the diagram contains two branches, A and B. Branch A applies only to liquids moving by laminar flow, and curves B, B', and B'' only to liquids moving by turbulent flow. With A goes a formula such as the one given by Jeffreys.[5] For branch B several empirical formulas are known, of which the most familiar is that of Chezy.

Palmer finds, on the basis of the Chezy and Kutter formulas, that the Alika flow moved 11 times more slowly than a stream of water flowing under identical conditions. As far as the abscissa is concerned, this results merely in a horizontal shift in the diagram, which is unimportant, since curve B is almost horizontal. With the abscissa, however, the fact that V for the lava was 11 times as small as for water means that $8gsd/V^2$ is 121 times as large as for water. Such a flow would be represented in the diagram by a point 121 times as high above the origin as most points of curve B, and therefore the Alika flow could not have been turbulent but must have been lami-

[5] Harold Jeffreys, "The Flow of Water in an Inclined Channel of Rectangular Section," *Phil. Mag.*, Vol. XLIX (1925), p. 794.

nar. However, Palmer assumed that the flow ran in a channel whose roughness coefficient (n in Kutter's formula) was approximately 0.014. If we assume that the channel was much rougher than this and had a roughness coefficient (n in Kutter's formula) of 0.037, which would seem to be much nearer the truth, then a point on a curve lying between curves B' and B'' of Figure 1 would represent a stream of water of the same dimensions as the Alika flow running

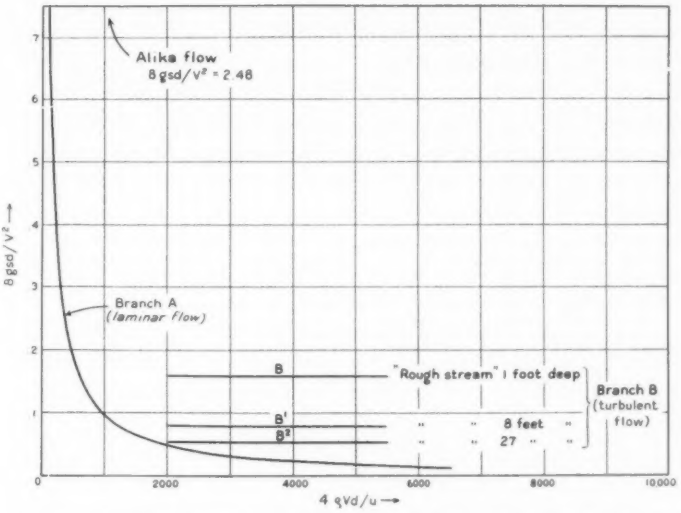

FIG. 1.—Branch A is a curve for laminar flows. If the depth, velocity, and slope of such a flow are known, the viscosity of the liquid can be obtained from this curve. Curves B, B', and B'' are for turbulent flows of various depths, having rough bottoms. If the depth, velocity, and slope of a turbulent flow are known, the viscosity of the liquid can be obtained from these curves.

under identical conditions. Calculation shows that $8gsd/V^2$ for the Alika flow is 2.48. As the value of $8gsd/V^2$ for any point on a curve lying between curves B' and B'' must have been less than 0.1, it is evident that on this assumption also the Alika flow must be represented by a point on branch A and that therefore it was not turbulent. Palmer's error lies in the fact that he applies to branch B a property which belongs only to A—namely, that velocity is inversely proportional to viscosity.

If the computed velocity of the stream of water had been about the same as that of the lava flow, two solutions for the viscosity of the lava would have been possible. The conditions of velocity, density, slope, and depth in this case could have been satisfied by a relatively fluid liquid flowing with turbulence and by another liquid of greater viscosity flowing with laminar motion. This can be seen graphically in Figure 1. From the value of $8gsd/V^2$, calculated from the velocity, slope, and depth of the flow, a value for $4\rho Vd/u$ can be obtained from the curve for laminar flow. From this value of $4\rho Vd/u$, a value for u (viscosity of lava) may be calculated, since V, d, and ρ are all known. Similarly, a smaller value for u (viscosity) may be obtained from the curve for turbulent flow. Gravity does not succeed in making the liquid of low viscosity flow more rapidly than the more viscous liquid, because the liquid of low viscosity uses up energy in turbulence, whereas in the case of the more viscous liquid the force of gravity is not so largely expended in overcoming internal resistance. Which is the correct solution can be determined only if it is known whether the flow was turbulent or laminar.

Becker[6] calculated the viscosity of the 1840 flow of Hawaii and found that it was 60 times that of water. He made the same error as did Palmer, for he also assumed that velocity is inversely proportional to viscosity. An analysis similar to that made for the Alika flow proves that the 1840 flow was also of the laminar type.

Since, however, Becker failed to give the essential data on which his computations rest, no further analysis of the 1840 flow is profitable.

In the application of this analysis to these problems, the help of Professor J. P. DenHartog is specifically acknowledged.

VISCOSITIES OF ALIKA AND 1887 FLOWS

As the Alika flow was of the laminar type, its viscosity can be calculated by the Jeffreys formula.[7] This formula applies to cross sections in which the width is much greater than the depth; however, no large error should be involved if this formula is used with cross sections of other dimensions. The Jeffreys formula in c.g.s. units is

$$V = \frac{g \sin A \, d^2 p}{3u},$$

[6] *Op. cit.*, p. 29.

[7] *Op. cit.*, p. 794.

where V is mean velocity with regard to depth, g is acceleration of gravity, A is angle of inclination, d is depth, u is ordinary coefficient of viscosity, and p is specific gravity. Jaggar[8] observed the pahoehoe stream in the main channel of the Alika flow to be moving at the rate of 11 miles per hour. He believes that the channel was from 20 to 40 feet wide and from 15 to 30 feet deep. Recent topographic mapping shows the gradient of the channel to be about 500 feet in $\frac{3}{4}$ of a mile, or about 12.6 per cent. If we assume that the depth of the Alika flow was 20 feet (Jaggar thought it to be between 15 and 30 feet), and that its specific gravity when liquid was 1.4, the vis-

TABLE 1

Substance	Temperature C.	Coefficient of Viscosity	Authority
Ice, glacier	.....	12×10^{13}	Deeley
Pitch	0°0	51×10^{10}	Trouton and Andrews
Pitch	15.0	1.3×10^{10}	Trouton and Andrews
Wax, shoemaker's	8.0	4.7×10^{6}	Trouton and Andrews
Water	20.0	.01005	Bingham and Jackson
Glycerin	20.3	8.30	Schöttner
Sugar	109.0	2.8×10^{4}	Tammann
Alika flow	.....	4.3×10^{4}	Calculated by the Jeffreys formula
1887 flow	.....	4.77×10^{4}	Calculated by the Jeffreys formula

cosity as calculated by the Jeffreys formula is 4.3×10^4 poises. This is about 287,000 times the value calculated by Palmer for this flow.

Thanks to the careful mapping of the 1887 flow of the Kau district, Hawaii, by Stearns,[9] it is possible to estimate its viscosity. From Stearns's work it appears that the average velocity of the 1887 flow was 0.7 mile an hour, its average thickness is 7 feet 3 inches, average gradient 354 feet to the mile, average width 4,000 feet, and the specific gravity when liquid must have been approximately 1.4. Using these data and the Chezy and Kutter formulas it is found that water would flow under the same conditions 40 times as fast as did the 1887 flow. Therefore, the 1887 flow was also of the laminar type. Using the Jeffreys formula and Stearns's data, its viscosity is

[8] Palmer, *op. cit.*, p. 2.

[9] Harold T. Stearns and William O. Clark, "Geology and Water Resources of the Kau District, Hawaii," *U.S. Geol. Surv. Water-Supply Paper 616* (1930), p. 74.

4.77×10^4 poises, or about the same as that calculated for the Alika flow, using the same method.

From the table of viscosities of familiar substances (Table 1), it will be seen that the viscosities of both the Alika and 1887 flows as calculated by the Jeffreys formula seem reasonable. They are smaller than the viscosities of glacial ice, pitch, and shoemaker's wax, but larger than those of water and glycerin. It will also be noted that the viscosities of the two flows are similar to that of sugar at 109° C. Sugar at this temperature is a somewhat pasty liquid, which nevertheless flows out of an inclined test tube.

EXPERIMENTAL WORK ON VISCOSITY

In order to measure the relative viscosity of the lava in the lake of Halemaumau and in the lower southwest rift cone, Jaggar[10] built a cylinder 27 inches long with an inside diameter of 3 inches, which was attached by a reducer to a 1-inch pipe. A flat iron cap with a central circular orifice 1.5 inches in diameter was fastened over the open end of the cylinder. After being heated over the hot lava, the cylinder and pipe were thrust into the lava to a depth of 1 meter and held there for four minutes. At the first locality it was found on withdrawal that the lava had filled approximately 83 per cent of the cylinder, while at the lower southwest rift cone only a third of the cylinder was filled. The temperature of the lava in Halemaumau pit was found to be 1,200° C. and the temperature in the lower southwest rift cone was 1,100° C. Although it is not possible with these data to make an accurate calculation of the viscosity of the lava either in the lake or in the cone, it is obvious that the viscosity was of a very high order, much greater than that calculated by Palmer and Becker and probably of the same order as that here determined for the Alika and 1887 flows. In so far as the lava in the lake and in the southwest rift cone is similar to that which formed the Alika flow, these experiments favor the estimate of viscosity obtained with the Jeffreys formula over those made by Palmer.

Volarovich[11] has measured the viscosity of dry melts of basalt at various temperatures. His results are shown in Table 2.

[10] T. A. Jaggar, "Experimental Work at Halemaumau," *Bull. Hawaiian Vol. Observ.*, Vol. IX (1921), pp. 28–29.

[11] M. P. Volarovich, D. M. Tolstoy, and L. I. Korčemkin, "A Study of the Viscosity of Molten Lavas from Mount Alaghez," *Compt. Rend. (Doklady) Acad. Sci. U.S.S.R.*, Vol. I(X), No. 8(85) (1936), p. 334.

It will be noticed that two values for viscosity are given for 1,160° C. This is due to the fact that at 1,160° C. the basalt began to crystallize during measurement. Consequently, the viscosity at this temperature increased with progressive crystallization.

TABLE 2

BASALT

Temperature C.	Absolute Value of Viscosity—Poises
1,400°	3.53×10^2
1,340	6.50×10^2
1,320	8.20×10^2
1,280	1.34×10^3
1,220	2.96×10^3
1,160	6.82×10^3
1,160	1.36×10^4

Kani[12] also has measured the viscosity of dry melts of an olivine basalt at various temperatures. His results, which check rather closely those of Volarovich, are shown in Table 3.

TABLE 3

OLIVINE BASALT

Temperature C.	Absolute Value of Viscosity—Poises
1,400°	1.37×10^2
1,350	1.76×10^2
1,300	2.96×10^2
1,250	6.56×10^2
1,200	3.18×10^3
1,150	3.79×10^4

The temperatures of the Alika and 1887 flows were probably between 1,150° and 1,200° C. It will be noticed that the viscosities obtained by the Jeffreys formula for these flows are slightly higher than those of the dry melts at these temperatures. One should, however, expect the viscosities of the Alika and 1887 flows to be lower than those of these dry melts at similar temperatures, because lava flows when molten contain dissolved gases as well as bubbles of gas that may make up as much as 50 per cent of the volume of the flow. It is impossible to say in a quantitative way how the presence of this

[12] K. Kani, "The Measurement of the Viscosity of Basalt Glass at High Temperatures, II," *Imperial Acad. Tokyo Proc.*, Vol. X (1934), p. 82.

gas would affect the viscosity. However, it seems unlikely that it would lower it to anything like the figures given by Becker and Palmer. The fact that the viscosities here calculated are higher than those of the dry melts, whereas because of their dissolved gases we should expect them to be lower, may be explained, first, by assuming that crystallization had already started while the flows were still in motion; second, by the fact that in the case of the 1887 flow the velocity used was the average rate at which the front of the flow advanced rather than the channel speed, which, if used in the calculation, would have given a lower figure for the viscosity of the flow; third, the temperature of the flows may have been lower than 1,150° C., the lowest temperature at which viscosities were experimentally measured; and, fourth, the 1887 flow undoubtedly had to fill in depressions in the terrane over which it flowed. This ponding delayed advance and consequently the estimate of its velocity is undoubtedly too low and therefore its calculated viscosity is too high.

SUMMARY ON VISCOSITY

In conclusion, it has been shown that the viscosities calculated by Palmer and Becker for the Alika and 1840 flows are based on the faulty assumption that the flows were turbulent. The viscosity of the Alika flow calculated by means of the Jeffreys formula, which assumes laminar flow, was found to be 4.3×10^4 poises or 287,000 times that calculated by Palmer. The viscosity of the 1887 flow was 4.77×10^4 poises. The experimental data of Jaggar, Volarovich, and Kani are consistent with these estimates but are not in harmony with those of Palmer and Becker.

APPLICATION OF THE JEFFREYS FORMULA TO THE McCARTYS FLOW

THE McCARTYS FLOW

The McCartys flow[13] in Valencia County, New Mexico, is a pahoehoe basaltic flow, more than 30 miles long, which is probably of historic age. The last 6 miles of the flow were studied in great detail during the field seasons of 1934 and 1935. The following assumptions and calculations are made with the object of obtaining an

[13] Robert L. Nichols, "Quaternary Geology of the San José Valley, New Mexico," *Geol. Soc. Amer. Proc. for 1933* (Abst.), p. 453.

estimate of the velocity of the flow in this area and the rate of extrusion of lava from the source.

VELOCITY

The gradient of the last 6 miles of the McCartys flow is about 30 feet per mile. The roughness of the terrane over which it moved was probably similar to that of a channel having a high roughness coefficient. Unfortunately, since the flow is uneroded, it is difficult to

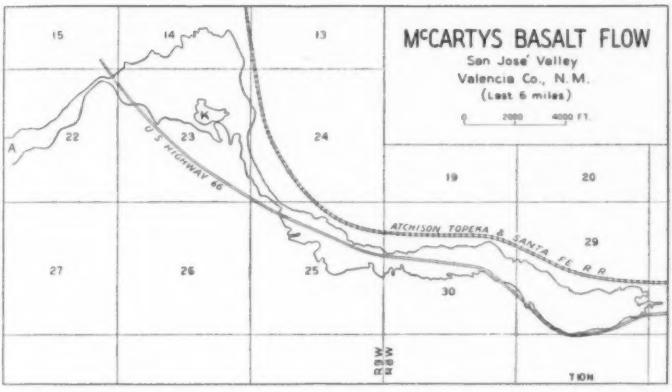

FIG. 2.—Map showing the last 6 miles of the McCartys flow, central New Mexico. The area marked *K* is a kipuka.

get accurate data on its thickness in this area. However, an approximate figure may be obtained from the depth of the larger cracks, from the depth of the collapse depressions, by a study of the edge of the flow around a kipuka, and by a comparison with the Laguna flow,[14] which is similar petrographically but eroded so that its thickness can be measured. Measurements around the kipuka shown in Figure 2 indicate that the flow in this area is about 15 feet thick; however, where the flow is narrow it is probably as much as 50 feet thick. Thirty feet is probably a good figure for the average thickness of the last 6 miles of the flow and its average width is about 1,500 feet. Using these data and the Chezy and Kutter formulas,[15] it appears that a stream of water of the same dimensions as the

[14] *Ibid.*

[15] Harris, *op. cit.*, pp. 108–11.

McCartys flow, flowing under identical conditions, would flow with a speed of 24 miles per hour. If it is assumed that the McCartys flow moved with less than one-half this speed, and this seems reasonable, an analysis similar to that made for the 1887 and Alika flows of Hawaii proves that the McCartys flow flowed by laminar motion.

If it is assumed that the viscosity of the McCartys flow was similar to that of the 1887 flow of Hawaii as calculated above, an assumption which is probably not greatly in error as both are basaltic flows, and if it is also assumed that the specific gravity when liquid was 2.0, then by using the data given above and the Jeffreys formula,[16] which assumes laminar flow, it is found that the average velocity for the last 6 miles was 4.8 miles per hour. At this velocity the lava would have moved from point *A* on Figure 1 to the end of the flow in approximately 1.2 hours.

The foregoing analysis, however, assumes that the lava moved as a single-unit flow. This, however, is not in agreement with the field facts which suggest that the flow, at least in part, moved by the flow-unit mechanism.[17] A flow which moves by multiple units will flow more slowly than one of similar dimensions which flows as a single unit. The slower movement results, first, from the fact that there is a time interval between the extrusion of individual units, and, second, because the units themselves move more slowly than would the whole mass as a single unit, since velocity, other things being equal, is proportional to the square of the thickness. The total time required to cover the last 6 miles must, therefore, have been in excess of the minimum figure of 1.2 hours. Just how much longer it took is difficult to say. However, if we assume that the flow is composed of 3 flow units of equal thickness, a reasonable assumption, then each unit being one-third the total thickness of the flow would take 9 times as long to move the last 6 miles (approximately 10 hours) as would the flow moving as a single unit. If it is further assumed that the time interval between the extrusion of the units was 5 hours, then approximately 40 hours would be required to cover the last 6 miles. However, the field evidence indicates that only a small fraction of the last 6 miles moved by the flow-unit mechanism. In

[16] Jeffreys, *op. cit.*, p. 794.

[17] Nichols, "Flow-Units in Basalt," *Jour. Geol.*, Vol. XLIV (1936), pp. 617–30.

view of this, 12 hours is probably a good estimate for the time required to cover this distance.

Furthermore, the rate of flow varied at different points within the last 6 miles as shown by the following analysis.

The Jeffreys formula[18] in c.g.s. units is

$$V = \frac{g \cdot \sin A \cdot d^2 p}{3u},$$

where V is mean velocity with regard to depth, g is the acceleration of gravity, A is angle of inclination, d is depth, u is the absolute viscosity, and p is specific gravity. If it is assumed that the density and viscosity of the lava remained constant while the flow was advancing over this 6 miles, and that the gradient was more or less uniform, then it can be seen from the formula that the velocity of the flow must have varied as the square of its thickness. As the lava, due to topography, does vary in thickness, its velocity could not have been uniform but must have been more rapid at one place and less rapid at another. This is, of course, in accord with observations on historic flows in the Hawaiian Islands and elsewhere.

RATE OF EXTRUSION

The area of the flow downstream from point A on Figure 2 is approximately 38,000,000 square feet. If we take 30 feet as the average depth for this part of the flow, its volume is 1,140,000,000 cubic feet. However, collapse depressions resulting from the collapse of the roofs of lava tubes are common in part of this area. The area of the lava tubes was approximately 3,500,000 square feet. If it is assumed that their average height was 20 feet, a figure which seems reasonable when compared with the depth of the depressions which now occupy their sites, and that their cross sections were square, their volume was about 70,000,000 cubic feet. This figure should be subtracted from the volume of the flow calculated above, giving 1,070,000,000 cubic feet for the corrected volume.

Assuming that all of this lava flowed through the lava tube at A in approximately 12 hours, according to the foregoing estimate, about 89,160,000 cubic feet flowed through every hour. However,

[18] *Op. cit.*, p. 794.

as the flow may have been increasing in area upstream from A while it was advancing downstream from A, it is apparent that this is a minimum figure for the rate of extrusion from the cone which fed the flow. If we multiply 89,160,000 cubic feet by 2 for this factor, we are probably not far from the truth. If 120 pounds is taken as the average weight of each cubic foot, then approximately 10,699,000 tons of lava per hour were extruded.

Stearns and Clark[19] found that the rate of extrusion for the 1887 flow of Hawaii was 2,250,000 tons per hour. This is about one-fifth the rate of extrusion for the McCartys flow.

ACKNOWLEDGMENTS.—Professor J. P. DenHartog, as acknowledged in the text, furnished the requisite data and method for the application of dimensional analysis to the problem of the flow of lava. Helpful suggestions of a more general character have also been made by Professors Kirk Bryan and R. A. Daly of Harvard University and Dr. Richard Tousey of Tufts College. Professor Bryan also assisted the author in the preparation of the manuscript. Thanks are due to Dr. Karl T. Benedict, Mr. Robert S. Folsom, and Mr. Charles E. Stearns for field assistance.

[19] *Loc. cit.*

GRAVITATIONAL ACCUMULATION OF OLIVINE DURING THE ADVANCE OF BASALTIC FLOWS[1]

RICHARD E. FULLER
University of Washington

ABSTRACT

Late Tertiary basaltic flows in southeastern Oregon show locally a surface depletion and a basal concentration of olivine above a chilled basal zone containing scattered phenocrysts of that mineral. Field and laboratory evidence indicates that the mafic grains gradually accumulated in a manner somewhat analogous to the deposition of sand at the delta of a river.

INTRODUCTION

In southeastern Oregon, the most northerly faults of the Great Basin cut a series of basaltic flows which were extruded during the late Tertiary, subsequent to the lavas of the Columbia River Plateau.[2] The most extensive exposure of the series occurs on the high eastern scarp of Steens Mountain and shows the basalt to have a thickness of over 3,000 feet, in spite of the fact that at that locality it directly overlies the thick near-vent facies of intermediate and acidic flows. The glaciation of the youthful valleys which cut the scarp has given rise to remarkably extensive exposures, preserved by the aridity of the climate.

Although the basalt throughout the series is relatively normal both in its mineralogical and chemical composition, the flows exhibit many peculiar characteristics which may be attributed to the initial high volatile content of the lava. The level surface which has been attained even by thin sheets, less than a foot in thickness, testifies to the remarkable fluidity of the lava. The speed with which the series was extruded is indicated by the local merging of successive

[1] Presented in abstract under the title, "Evidence on the Gravitational Accumulation of Olivine during the Advance of a Basaltic Flow," *Bull. Geol. Soc. Amer.*, Vol. XLII (1931), p. 190.

[2] Richard E. Fuller, "The Geomorphology and Volcanic Sequence of Steens Mountain in Southeastern Oregon," *Univ. Wash. Pub. in Geol.*, Vol. III, No. 1 (1931), pp. 101–21.

sheets. A contact which may be clearly defined by vitreous surface features, a change in jointing and a variation in the distribution of vesicles, is locally found to lose its sharp definition and even to become imperceptible on being traced laterally for a few feet, thus indicating that the surface of the lower flow was only partially solidified when submerged by the succeeding flood. The fluidity of the lava may in part be explained by the proximity of the vents from which it was extruded, for a series of dikes which are exposed on the Steens Mountain scarp are similar to the flows in composition.

The fact that the fluidity of the basalt was due principally to a high volatile content is indicated by its characteristic "diktytaxitic" (Greek, *diktuon*, "net," + *taxis*, "arrangement")[3] texture, which is caused by the escape of the volatile constituents of the final mesostasis, leaving a mesh of plagioclase laths together with augite and olivine. This open texture commonly gives the fresh rock a light-gray color near the surface of the flow and adjacent to the major joint cracks. In marked contrast, in the center of the joint blocks, where the volatiles were unable to escape, the rock is characteristically dark, owing to the decomposition of the olivine and the impregnation of the rock with the resulting unstable hydrous product.[4]

FIELD RELATIONS

Although no marked variations were detected to suggest the differentiation of the series as a whole, scattered grains of olivine of megascopic proportions appeared to be increasingly common in the lower flows. The mineral is usually rendered apparent by a thin film of alteration, which gives it a dark iridescent appearance. As a rule, these small phenocrysts, which are about 1 mm. in diameter, appear to be uniform in their distribution, but a remarkable basal concentration occurs in some of the lowermost flows exposed in the valley of the north fork of Willow Creek. The occurrence is accessible on the southern margin of the main cirque at about 200 feet above its base, and also about a half a mile to the north in the cirque of a minor tributary. The exposures in both instances are ideal for

[3] *Ibid.*, p. 116.

[4] Fuller, "Deuteric Alteration Controlled by the Jointing of Lavas," *Amer. Jour. Sci.*, Vol. XXXV (1938), pp. 160–71.

study and the flows locally are relatively free from the effect of deuteric alteration.

In each instance, the specific flows are confined to a section about 50 feet in thickness. Although the individual flows at both localities differ in magnitude, they exhibit similar facies. As is usually characteristic of the series, each flow had sufficient fluidity to attain a relatively level upper surface, which locally shows a thin aphanitic coating superficially oxidized to a fairly brilliant shade of red. Adjacent to the upper surface, the lava, as a rule, exhibits a fairly high concentration of fine round vesicles. With depth, they decrease in number and become larger and more irregular in shape. In marked contrast, long, thin pipe vesicles extend upward from the base of the major basaltic sheets for usually 6 inches to a foot or more, with a fairly constant inclination of about 60°. In this instance, the fact that traced upward they curve predominantly toward the south indicated that the lava was advancing in that direction when air imprisoned beneath it attempted to rise.

These specific flows vary in thickness from approximately 18 inches to 30 feet. Irrespective of their magnitude, they exhibit at their basal surface a sparse content of olivine grains (Fig. 1). Upward, these increase so rapidly in number that they attain a marked concentration even adjacent to the upper portion of the pipe vesicles. The basal olivine-poor zone is thus, as a rule, only a few inches in thickness and is unrelated to the magnitude of the flow. In the overlying zone the olivine attains a maximum concentration of about 30 per cent. Invariably, the flow was found to be capped by a zone which is free from the coarse grains of olivine, although it contains microscopic fragments of that mineral. The relative magnitude of these three zones is independent of the size of the flow.

At the previously mentioned locality to the south of the main cirque, a flow 30 feet in thickness shows these characteristics very clearly. In less than a foot above the base of the flow, the olivine-poor zone grades upward into a remarkably homogeneous olivine-rich zone, which averages approximately 20 feet in thickness. This zone contains about 30 per cent olivine, and has the appearance of a light-gray, coarsely granular rock, because it has been uniformly

impregnated with soda-lime zeolites, which were formed by the partial decomposition of the labradorite laths.

At its upper surface, this zone locally grades rapidly into the capping olivine-free zone, but, as a rule, the slightly irregular contact between the two facies is sharply defined, and even accented by scattered zeolitic amygdules. The fact that an irregular patch of

FIG. 1.—The base of a basaltic sheet less than 2 feet in thickness shows an increase upward in the concentration of olivine grains, which may be observed as dark specks. A 1¼-inch disk adjacent to the contact gives the scale.

vesicular lava in the basal portion of the olivine-free zone may be traced directly into a line of amygdules in the olivine-rich zone gives definite proof of the contemporaneous fluidity of the two zones (Fig. 2). This capping olivine-free zone averages 10 feet in thickness and has a surface which is approximately level, in spite of increasing vesicularity.

The depletion of olivine in the upper portion of the flow and its accumulation in the thick central zone obviously suggest the gravitational separation of that heavy constituent. The chilled base of

the flow, with its low content of olivine, presumably preserves the initial composition of the advancing lava, which had attained a viscosity too great to permit enrichment by the sinking grains. The thinness of this zone, however, indicates that within this insulating coating the fluidity of the lava must have rapidly increased sufficiently to permit the settling of the coarse grains from the overlying

FIG. 2.—The contact of the olivine-rich zone with the overlying olivine-free zone of the 30-foot basaltic flow. The olivine-rich facies speckled with the dark mafic grains is apparent in the lower left. In the center, a line of amygdules leads from the olivine-rich zone to an irregular vesicular patch in the olivine-free zone. Vertical extent of view, 16 inches.

lava. Petrographic examination of the three types supports the evidence of gravitative differentiation and shows the essential difference between them to be dependent on the concentration of olivine.

PETROGRAPHY

The olivine in these flows occurs both as phenocrysts, which attain a length of over 2 mm., and as small grains 0.1–0.3 mm. in diameter. The latter, which appear ubiquitous, are invariably altered in part to a brownish material, which also rims the larger

crystals. This alteration product locally grades into green isotropic chlorophaeite,[5] from which it has been oxidized by atmospheric agencies. The olivine in the basal zone is less altered (Fig. 3). The larger grains are predominantly idiomorphic crystals or angular fragments, although they are locally slightly embayed by the

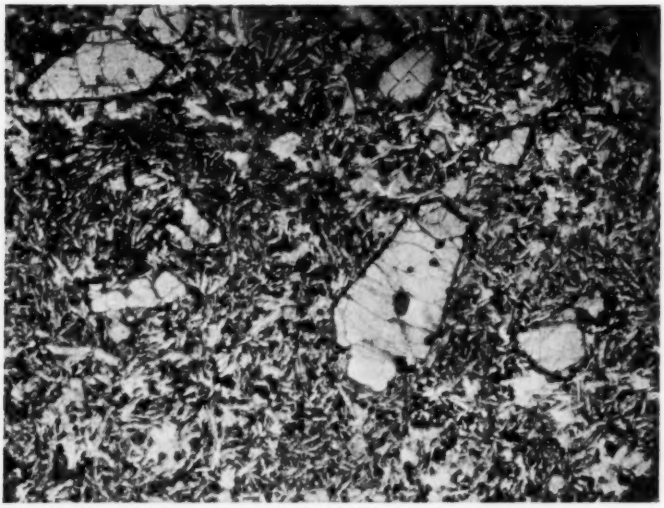

FIG. 3.—Photomicrograph of the basal olivine-poor zone of the 30-foot flow. The coarse olivine appears as idiomorphic crystals or as angular fragments in a ground composed largely of feathery labradorite with interstitial ferruginous material. The small light patches are formed of zeolites. The field is 7.5 mm. in lateral extent.

groundmass. In the olivine-rich zone (Fig. 4) the idiomorphism is less apparent, owing to the progress of marginal alteration, resorption, and fracturing, which is indicated by the contrast of the altered and unaltered margins on the same crystal.

Aside from the concentration of olivine, which forms approximately 30 per cent of the olivine-rich rock, the most marked distinction between zones lies in the mafic constituents of the groundmass. In the basal zone the augite is barely distinguishable in the dark ferruginous ground, while in the central olivine-rich zone it

[5] M. A. Peacock and R. E. Fuller, "Chlorophaeite, Sideromelane, and Palagonite from the Columbia River Plateau," *Amer. Min.*, Vol. XIII (1928), pp. 361–69.

occurs in ophitic texture as crystals ranging up to 1.5 mm. in diameter. This marked change in grain size, observed in the 30-foot flow in the main cirque of the north fork of Willow Creek, has been accompanied by only a slight increase in the length of the labradorite laths from an average about 0.4–0.6 mm. and the development of a

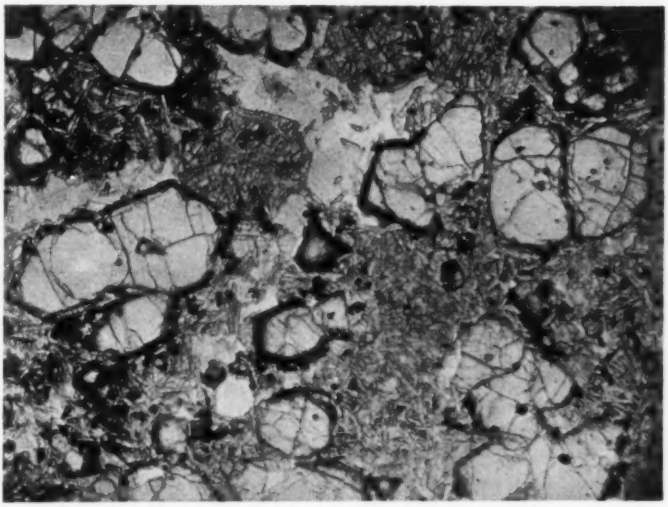

FIG. 4.—Photomicrograph of the olivine-rich zone of the same flow as Figures 3 and 5. The numerous olivine phenocrysts are here more altered at their margins to a reddish brown. The ophitic augite, which is in part idiomorphic, includes altered laths of labrodorite, which locally protrude into the colorless thompsonite and chabazite. Lateral extent of field is 7.5 mm.

slightly less feathery appearance. In both upper facies the plagioclase is largely altered to zeolites at the margins of the laths and in a minute network of intersecting fractures. Since the hydrous content of the final mesostasis thus resulted in the resorption of feldspathic material, it apparently impeded the growth of the laths.

In the capping zone (Fig. 5) the augite, as well as the included laths of plagioclase, shows the alteration to zeolites, which here are more abundant and contain turgid patches which were presumably formed by the mafic constituents liberated by the reaction. The zeolites occur principally as amygdules which fill either vesicles or irregular cavities normally left by the escape of the final volatiles

of the mesostasis. The zeolites, by impregnating the diktytaxitic rock, appear to be intergrown with idiomorphic crystals of labradorite, augite, and olivine. These zeolitic patches are usually bordered by fibrous thompsonite, while the center is formed of chabazite. These minerals, which indicate the hydrous content of the lava, are

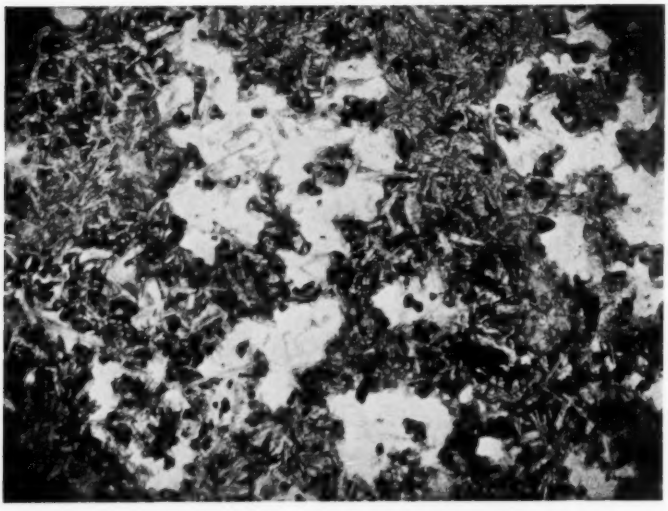

FIG. 5.—The upper zone of the flow free from the coarse crystals of olivine, but still containing minute particles of that mineral partly discolored to a reddish brown. The irregular white patches are diktytaxitic cavities filled with thompsonite and chabazite derived from the decomposition of the labradorite and part of the ophitic augite. Lateral extent of field is 7.5 mm.

not so apparent in the thin sheets where the volatiles could have escaped more easily.

CHEMICAL ANALYSES

Chemical analyses of the three zones of the 30-foot flow give definite quantitative figures for studying the relative change in the composition of the flow during its differentiation (Fig. 6). The two upper zones appear to be so homogeneous that the original location of the specimen has probably little significance, but, owing to the gradation in the thin basal zone, its composition undoubtedly would show considerable variation, depending on selection. For the analysis of this zone, the rock came from 3 to 4 inches above the base of

the flow. It shows a low concentration of olivine, but not the extreme minimum.

An analysis of the olivine confirmed the fact that it is fairly close to forsterite in composition, having an MgO content of over 43 per

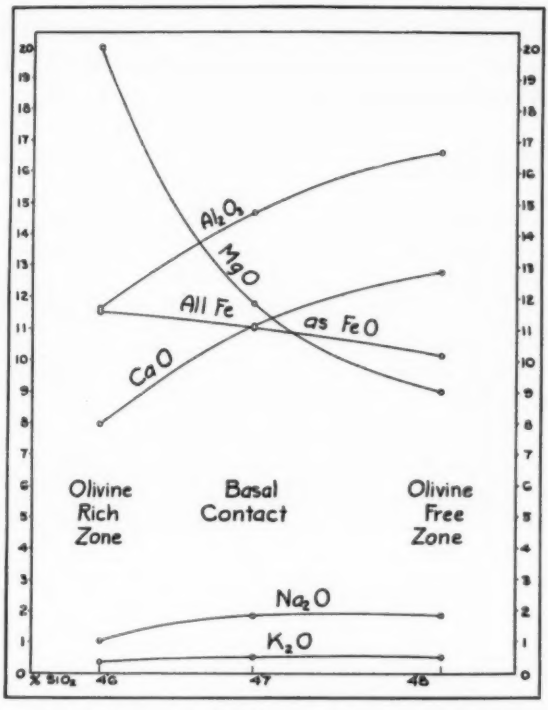

FIG. 6.—Variation diagram plotting chemical analyses by W. H. and F. Herdsman of the three zones of the 30-foot flow exposed at the base of the main cirque of the north fork of Willow Creek. These rocks had a relatively uniform hydrous content of approximately 4 per cent. The oxides are calculated water free.

cent, while the FeO was recorded as less than 15 per cent. As would therefore be expected, a variation diagram of the major chemical constituents of the three rocks showed the central zone to be enriched only in magnesia and, to a slight degree, in ferrous oxide, the only two components in which the upper zone has been impoverished. In each instance the basal zone lies between the two extremes.

The diagram, however, indicates that the enrichment of the central zone in its content of MgO was nearly three times greater than the degree to which that constituent was reduced in the upper zone. Since the upper zone has now only half the thickness of the central zone, this depletion in olivine can account for the enrichment of only one-sixth of the concentration beneath it. If the mass of the rock is considered, the vesicularity of the surface lava renders this discrepancy even greater.

TABLE 1*

CHEMICAL ANALYSES

	I†	II†	III†
SiO_2	44.40	46.10	43.60
Al_2O_3	13.86	14.90	11.09
FeO	5.53	8.28	8.36
Fe_2O_3	5.47	1.54	2.92
MgO	11.17	8.60	19.12
CaO	10.50	12.24	7.60
Na_2O	1.70	1.80	1.02
K_2O	0.45	0.51	0.33
H_2O+	3.90	3.75	3.90
H_2O-	1.50	0.50	0.90
CO_2	none	none	none
TiO_2	1.38	1.60	1.05
P_2O_5	0.12	0.12	0.16
S	none	none	none
MnO_2	0.18	0.24	trace
	100.16	100.18	100.05

* By W. H. and F. Herdsman, of Glasgow.

† I, Base of olivine rich flow; II, capping lava free from the coarse grains of olivine; and III, olivine rich zone.

INTERPRETATION

All these facts may be explained by postulating the gradual accumulation of the olivine phenocrysts at the base of a relatively stagnant flood of basalt, which was being continuously augmented in depth by the advance of very fluid surface lava. Presumably, the fresh lava advanced with a relatively constant low rate of flowage, which permitted the sinking of the olivine crystals into the still fluid earlier lava beneath it. The grains would have finally come to rest on the upper surface of the solidified basalt, which would have been progressively crystallizing from the chilled base of the flow. The high volatile content of the lava is indicated both by the presence of zeolites and by the hydrous content recorded in the chemical analy-

ses. These constituents, which undoubtedly contributed greatly both to the fluidity of the mesostasis and to the reduction of its specific gravity, would have been retained in the lower zone of the flow because they were unable to escape through the more highly heated upper zone.

A temporary change in the rate of flowage would have locally permitted the surface of the lava to solidify and would have thus formed an impervious layer through which the olivine grains from the subsequent floods of surface lava were unable to sink. This is indicated by intermittent flow contacts at both localities, defining differentiated sheets less than 2 feet in thickness and yet exhibiting the same characteristics as the larger flows, except for a lower degree of crystallization of the groundmass (Fig. 1). Some of these contacts have a very limited extent, and disappear horizontally within a few feet, thus permitting the upper sheet to merge with the underlying flow. With the disappearance of this glassy contact, the local accumulation of olivine grains also ceases, indicating that the mafic grains were successful in sinking through the still fluid lava to accumulate on the surface of the main olivine-rich zone.

Daly,[6] in referring to the original brief description of this occurrence, which the writer published in abstract,[7] remarked that no statement had been made as to why "the crystals were dropped in special number at this particular spot." An explanation of this phenomenon depends on the proximity of the above-mentioned fissures from which the lava must have been extruded. Presumably the grains of olivine accumulated adjacent to the vent where the lava, still retaining its maximum fluidity, experienced a reduction in velocity, owing to the low gradient on which it advanced. The coarseness of the ophitic texture in the olivine-rich zone indicates an absence of movement during solidification and suggests that the flow actually ponded while it was being deepened by fresh floods advancing on its surface. The basal accumulation of olivine was, therefore, somewhat similar to the deposition of sediments at the delta of a river. The viscosity of the lava, however, being greater than that of water, delayed the process and widened the area of deposition.

[6] R. A. Daly, *Igneous Rocks and The Depths of the Earth* (New York: McGraw-Hill Book Company, 1933), p. 350.

[7] "Evidence on the Gravitational Accumulation of Olivine . . . . ," *op. cit.*

DETAILED GEOLOGICAL MAPPING AND FAULT STUDIES OF THE SAN JACINTO TUNNEL LINE AND VICINITY

L. H. HENDERSON
Banning, California

ABSTRACT

In driving the 13-mile San Jacinto Tunnel on the Colorado River Aqueduct water was tapped in a fault intersected a short distance from the Potrero shaft. A geological investigation was made in an effort to determine whether additional faults were present in the mountain mass to be penetrated by the tunnel. The use of aerial photographs facilitated structural studies and geological mapping of the area. During the course of this survey, a number of faults were identified which were expected to be sources of difficulty in driving this tunnel. The geological features involved in a change in the alinement of the tunnel and the location of an additional access to expedite the completion of the tunnel are herein described.

The 13-mile San Jacinto Tunnel, located near Banning, California, is one of 38 tunnels which comprise 108 miles of the 392-mile Colorado River Aqueduct being constructed by the Metropolitan Water District of Southern California. In the early stages of the construction of the San Jacinto Tunnel, excavation had advanced only 160 feet east from the Potrero shaft when a shear zone was penetrated. As this fault was entered a flow of water estimated at 7,500 g.p.m. surged into the heading accompanied by over 1,000 cubic yards of rock debris. The tunnel was quickly flooded and the water finally filled the 815-foot shaft to within 160 feet of the surface. When these workings were ultimately de-watered, a detailed geological investigation of the San Jacinto Tunnel line was initiated to determine whether or not, in the light of current developments, additional faults might be encountered in driving this bore.

The San Jacinto Tunnel line traverses the western slope of the San Jacinto Mountain, through the rugged, brush-covered highlands which divide the San Gorgonio Pass and the San Jacinto Valley.

The rock units involved in the immediate vicinity of the San Jacinto Tunnel line are predominantly granites, with subordinate masses of metamorphic rocks, including schists, crystalline limestone, and quartzite. Inconspicuous patches of Tertiary sandstones and shales also occur near Potrero shaft.

Particularly in localities where crystalline rocks prevail, faults are seldom so obvious that they make themselves immediately known to the observer, and the detection of faults is usually somewhat difficult, generally requiring very close observation and tedious work on the part of the geologist.

FAULT CRITERIA

Faults may be expressed at the surface of the earth in a number of different ways. By virtue of the movement along faults, geologic and topographic phenomena are developed to varying degrees, depending largely upon the class and the intensity of the faulting. These fault expressions may be presented on a grand scale or may be obscure. Subsequent to the occurrence of a fault, erosion and weathering soon modify its surface expressions, sometimes by accentuating but more frequently by masking the previously existing evidence.

Some of the more important features expressed by faults are as follows:

1. Gouge in and along a fissure.
2. Brecciation of rock in and along walls of a fissure.
3. Striations and polish (slickensides) along a fracture surface.
4. Shear zones: Parallel fractures which divide the rock into thin slices.
5. Offset dikes: Quite often dikes or other original structures do not match up on opposite sides of a fissure, thus indicating displacement.
6. Rifts: Narrow depressions.
7. Kernbuts and kerncols: Narrow benches or ridges along the downhill side of a fault and paralleling the mountain slope instead of trending to the more natural direction down the slope.
8. Alinement of springs: Springs commonly issue along faults. Therefore, an alinement of springs strongly suggests a fault.
9. Unconformable drainage lines: Drainage channels are often developed along faults because of the weak crushed material along the fault. Fault-controlled drainage lines are generally straight and ignore in trend the natural drainage gradients.
10. Alinement of saddles: Owing to the easily eroded, triturated material along a fault, saddles are frequently formed where the fault crosses ridges.

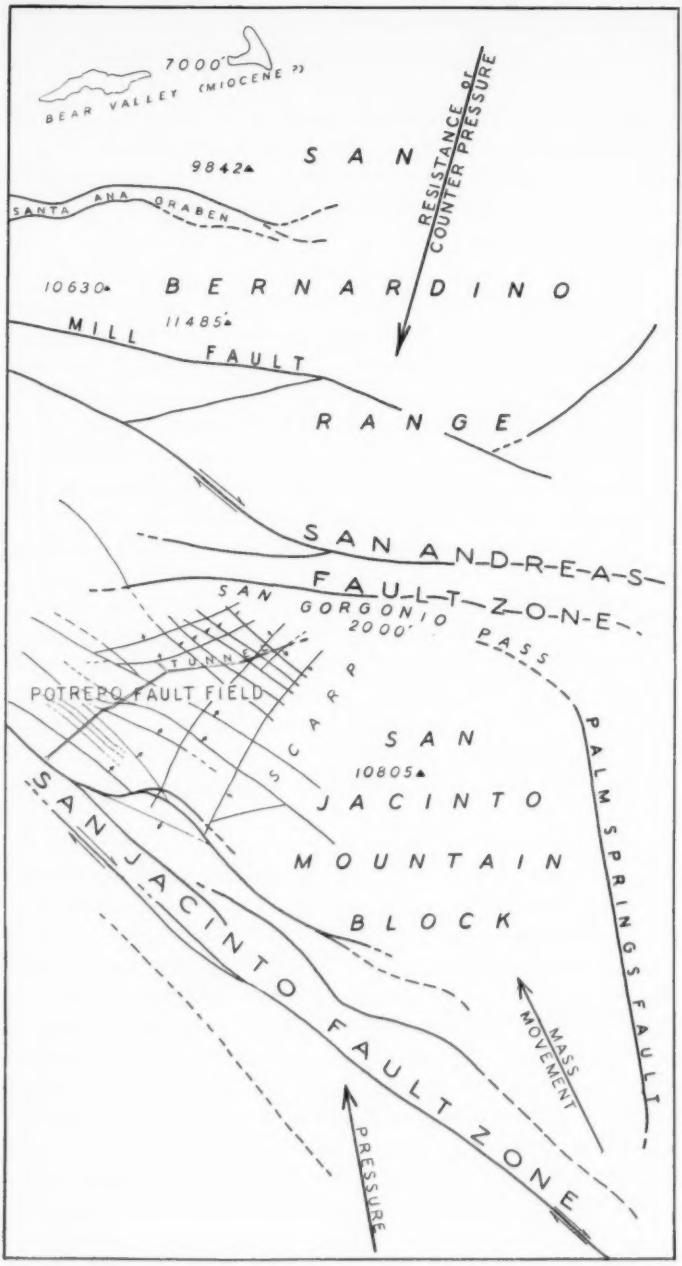

FIG. 1.—Prominent faults in the vicinity of the San Jacinto tunnel (Potrero fault field) and fault systems of adjoining areas. (Stress analysis after Willis.)

11. Scarps: Straight cliffs or steep slopes quite frequently are due to faulting. A fault scarp when identified is a direct evidence of faulting. Erosion quickly dissects and eventually destroys these steep faces, and, except where the faulting is of rather recent origin, fault scarps are comparatively rare. However, vestiges of these fault features are commonly represented by conspicuously alined faceted spurs and spur ends.

Of the foregoing list of fault manifestations, only those from 1 to 5 inclusive can be accepted as prima facie evidence. The remaining phenomena, although typical of faulting, may also be attributable to other causes and must therefore be applied with discrimination in the identification of faults. This does not mean, however, that the presence of a fault cannot be satisfactorily established unless an actual exposure is found. A fault usually reveals itself slowly by exhibiting bits of evidence which require careful analysis and correlation. When fault indications of questionable character are observed they must be put to test, and when found to be explainable only by faulting, under the prevailing circumstances, they may be confidently used as fault identifications. The various fault criteria other than direct evidence can thus be dependably used, but one alone rarely proves conclusive. Having satisfied these stipulations, a geologist is justified in mapping a fault, even though direct evidence is not available, and he can feel assured of reasonable accuracy in his prognostications.

PRELIMINARY STUDIES AND DETAILED GEOLOGICAL MAPPING OF THE AREA

During the early part of January, 1935, approximately ten days were devoted to a more or less detailed study of the geologic structure in the general vicinity of the Potrero shaft of the San Jacinto Tunnel. This initial study covered a strip approximately 2 miles wide from a point roughly $\frac{3}{4}$ of a mile east of the shaft to about $1\frac{1}{2}$ miles west of the shaft. An adequate topographic map necessary for detailed geological mapping was not available except for a small area in the immediate vicinity of the Potrero shaft. Therefore, no attempt was made at this time to map the various masses of different kinds of rock which occur in the area investigated. All topographic

forms and other features observed which gave rise to a suspicion of faulting were investigated. A careful search was made along the trend of the suspected fault and either by actual exposures or cumulative evidence the presence of a number of faults was established. During the course of this examination nine northwest-striking faults were revealed, which cross the San Jacinto Tunnel line in the section inspected.

Following this work, several days were spent in a preliminary inspection of the area adjacent to the tunnel line between Potrero and Cabazon. During this reconnaissance, indications were noted which strongly suggested the presence of a considerable number of northwest faults crossing the tunnel line in this section. Four faults crossing this area were conclusively identified by either actual exposures or by almost irrefutable evidence. The most conspicuous of these faults is the McInnes fault, which passes through the McInnes ranch located on the Banning-Idyllwild road and near the tunnel line. The McInnes fault is a strong fault of relatively major proportions, which is traceable by exposures, alinement of springs, and strongly evident topographic forms to the northwest and southeast of the McInnes property for many miles.

On May 4, 1935, aerial photographs were obtained of the area 1 mile on either side of the San Jacinto Tunnel line from the east portal to approximately $1\frac{3}{4}$ miles west of Potrero shaft. These photographs afforded excellent control for detailed geological mapping. The photographs, furthermore, made possible a stereoscopic study of the physiographic features of the area, which revealed indications of unsuspected faults and corroborative evidence of those previously suspected and those already designated.

The mapping of the geology of the area covered by the aerial photographs was immediately begun. The contact prints, which cover an area approximately 2 miles by $2\frac{1}{2}$ miles square, were used in conjunction with this work. On these photographs the various rock masses were mapped and a considerable number of northwest-trending faults were traced across the tunnel line in addition to those previously discovered in the Potrero shaft region. Where an actual dip exposure was not found, the dip was generally determined from the attitude of the surface trace of the fault with respect to topo-

graphic anomalies along its course. The faults of the northwest-trending system were found to dip steeply to the northeast, usually about 65°, and few were found to deviate appreciably from this angle of dip.

Four of the faults traced across the San Jacinto Tunnel line during the combined studies are conspicuously strong. These faults were named, respectively, the McInnes, the Goetz, the Potrero, and the Lower Potrero. All consist of a comparatively wide belt of shearing and crushing which is traceable for many miles.

In addition to the numerous northwest faults cutting the area surveyed, several east-west and also northeast trending faults were found. Exposures of a number of very minor faults were also seen which were too inconspicuous to be successfully traced.

The detailed geological mapping of the area, 1 mile to either side of the San Jacinto Tunnel line and from the East Portal to approximately 1½ miles west of Potrero shaft, required about four weeks of field work. Upon the completion of the field work an aerial mosaic was prepared of the area mapped, on which the results of the field work were shown. In addition, a geological section along the tunnel line was prepared on which prognostications were given as to the geological conditions probably to be encountered in driving the tunnel.

Granitic rocks, including granodiorite, quartz monzonite, and quartz diorite are by far the most prominent rock units of the area through which the tunnel line passes. Conspicuous irregular bodies of ancient metamorphic rocks consisting of mica schist, quartzite schist, and crystalline limestone also occur as roof pendants and probably in some instances xenoliths which have been exposed by erosion. With one or two exceptions it was not expected that the masses of metamorphics seen along the tunnel line would extend below the surface to tunnel elevation. Roughly 2 miles west of Cabazon shaft a complex of biotite and quartzite schist is exposed for almost a mile along the tunnel line and it was believed likely that a considerable length of tunnel would be driven in schist in this locality.

As a result of these studies twenty-one faults, striking northwesterly across the tunnel line, were located which were expected to

be sources of difficulty in driving the remainder of the bore. Prior to the completion of the field mapping, two of the faults recognized and their tunnel intersections predicted during the early preliminary work had already been encountered—one at the Cabazon west heading and one at the Potrero west heading. Both were accompanied by large inflows of water. The approximate locations at tunnel elevation of nineteen additional fault intersections were predicted on the geologic section.

In addition to the northwest-trending faults, segments of east-west faults were mapped which might give rise to difficulties in driving the tunnel. For approximately 4 miles east of where the Goetz fault is crossed by the tunnel line, the tunnel line is paralleled on both north and south by segments of east-west faults. These faults exhibit dips to the north varying from 45° to 65°. The position and attitude of the east-west faults to the south are such with respect to the tunnel line (original alinement) that at tunnel elevation these faults are likely to be in close proximity to the tunnel. It was believed within the realm of probability that the tunnel (original alinement) would be within the zone of influence of these faults for considerable distances.

At odd times subsequent to June, 1935, the area of investigation was expanded. Some additional study was given portions of the area already mapped, particularly along the north border of this strip, and the geological investigation was extended to cover the intervening territory between the tunnel line and San Gorgonio Pass from the East Portal to Potrero.

GEOLOGICAL FACTORS INVOLVED IN THE LOCATION OF LAWRENCE ADIT AND REALINEMENT OF THE SAN JACINTO TUNNEL

In order to expedite the completion of the San Jacinto Tunnel another entry was proposed, which would permit two additional working faces. A 5,600-foot inclined adit to be driven on a 25 per cent slope from Lawrence Gulch at a point approximately midway between the Cabazon west heading and Potrero east heading was considered the most feasible means of providing such an entry (see Fig. 2). The various geological factors involved were given careful study and consideration in the adoption of this measure to accelerate

the tunnel driving. Construction of this adit was started in March, 1936.

The location of the Lawrence adit appeared to be an excellent one from a geological viewpoint. The adit was located on the south side of Lawrence Gulch, in apparently a relatively undisturbed slice of granite between the McInnes fault and a parallel fault to the east. The adit was located to parallel the northwest fault system, and it was considered highly improbable that faults of any consequence or other adverse conditions would be encountered in the driving of this access. It was realized that two rather inconspicuous northeast faults were likely to be intersected by the adit, but these faults were

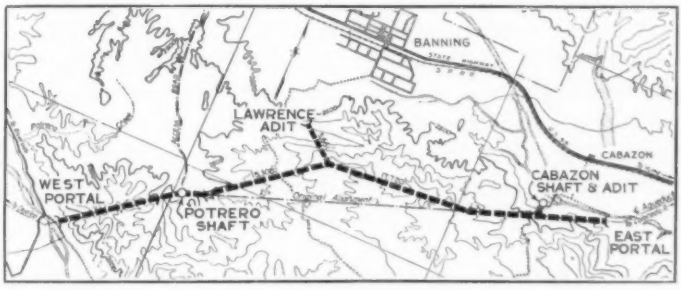

FIG. 2.—The new alinement of San Jacinto Tunnel

determined to be very minor local features with little lateral extent and they were not expected to present any unusual trouble in sinking this incline. The adit was recently completed in record time and the prognostications as to the geological conditions to be encountered proved to be essentially correct.

Before the full significance of the geological factors pertinent to the change of alinement can be fully appreciated, they must be considered in the light of experience gained in tunneling through the various faults encountered in the San Jacinto Tunnel previous to the date of the realinement. By March of 1936 eleven of the twenty-one northwest-trending faults identified during the detailed geological studies conducted early in 1935 had been intersected. The attitude of the respective faults as determined along their surface trace proved to be unusually consistent with depth, and the projected

location at tunnel elevation was consequently found to be a close approximation in each instance. All of these faults were accompanied by inflows of water, the majority of which were large inflows under very high pressures.

It was found that the water occurred in open interconnected fractures and joints in the hanging wall or northeast wall of the northwest-striking, northeast-dipping faults. Out in the hanging wall the fractures became tighter with increased distance from the fault. Where the tunnel heading approached these faults from the east, water under high pressure was generally developed some distance away from the fault plane in hard but somewhat fractured rock. As the heading neared the fault the open fracturing became more prevalent and the volume of water increased accordingly. However, normally, by the time the footwall was reached where gouge and crushed material occurred, the hydrostatic head had been lowered by drainage to a point where no great difficulty was entertained in driving through the soft, crushed material of the fault plane.

On approaching the faults from the west or footwall side, the conditions were found to be considerably more hazardous and difficult. Open fractures at the footwall are few, and the gouge and crushed material present an almost impermeable diaphragm to the waters which may percolate more or less freely along the open fractured hanging wall. When approached from the west the gouge and crushed material of a fault was generally exposed before any great quantities of water developed. As excavation advanced into the fault and the diaphragm was thinned to where the pressures ahead overbalanced the resistance of the remaining interposed material, heavy surges of water, frequently accompanied by tons of material, would result. Encountering large quantities of water under high pressure in the soft, crushed ground made it necessary to advance with extreme caution and to adopt slow and tedious tunneling methods. The records of progress made in fault zones at the Cabazon and Potrero west headings as compared with those of the Potrero east heading demonstrate clearly the advantage of entering the faults from the hanging-wall side.

The construction of the Lawrence adit offered a means of attack-

ing from the hanging-wall side the McInnes fault, which appears to be one of the most menacing faults crossing the tunnel line.

In so far as the geology was concerned, the proposed alinement change offered several distinct advantages over the original line. From the angle point east of Potrero to the Lawrence adit junction, the proposed line crossed all northwest faults, including the strong Goetz and McInnes faults, at a more obtuse angle, thus minimizing in each instance the section of crushed and brecciated material to be penetrated by the tunnel. Furthermore, this alinement avoided a plexus of faults in the Goetz Spring area. Here the Goetz fault bifurcates and is intersected by an east-west fault forming a triangle of probably badly sheared and broken ground. It is believed that on the old alinement the tunnel would probably have encountered in this vicinity from 2,000 to 3,000 feet of sheared and badly fractured ground attended by heavy inflows of water. The new alinement, moreover, would preclude the probability of serious trouble presented by the east-west faults which parallel the original line on the south for a number of miles east of Goetz Spring. It appeared that on the proposed realinement the tunnel would probably intersect an east-west fault immediately east of the Goetz fault crossing. However, the bearing of the alinement change was such that in the event this east-west fault should be encountered, it would be crossed at an acute angle but not paralleled by the tunnel.

On the new alinement the crossing of the northwest faults between the angle point west of Cabazon and Lawrence adit junction would be made at a less favorable angle than on the old line. The faults involved at this section are relatively minor features as compared with the strong McInnes and Goetz faults of the Potrero-Lawrence adit section. Furthermore, the majority of these faults would be approached from the east, which makes them considerably less formidable, and the angle of penetration at this section is obviously of much less importance than it is in the Potrero-Lawrence section where the faults present a much more serious problem.

In brief, the realinement of the San Jacinto tunnel, attendant upon the location of the Lawrence adit, was superior in many respects to the original line, from the standpoint of the geology. Two sources of probably serious trouble were entirely avoided. The major

faults which had to be crossed in any event were to be penetrated at a more favorable angle. The construction of the adit would provide a means of penetrating the strong McInnes fault from a much more advantageous position. By this change in alinement of the tunnel, a number of important advantages were gained and no adverse geological factors of any consequence were introduced.

Following the location of the Lawrence adit, aerial photographs were obtained covering an additional strip to the north of the original area mapped, which included the adit location. The geology was mapped of the added area, which had previously been investigated for faults. A drawing was prepared on which was shown the geology in plan and section of the Lawrence adit and the relocated tunnel line. On this drawing were given the prognostications as to the geological conditions to be encountered in driving the Lawrence adit and the tunnel on the new alinement. Ten northwest faults and one northeast fault were shown crossing the remainder of the tunnel on the new alinement, and two northeast faults crossing the adit. By January of 1938 the two faults had been penetrated by the adit and five of the remaining eleven indicated on the alinement change had been crossed by the tunnel. These faults have also proved to be fairly uniform in attitude with depth, and consequently their predicted locations at tunnel level were found to be reasonably close. Comparatively very little water was developed in the faults crossed by the adit. Of the faults crossed by the tunnel subsequent to the alinement change, the Goetz fault zone, entered from the Potrero east heading, developed considerably the largest inflows thus far tapped.

Nineteen of the twenty-four faults indicated as a result of the detailed geological investigations have thus far been crossed by the tunnel and adit combined. Although no particularly impressive faults occur in the remaining 1½ miles between the Cabazon west and Lawrence east headings, the strong McInnes fault, together with its branches, comprises a wide belt of shearing that must be traversed by the Lawrence west heading. However, inasmuch as this fault will now be approached from the hanging-wall side, it is anticipated that the tunneling difficulties throughout this section will therefore be minimized.

MASS TRANSPORTATION OF SEDIMENTS ON SUBAQUEOUS TERRACES

O. F. EVANS
University of Oklahoma

ABSTRACT

Sand ridges having a steep slope on one side and a gradual slope on the other occur on some subaqueous terraces in Lake Michigan which have a plentiful supply of sand. The origin and behavior of these ridges is explained in connection with one class of beach cusps. A similar subaqueous mass movement of sand on a larger scale is described as it occurs off a large cuspate projection such as a cape. An understanding of the behavior of subaqueous dunes is important in explaining the common occurrence of cross-bedding, the preservation of ripple marks and other bottom irregularities, and the embedding in sediments of organic remains and other objects.

In a discussion of the origin of beach cusps the author[1] mentioned the existence of ridges on certain subaqueous terraces having a plentiful supply of sand. One class of beach cusps was explained as being formed by these sand ridges joining the shore. At the time this article was written, the origin and behavior of the ridges had not been carefully studied and consequently there was lacking a proper evaluation of their importance as shore features.

Scott[2] mentions the occurrence of such ridges in Douglass Lake and Long Lake in Michigan. They were first observed by the author in Silver Lake near Little Point Sable in Michigan. They appear to form only on certain subaqueous terraces which have an abundant supply of sand and whose slope outward from shore is very gentle. Their outer ends are often a considerable distance from shore, sometimes as much as 200 or 300 feet. Where they join the shore a cusp is present. Occasionally a ridge is found which does not join the shore. In all such cases observed, the ridge after having been formed appeared to have been cut off from the shore by the work of the waves and currents.

The ridges vary in width from a few feet up to about 60 feet. In

[1] O. F. Evans, "The Classification and Origin of Beach Cusps," *Jour. Geol.*, Vol. XLVI (1938), pp. 615–27.

[2] I. D. Scott, "Inland Lakes of Michigan," *Mich. Geol. Survey Pub. 30* (1920), pp. 111 and 246.

Silver Lake, which is the only inland lake where they were studied by the author, their height above the lake bottom is never more than 10 or 12 inches. They are not symmetrical in cross section but slope off gently on one side and more steeply on the other. The steep side usually has the highest gradient near the junction of the ridge and the shore. Here it characteristically stands at the angle of repose for sand under water. Where the ridge joins the shore obliquely, the steep side is nearly always on the side of the acute angle.

Studies during the past summer along the shores of Lake Michigan show that these ridges are the result of an important type of transportation of sediment occurring extensively along the shores of lakes, especially where the subaqueous terrace is above the curve of equilibrium.

As is well known, the east shore of Lake Michigan has an abundant supply of sand. This is easily moved by the waves and currents; consequently the local outline of the shore changes with every storm wind. Sand points of large size form and are in turn destroyed as the waves and currents deposit or carry away the material of the beach. This action is particularly noticeable when the wind blows at an oblique angle to the shore. At such times inequalities in the strength of the waves and currents that impinge on the shore, or differences in the resistance of the shore itself, cause it to be worn away faster at one place than another. Consequently indentations are formed and the material taken out is carried and deposited to leeward along the beach. Much of this sediment is deposited in ridges along the course of currents which leave the shore, forming cusps and ridges somewhat similar to those described above for small lakes. The transportation and deposition of the material takes place essentially as described in textbooks in explaining the formation of spits. Because of dissimilar conditions of lake bottom and difference in the size of waves, these ridges are relatively higher and shorter on the Lake Michigan shore than on the small lakes, although the conditions and processes of formation are the same.

Figure 1 shows typical cusps and ridges on the beach of Lake Michigan. Sometimes only a single cusp is present but frequently a series of two or more are formed simultaneously. The distance between cusps of this type on the Lake Michigan shore varies greatly

but is usually from 100 to 400 feet. In the diagram the wind is from the southwest. The waves are from the west-southwest, being turned somewhat as they enter the shallowing water in approaching the shore. At first, deposition off the points C_1 and C_2 is not very great, but as erosion continues the irregularity of shoreline thereby produced causes a more rapid growth. As the process goes on subaqueous deposition of sand continues at the ends of the cuspate forms. They are thus lengthened, and submerged ridges are formed which increase in length to the northwest. As soon as the formation

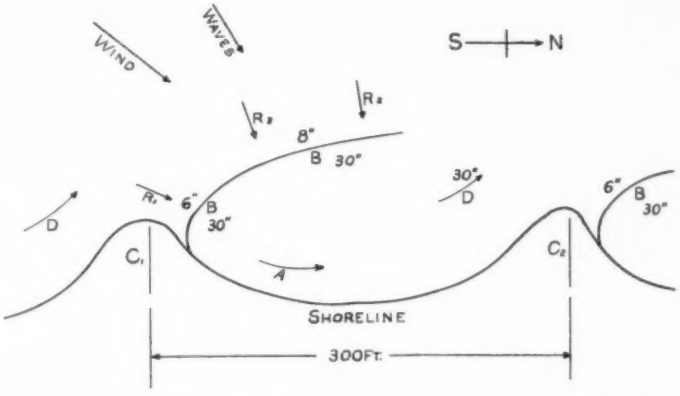

FIG. 1.—Diagram of cusps and subaqueous sand mass at its outer end being driven toward shore by the waves and currents. Figures show depth of water in inches.

of a ridge starts, the incoming waves begin driving it toward the shore. As a result it becomes dune-shaped with the steeper face at B where the sand lies at the angle of repose. On the windward side of the ridges the water deepens very gradually. In the cases observed, the top was almost flat for the first 20 or 30 feet and then sloped toward deep water at the rate of about 1 foot in 15 feet. With waves 18 inches high the current at R_1 was strong, perhaps 10 miles per hour, and current ripples 4–6 inches high and 24–60 inches long were formed. At R_2 the ripples were still unsymmetrical but considerably smaller. Between the steep face of the ridge at B and the shore the bottom was covered with oscillation ripples parallel to

the shoreline. They were thus at an angle to the trend of the face of the advancing ridge and were being covered as it moved toward the shore. In the cases observed, the rate of advance of the bank was about 1 inch in 30 minutes. It is evident that should these sediments become indurated fossil ripple marks would result. The water brought over the ridge by the incoming waves caused a current at *A*, which was in some cases strong enough to superimpose current ripples in the troughs of the oscillation ripples. This water in finding its way out again to deeper water produced an undertow at *D*. This outward-moving current was distinctly felt by a person standing in the water at that point and was also indicated by the shape of the ripples on the bottom. It is evident that some of the sediment carried by this current enters into the building of the next subaqueous ridge extending out from C_2.

One result of the movement of these subaqueous dunes is a migration of the cusps along with them. Measurements made on a series of the cusps near Whitehall, Michigan, showed a migration of 12 feet in three days with a steady southwest wind averaging about 15 miles per hour. It is evident that some erosion takes place on the windward side of the cusp at the same time the ridge moves toward shore, and that the distance between the steep face of the ridge and the shore depends on the relation between the rate of migration of the dune and the rate of erosion of the shore. These in turn are determined by the size and velocity of the waves and the angle at which they approach the shore. Also, as the subaqueous dune ridge from C_1 is extended it tends to protect the shore on the windward side of C_2 from such erosion. The usual result is that the ridge gradually approaches the shore and finally reaches it, thus filling the embayment between C_1 and C_2. The sand of the resulting shallows is then driven toward shore by the incoming waves and again becomes a part of the beach ridge, and thus the cusps disappear. Several cases were observed where the trough between the bank and the shore had been narrowed to a width of from 1 foot to 5 feet, with the bank still approaching the shore and the current running strongly along the trough. In such cases, as is evident, the windward end of the trough, which is the first to become completely filled, is a considerable distance to leeward of the place where the cusp started.

Sometimes this process of subaqueous dune building takes place where only a solitary cusp is present. In such case, if the shoreline is straight for a considerable distance, a ridge of sand may be built from the cusp point to parallel the shore at a distance of 30–50 feet from it. Such ridges may be 1,500–2,000 feet long, and an unwary observer might easily confuse them with the first member of the "ball and low" commonly found along this coast. With strong incoming winds these ridges take on the dune shape and migrate to the shore where the sand in them again becomes a part of the beach ridge.

It is evident that a 45°–90° change of wind and waves will destroy or reverse the system, as shown in the diagram. If the waves drive directly on shore the subaqueous dunes move to the shore, and the system is destroyed although the cusps in a modified form may remain. If there is a 90° change of wind, as from the southwest to the northwest, the system is broken up and a new one may be formed in the opposite direction. One interesting result of such a reversal is that the new system of waves and currents guided by the trough between the subaqueous dune and the shore may succeed in cutting off the ridge at the tip of the cusp, thus forming an isolated shallows some distance out from shore.

The chief importance of these migrating dunelike ridges is that they are the medium by which large amounts of sediment are transported along the shore and over the subaqueous terraces. As a result of such mass transportation, any irregularities of the bottom, such as ripple marks, will be buried and any masses of material, such as shells or pebbles, will be embedded and, in case of later induration of the sediments, will be preserved.

The ridges found on the subaqueous terraces of Silver, Douglass, and Long lakes, as stated earlier in this article, are formed in the same way as those of Lake Michigan. The relatively greater extension in the small lakes of these ridges out from shore and the radial arrangement of some can be explained by the somewhat different conditions of waves and currents which prevail on small lakes. Where ridges are present in Silver Lake the slope of the terrace from the shore outward is very gentle, not more than one-fourth or one-fifth that in Lake Michigan. Also, the waves are very much smaller

and the currents on the shelf are weaker. Winter storms on Lake Michigan sometimes produce waves 15–18 feet high and 200 feet long. Silver Lake is nearly circular and from $1\frac{1}{4}$ to $1\frac{1}{2}$ miles across; the extreme height of the waves on it cannot be much over 3 feet. Also, the curved shoreline causes a constant deflection of the currents set up by the wind. Therefore, when an indentation is produced in the shore, the transported material is carried out more nearly perpendicular to the shoreline and the waves of the smaller lake are less efficient in driving the ridge toward the shore. In both the large and the small lakes, the first material of these ridges comes from the shore, but it is quite probable that during its growth some material is also picked up from the shelf itself and built into the ridge.

It has been shown that cusps, which are comparatively minor topographic features, often play an important part in directing the deposition of sediment by littoral currents. To pass to a more general case, it might be expected that any projection in the shoreline would have a similar effect on the littoral current and would play an equally decisive role in determining the transportation of sediment. Permanent projections, such as capes, may and often do cause the formation of subaqueous dunes much larger than those usually accompanying temporary cusps. A good example is afforded in Crystal Lake, near Frankfort, Michigan.

Crystal Lake was formerly a part of Lake Michigan and still has sandy shores and remarkably clear water and hence is an ideal place for the study of sand movements. About sixty-five years ago a cut was made at its outlet which lowered the level of the lake about 7 feet. This started a readjustment of the shorelines that is still going on. The lake has a length of 8 miles and an average width of about 2 miles. Its trend is from north of west to south of east, and thus the south shore is frequently subject to the strong north and northwest winds of this region. These cause strong currents from west to east which, aided by the waves, are producing extensive erosion and transportation of the sandy material.

Robinson's Resort (see Fig. 2) is situated on the south shore about 3 miles from the west end of the lake. Mr. Robinson, who is an old resident of the region, estimates that the shoreline along his property has been eroded away as much as 200 feet in some places since the

lowering of the lake. To the east of Robinson's the shoreline is somewhat irregular. There are several bays, the largest of which is known as Outlet Bay. Here the overflow from the lake forms a stream that is tributary to the Betsie River. It is here that the cut was made which lowered the lake and that a dam is now maintained which keeps its level fairly constant.

The original shores of the lake along the south side consist of rocky moraines. When the lake was at its old level, the waves cut

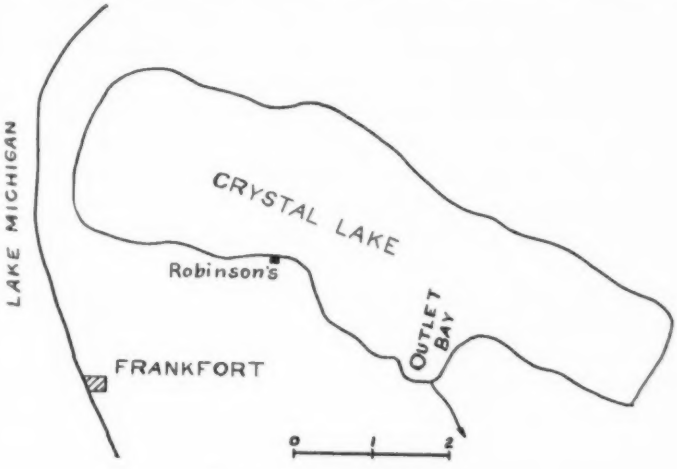

FIG. 2.—Sketch of Crystal Lake

into these and formed terraces, which in many places are paved with glacial boulders. Partly because of this and partly because of the ice push, which is very strong along this shore during the winter, beach ridges are not formed to any extent. Consequently, the movement of sand takes place mostly out beyond the shoreline. This sand is deposited in large quantities wherever the currents are deflected outward from the shore, and the result is the formation of large subaqueous dunes. Their most extensive development is in Outlet Bay.

At Outlet Bay (Fig. 3) the northwesterly winds have a fetch of from 3 to 5 miles. This causes a strong current from the west along the shore at point *P*. The sand brought by this current is deposited offshore to the east of *P*, and the formation of two great dune banks

at A and B has developed. From P to the outer edge of B is about 1,500 feet. Along the edge of A, where the depth changes from 3 to 6 feet, the slope is as steep as it can be in loose sand under water. This slope decreases from A to D, until at D it is the same as at T. The slope of the subaqueous bank at T, being at the edge of the "drop-off," is probably in a state of permanent equilibrium and stands at an angle of about 10° or 15°. To the westward from B the slope decreases in the same way. As the sand is moved by the current out from the shore past the point P, the northwest winds set up currents

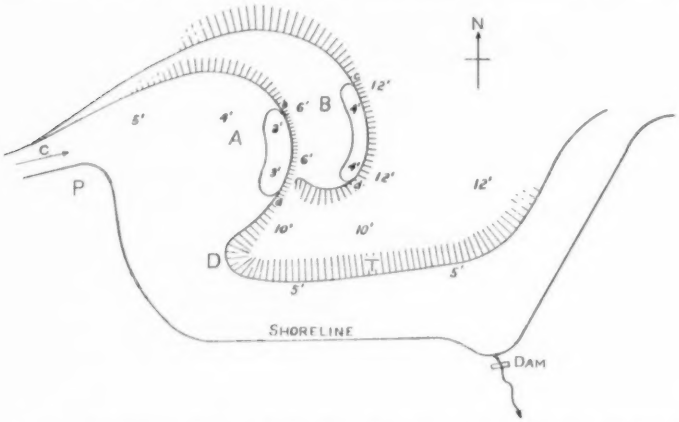

FIG. 3.—Subaqueous dunes at Outlet Bay, Crystal Lake, near Frankfort, Michigan. Figures show depth of water in feet.

that push it to the southeast. The form taken by the mass was probably at first that of a hook under water, but, as more sand was brought in, the formation became wider where it joined the shore until it took the present form. At the 3-foot depth unsymmetrical ripples on the bottom indicate that some movement of the mass to the east and southeast is still going on.

The mass B is the result of further deflection of the current from the west as the size of the mass A increased. On B the depth decreases eastward from 6 feet to 4 feet. This depth of 4 feet at the crest of the subaqueous dune B corresponds to the 3-foot depth on A, and the unsymmetrical ripples again indicate, as on A, a movement of the sand toward the steep slope to the east. Here the depth

suddenly changes from 4 feet to 12 feet, with the sand in the bank standing at the angle of repose. This slope begins to decrease in each direction at *C* and *D*.

It was impossible to get any information from local residents as to the rate of growth of the formations. It has been so slow as to attract little attention. I. D. Scott,[3] who made a geological survey of the lake in 1913, speaks of the formation *A* and the 3-foot depth of water at its edge but says nothing of the shallows at *B*. At the present time the shallow area at *B* is easily seen at the shore; apparently most of its growth has occurred since 1913.

It is evident that the subaqueous dune masses *A* and *B* move parallel to the shore of the bay and in toward it in a way similar to that described in the foregoing discussion of beach cusps. As a result, the bay will finally become filled to a depth of 3 or 4 feet by the continued migration of these dunelike masses. As the shallows become wider, their approach to the south shore will become slower and the last filling of the resulting trough may be by the finer materials from suspension, perhaps aided by the growth of vegetation. After the bay has become shallow or perhaps before it is entirely filled, a spit will probably begin to build out from near point *P*. As this increases in size the winds will build a beach ridge along its windward side. Thus Outlet Bay will finally be separated from the main body of water and become a shallow lagoon or swamp.

It is evident that the movement of sand masses which has been described is in many respects similar to the movement of sand dunes. There is a forward movement of the sand, partly in suspension and partly in ripples, and the formation of a steep lee slope, much the same as in the case of dunes formed above water. The windward slope is less steep than that of a sand dune and the whole mass is much wider in relation to its height. However, the behavior of the sediments is so nearly the same in the two cases as to warrant the use of the term "subaqueous dune." This term is also used by Bucher[4] in describing downstream mass movement of sand in rivers, in which the behavior of the sediments is very similar to that described in the foregoing paragraphs.

[3] *Op. cit.*

[4] W. H. Bucher, "Origin of Ripples and Related Sedimentary Surface Forms," *Amer. Jour. Sci.*, Vol. XLVII (1919), p. 170.

It seems from a general reading of geological literature[5] that the usual mental picture which the geologist has of the deposition of sediments in water is that it takes place gradually and rather uniformly as a result of the finer particles settling from suspension and of the coarser ones being dragged and rolled over the bottom individually or sometimes in ripples. These processes are important in both deep and shallow water, but, where loose sediments are abundant on the subaqueous shelf, mass movement is very common and of great importance.

Among other things, the subaqueous dune movement of sediments is important in explaining the following:

1. Common cross-bedding of shallow-water sediments. It is well known that cross-bedding is produced by sand-dune movement, so it is quite probable that a similar effect is brought about by the movement of dunes under water, especially in those cases where the sand mass crosses and fills a depression.

2. The abundant occurrence of fossil ripple marks. At present there are very few definite criteria for determining the depth at which ancient ripples marks have been formed, but it seems that in a great many cases those found preserved in rocks have been formed in shallow water. Johnson[6] has even expressed the opinion that, because of the constantly changing sediments on a beach, ripple marks are much more likely to be preserved on the sea bottom than close to shore. It would seem that the mass movement of sediments which buries the ripple marks as the subaqueous dunes move forward provides excellent conditions for their eventual preservation.

3. Preservation of shells and other hard materials. The movement of subaqueous dunes provides the same suitable conditions for the burying and preservation of shells and bones as of ripple marks.

4. Occurrence of thin layers of gravel in sandstone. Thin layers of gravel are frequently seen embedded in sandstone. These are somewhat difficult to explain on the basis of settlement of sediments from suspension but are readily explainable on the basis of the covering of the gravel by an advancing sand mass.

[5] D. W. Johnson, *Shore Processes and Shoreline Development* (New York: John Wiley & Sons, Inc., 1919), pp. 113–15, 124–25, and 235–37; Bucher, *op. cit.*, p. 242.

[6] *Op. cit.*, p. 510.

REVIEWS

"Miocene and Pliocene Floras of Western North America," by RALPH W. CHANEY, MAXIM K. ELIAS, ERLING DORF, DANIEL I. AXELROD, CARLTON CONDIT, and CURTIS J. HESSE. *Carnegie Institution of Washington, Publication 476*. Washington, 1938. Pp. 272; pls. 30; figs. 15.

Issued as a unit are five papers dealing with late Tertiary floras of western America: (I) "Late Tertiary Floras from the High Plains," by Ralph W. Chaney and Maxim K. Elias. "With a Chapter on the Lower Pliocene Vertebrate Fossils from the Ogallala Formation of Beaver County, Oklahoma," by Curtis J. Hesse. (II) "A Late Tertiary Flora from Southwestern Idaho," by Erling Dorf. (III) "A Pliocene Flora from the Mount Eden Beds, Southern California," by Daniel I. Axelrod. (IV) "The Deschutes Flora of Eastern Oregon," by Ralph W. Chaney. (V) "The San Pablo Flora of West Central California," by Carlton Condit.

The first paper describes fossil floras recently collected from the Ogallala formation of the western plains. Thirteen species of vascular plants are described from localities in Nebraska, Kansas, and Oklahoma. Consideration is given also to thirty-one species of diatoms from the same localities. Although vertebrate faunas have been collected from these areas for several decades, plant fossils have been relatively unknown. From the floral aspect, it is concluded that a trend toward greater aridity occurred throughout the plains region during the time represented.

The next paper of the series describes forty-five plant species collected from the lower Idaho formation within a 20-mile radius of Weiser, Idaho. The flora, as a whole, has its closest living counterpart in the forests of the Pacific states. Comparisons with other closely related floras indicate a steady decrease in annual precipitation in the region during the late Tertiary. The age of the Weiser flora is considered to be uppermost Miocene or lowermost Pliocene.

The third paper describes thirty species of plants from the Mount Eden beds at San Gorgonio Pass in southern California. Twenty-one of the species are considered to be new, and more than a third of the total number are definitely known to be shrubs. The flora represents six distinct habitats such as might exist on mountain slopes adjacent to a depositional basin. A comparison with other California floras of Pliocene age, together with vertebrate evidence, indicates a Middle Pliocene age for the Mount Eden beds.

Fourth in the series is a paper describing five plant species collected

from the base of an ancient mudflow in the Deschutes formation near Madras, Jefferson County, Oregon. The composition of the flora, which is dominated by *Populus pliotremuloides*, indicates a cool, arid climate at a relatively high elevation. The flora is considered to be Pliocene in age. A close relationship with previously known floras in the Dalles and Hood River formation suggests a time equivalent to them.

The last paper in the volume describes twenty-six species of plant fossils obtained from several localities in the Neroly member of the San Pablo beds in Contra Costa, Alameda, and San Joaquin counties, California. The majority of the species are arborescent dicotyledons. The flora has its closest modern equivalent in the Taxodium forests of southeastern United States. A climate having only slightly higher temperatures but much greater annual rainfall than the region has at present is indicated by the flora. On the basis of specific content and climatic indications, the age of the Neroly horizon is believed to be Upper Miocene.

Each paper is illustrated with excellent photographs. The articles are presented in a uniform style with numerous tables, drawings, and maps adding to the usefulness of the text. The volume as a whole is a valuable addition to our knowledge of Tertiary paleontology and geology.

RAYMOND E. JANSSEN

"The Geology of the Baguio Gold District," by ANDREW LEITH. *Technical Bulletin No. 9, Department of Agriculture and Commerce, Commonwealth of the Philippines.* Manila, 1938. Pp. 91; pls. 2; figs. 5.

The Baguio gold district in the northwest highlands of Luzon is the foremost gold-producing district in the Philippines. Baguio is located on the west limb of a great eroded arch. To the east, along the axis of this arch, crystalline rocks of the basement complex are exposed. The sediments found on the west limb are of Tertiary age. They consist of marine and fresh-water clastics (chiefly pyroclastics) interbedded with limestones. These formations are pierced by numerous andesitic stocks.

The ores must have come in after most of the andesite had solidified, for the andesite in some places is traversed by ore veins. On the other hand, certain masses of the andesite seem to have been still sufficiently hot to cause a zonal deposition of ores in their immediate vicinity. The fractures occupied by the veins are attributed to forces acting at great depth, since they maintain their trend regardless of differences in the competency of surface rocks. Leith believes that the forces which gave rise to these great sets of fractures were also responsible for the formation of "regional crustal magmas" under Luzon and that the ore-bearing solutions emanated from these magmas.

WILLIAM F. READ

near
which
ate at
age.
Hood

plant
e San
Cali-
The
outh-
pera-
ent is
indi-
cene.
es are
maps
uable

EN

chni-
mon-

s the
ed on
f this
sedi-
arine
lime-

ified,
other
ently
The
great
n the
gave
ation
solu-

AD